

Development and comparison of a Heat transfer model for SLM in OpenFoam and commercially available FEM software

Diploma in
Mechanical Engineering

Submitted by
Ioannis Christodoulou

Under the supervision of
Angelos P. Markopoulos



SCHOOL OF MECHANICAL ENGINEERING

NATIONAL TECHNICAL UNIVERSITY OF ATHENS

15780, Iroon Polytecneiou 9, Zografou, Athens

JULY 2021

ACKNOWLEDGMENT

I wish to express my sincerest gratitude to Associate Professor Angelos P. Markopoulos for his continuous guidance and mentorship, not only during my diploma thesis development, but also during my years as a student at the National Technical University of Athens. He showed me the path to achieve my targets by explaining all the tasks to be done, and helped me be creative in a controlled manner, as well as he explained to me the importance of this project on the scientific society and its industrial relevance. He was always ready to help me and clear my doubts regarding any hurdles in this project. Without his constant support and motivation, this project would not have been possible. Finally, I would also like to express my gratitude to Manolis Papazoglou for his support throughout all this work. Without him, the project would not have been successful.

Υπεύθυνη δήλωση για λογοκλοπή και για κλοπή πνευματικής ιδιοκτησίας:

Έχω διαβάσει και κατανοήσει τους κανόνες για τη λογοκλοπή και τον τρόπο σωστής αναφοράς των πηγών που περιέχονται στον οδηγό συγγραφής Διπλωματικών Εργασιών. Δηλώνω ότι, από όσα γνωρίζω, το περιεχόμενο της παρούσας Διπλωματικής Εργασίας είναι προϊόν δικής μου εργασίας και υπάρχουν αναφορές σε όλες τις πηγές που χρησιμοποίησα.

Οι απόψεις και τα συμπεράσματα που περιέχονται σε αυτή τη Διπλωματική εργασία είναι του συγγραφέα και δεν πρέπει να ερμηνευθεί ότι αντιπροσωπεύουν τις επίσημες θέσεις της Σχολής Μηχανολόγων Μηχανικών ή του Εθνικού Μετσόβιου Πολυτεχνείου.

Ονοματεπώνυμο

Ιωάννης Χριστοδούλου

ABSTRACT

The focus of this work was to simulate the heat transfer on two different software, COMSOL 5.6 and OpenFOAM v5, during the additive manufacturing process named, Selective Laser Melting (SLM). A heat transfer model, in conduction mode, was implemented with Gaussian distributed laser beam striking down on the top surface. First of all, a brief presentation of SLM is given. Then the model assumptions are formed. Moreover, the governing Equations and Laser Boundary Conditions mathematical treatment are presented in this work. The generation of the code for OpenFOAM and the model for the COMSOL are presented, too. In addition, the workflow for each program is presented and the implementation of the heat transfer model is included. On OpenFOAM, *laplacianfoam* solver was used, whereas on COMSOL *Heat Transfer in Solids* Module was used. The results were compared in respect to three different laser speeds. The runtime, operating system resources management and user interface were compared, too. During comparison, both software operated adequately, and it is concluded that for different application each software maybe be more capable than the other.

In the end of this work, reader will be able to answer to questions such as what is the modeling workflow for the two programs? How to model conduction mode on SLM process? How far can the single-track simulation enrich? Which software is most suitable for which application? How OpenFOAM and COMSOL manage computer resources? And more...

LIST OF ABBREVIATIONS

Abbreviation	Description
3D	Three dimensional
AM	Additive Manufacturing
BC	Boundary Condition
CAD	Computer-Aided Design
CV	Control Volume
FEM	Finite Element Method
FVM	Finite Volume Method
GUI	Graphical User Interface
OpenFOAM	Open source Field Operation And Manipulation
PBF	Powder Bed Fusion
RnD	Research and Development
SLM	Selective Laser Melting
VOF	Volume of Fluid

NOMECLATURE

Symbol	Units	Description
v	[m/s]	speed
ρ	[kg/m ³]	density
c_p	[J/kgK]	Specific heat capacity
k	[W/mK]	Thermal Conductivity
DT	[m ² /s]	Thermal diffusivity
h	[W/m ² K]	Heat Transfer Coefficient
σ	[m]	Standard deviation of laser beam distribution
\mathbf{n}	-	Surface normal vector
\mathbf{e}	-	Unit vector of axis
d	[m]	Distance from Surface
V	[m ³]	Volume
T	[K]	Temperature
O	[m]	Beam origin
x	[m]	Beam striking surface point coordinates

CONTENTS

ACKNOWLEDGMENT.....	3
Υπεύθυνη δήλωση για λογοκλοπή και για κλοπή πνευματικής ιδιοκτησίας:	4
ABSTRACT.....	5
LIST OF ABBREVIATIONS	6
NOMECLATURE	7
CONTENTS.....	8
1. INTRODUCTION	12
Objectives	12
1.1 SLM TECHNOLOGY	12
1.2 SLM PARAMETERS	15
1.2.1 SLM MANUFACTURING ISSUES	16
1.3 ADVANTAGES AND DISADVANTAGES	17
1.4 KEY FACTORS IN SLM TECHNOLOGY - MELT POOL	18
1.4.1 DOMINANT FORCES.....	18
1.4.2 HEAT CONVECTION	19
1.4.3 HEAT CONDUCTION.....	19
1.4.3 CONDUCTION MODEL VS THERMAL-FLUID MODEL	20
1.5 FINITE ELEMENT METHOD SOFTWARE.....	21
1.5.1 INTRODUCTION	21
1.5.2 OPEN CODE SOFTWARE.....	21
1.5.3 ALTERNATIVE COMMERCIALY AVAILABLE SOFTWARE	22
1.5.4 STRENGTH AND WEAKNESSES OF EACH SOLUTION	22
2. BASIC THEORY – STATE OF THE ART	23
OBJECTIVES	23
WHY MODELING SINGLE TRACK	23
2.1 GOVERNING EQUATIONS	23
2.2 STATE OF THE ART	24
2.2.1 LASER BEAM MODELING	24
2.2.2 MELT POOL GEOMETRY	25
2.2.3 MESHING FOR SLM PROCESS SIMULATION	26
2.2.1 ANALYSIS OF PROCESS DYNAMICS IN LASER WELDING.....	27
2.2.2 MESHFREE SIMULATIONS FOR ADDITIVE MANUFACTURING PROCESS OF METALS.....	28
2.2.3 PAPERS ON UNITE ALL THE PHYSICS	30

2.2.4 BASIC FLUID DYNAMICS EQUATIONS FOR THERMAL-FLUID MODELING.....	32
COMPUTATIONAL FLUID DYNAMICS (CFD).....	32
FINITE VOLUME METHOD (FVM)	32
MASS CONSERVATION.....	32
ENERGY CONSERVATION	33
VOLUME OF FLUID (VOF).....	34
PRANDTL NUMBER	34
2.2.5 ANSYS AM MODULE	35
3. MODEL ASSUMPTION AND MATERIAL PROPERTIES	36
3.1 MODEL ASSUMPTION WHEN SIMULATING THE SLM PROCESS	36
3.2 MATERIAL PROPERTIES	36
4. MODEL DEVELOPEMENT USING OPENFOAM	37
OBJECTIVES	37
4.1 MODEL	37
4.1.1 LAPLACIAN SOLVER	37
4.1.2 LASER BC.....	37
4.1.3 CONVECTIVE BC.....	39
4.1.4 MATHEMATICAL TREATMENT OF THE BOUNDARY FACES IN OPENFOAM	40
4.1.4 MATHEMATICAL TREATMENT OF THE LASER IN OPENFOAM	40
4.1.5 MATHEMATICAL TREATMENT OF THE FINAL BOUNDARY CONDITION.....	40
THERMAL DIFFUSIVITY	41
4.2 OPENFOAM INTERFACE.....	41
4.1.1 SYSTEM DIRECTORY	43
4.1.2 CONSTANT DIRECTORY	43
4.1.3 TIME DIRECTORIES	43
4.2 MESH IN OPENFOAM	43
4.2.1 POINTS.....	43
4.2.2 FACES	44
4.2.3 CELLS	44
4.2.4 PATCHES	45
4.2.5 BOUNDARY	45
4.2.6 DIMENSIONS IN OPENFOAM.....	45
4.3 MESH GEOMETRY	45
4.4 SYSTEM, CONSTANT AND ZERO DIRECTORIES DURING SIMULATION	47
4.4.1 SYSTEM FOLDER	47
4.4.2 COMPILING THE laserConvectionBC	47

4.4.3 THE HEAT TRANSFER COEFFICIENT AND MATERIALS CONDUCTIVITY	48
4.4.4 PARALLELIZATION	48
4.4.5 ParaView	48
5. MODEL DEVELOPMENT USING COMSOL	49
OBJECTIVES	49
5.1 COMSOL	49
5.1.1 FILES:	50
5.2 WORKFLOW	50
5.2.1 GEOMETRY AND MESHING	51
5.2.2 MATERIALS	53
5.2.3 PHYSICS	54
5.2.5 ADDITIONAL FEATURES	57
ADAPTIVE MESHING	57
AUXILIARY SWEEP	57
LINEAR SYSTEM SOLVERS	57
5.3 UNITS IN COMSOL	58
6. RESULTS AND COMPARISON OF THE SOFTWARE	59
OBJECTIVES	59
COMPUTER CHARACTERISTICS	59
PROCESSOR	59
MEMORY	59
SYSTEM TYPE	59
6.1 MESH	60
6.2 MELT POOL GEOMETRY	62
6.3 PROCESSING TIME, COMPUTER RESOURCES MANAGEMENT AND PARALLELIZATION	72
7. CONCLUSIONS	75
OBJECTIVES	75
8. FUTURE WORK	76
Objectives	76
8.1 MODELING AND COUPLING OF FLUID DYNAMICS AND PHASE CHANGE	76
8.2 MODELING OF ELECTROMAGNETIC FORCES DUE TO PLASMA INTERACTION	76
8.3 COMPARING THERMAL, FLUID, ELECTROMAGNETIC MODELS TO DETERMINE IF IT HAS ANY EFFECT ON THE RESULTS	76
8.4 COMPARISON BETWEEN DIFFERENT MESH SIZES	76
8.5 PLASMA SHIELDING COUPLING (BEAM ENERGY LOSS)	77

8.6 TOWARDS AN OPEN-SOURCE AM SOFTWARE TOOLKIT, BASED ON OPENFOAM OPEN-CODE SOFTWARE	77
APPENDIX A	78
ControlDict	78
Bibliography	79

1. INTRODUCTION

Objectives

After reading Chapter 1, reader will be familiar with the AM processes and especially the SLM technology. Also, as an extensive presentation of FEM software (commercially available and open source) is included, the reader will also be able to identify the advantages and disadvantages of these software. Finally, a disclosure of the key components that a SLM machine consists of, is included.

1.1 SLM TECHNOLOGY

Additive manufacturing has already entered the industrial world with success, and more research is done on this field than ever before. The techniques used up to date are shown in the figure below:

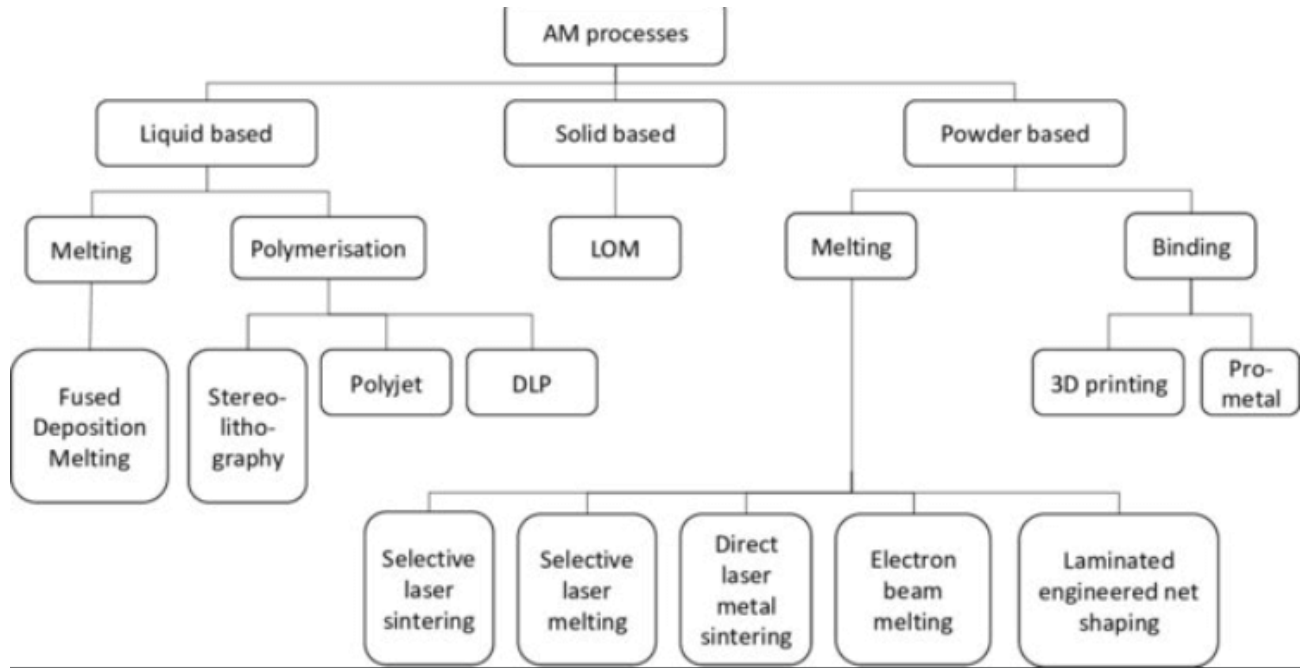


FIG1.1 ADDITIVE MANUFACTURING TECHNOLOGIES [1] FIG 1

Selective Laser Melting (SLM) or Laser Powder Bed Fusion (LPBF) is an Additive Manufacturing (AM) Technique that can produce complex three-dimensional (3D) parts through melting and solidification of the powder used. This process iterates for each layer of the sliced model produced from a Computer Aided Design (CAD) software[2].

The above technology has some main traits common to other similar technologies (SLS, DMLS etc.). These include:

- A thermal source, which melts the powder particles and fuses them together (laser)
- A control mechanism to control the melting of the particles to a specific area (galvano scanner)
- Ability to add a subsequent layer.
- Ability to smooth each layer before addition of the next layer.

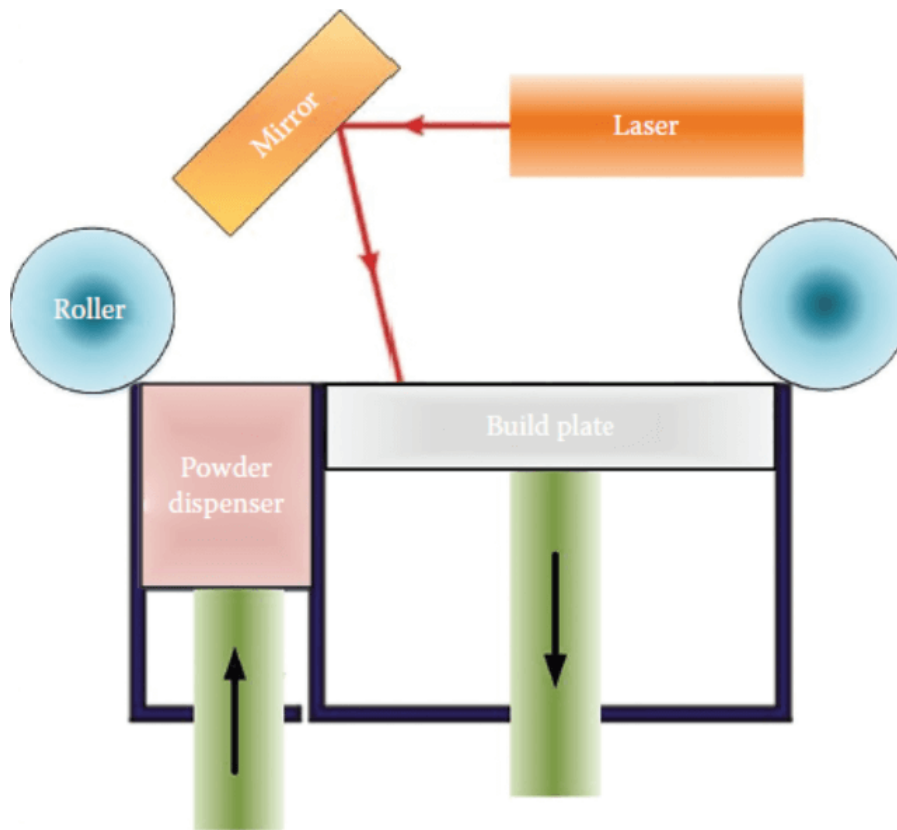


FIG. 1.2 SCHEMATIC OF SLM PROCESS [3]

Some applications of this technology are in the medical devices, aerospace, and automotive industry, where 3D complex geometries and weight are more important.

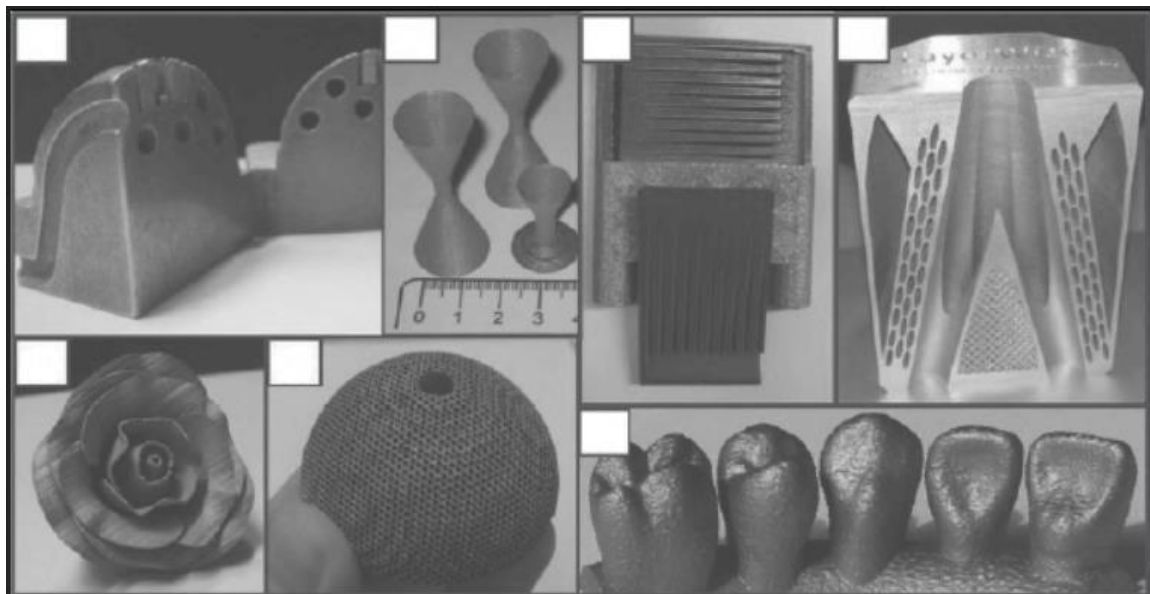


FIG 1.3 COMPLEX SLM PARTS: (A) STAINLESS STEEL MOLD, (B) TITANIUM ALLOY THIN-WALL STRUCTURE, © 316L SS HEATING PLATE FOR AEROSPACE INDUSTRY, (D) ADVANCED NOZZLE WITH INTERNAL COOLING, (E) SS ARTISTIC FLOWER, (F) TITANIUM ALLOY BIOMEDICAL ACETABULAR CUP, (G) COCR DENTAL PARTS [2] FIG 32

The discrete sub-systems that a SLM machine consists of are: (i) laser system, (ii) scanner system, (iii) bed, (iv) controller system, (v) build chamber. The laser and scanner system (fig.1.2) consists of two mirrors that oscillate, creating the desired pattern. However, the beam needs to be focused, so after the scanner system (galvano scanner head), the beam is guided through focusing optics to scan the desired geometry on the powder bed.

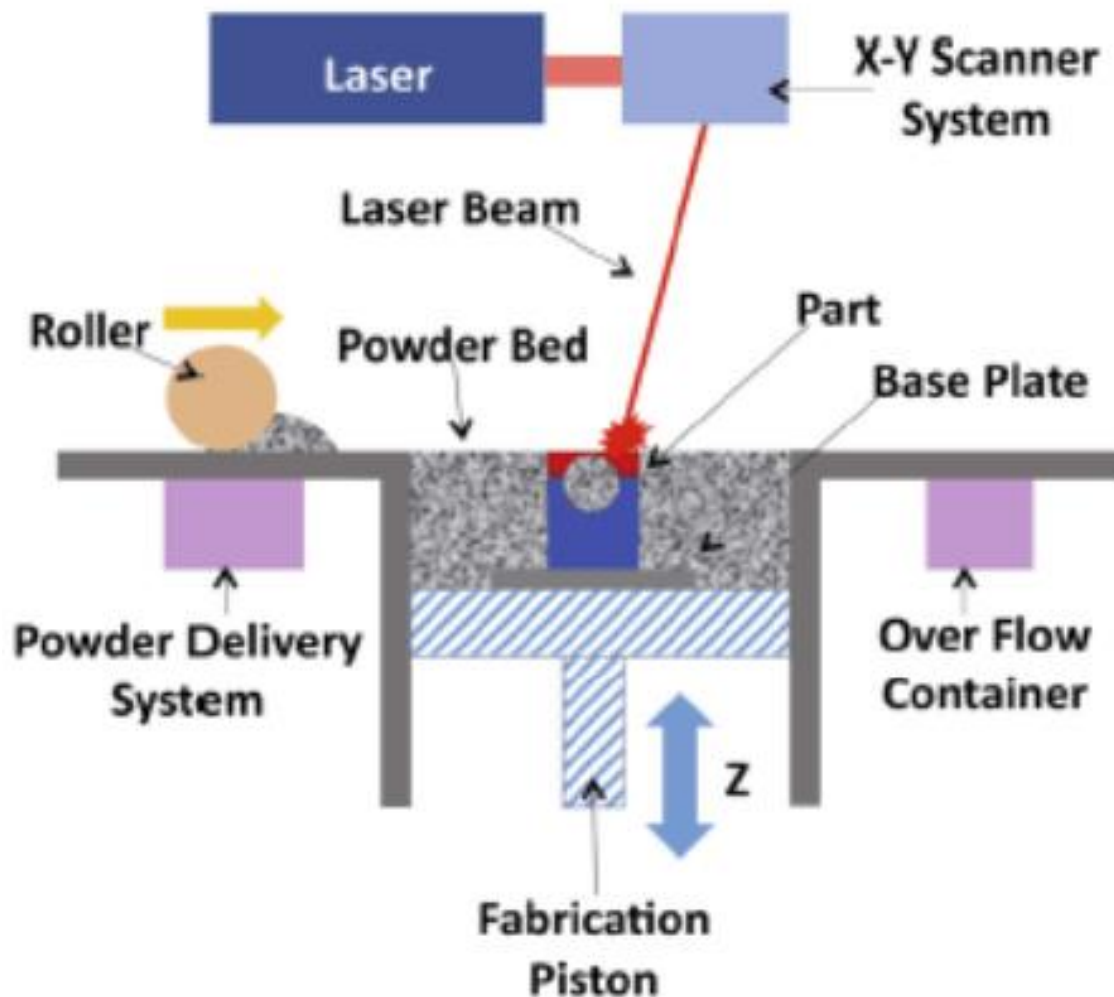


FIG1.4 AN OVERVIEW OF SELECTIVE LASER MELTING [4] PP 36-62

First, deposition of a uniform layer of powder on the bed is done. Then, the laser beam melts the desired area to build a single layer of the part. In addition, the melting pattern, or laser scanning pattern, is created through the galvano scanner and can have multiple geometries (continues lines, near-random pulses, etc.). The layer is completed by lowering the height of the deposited layer. This process is iteratively repeated for each layer until the part is produced [4].

1.2 SLM PARAMETERS

This technology has some key parameters that are important to not overlook. Some of them are [5]:

- Laser power: Power of laser that applied on powder melting.
- Scan speed: Velocity at which laser beam travels. This is controlled by galvano scanner.
- Scan spacing: Parallel laser scans are distanced by this parameter.
- Scan count: The count of laser beam traverses by layer
- Scan strategy: Scanning pattern on each layer
- Layer thickness: The distance that the build platform will lower for the new layer to be deposited.
- Build temperature: Temperature of bed and/or chamber.

Many factors of this process are shown below:

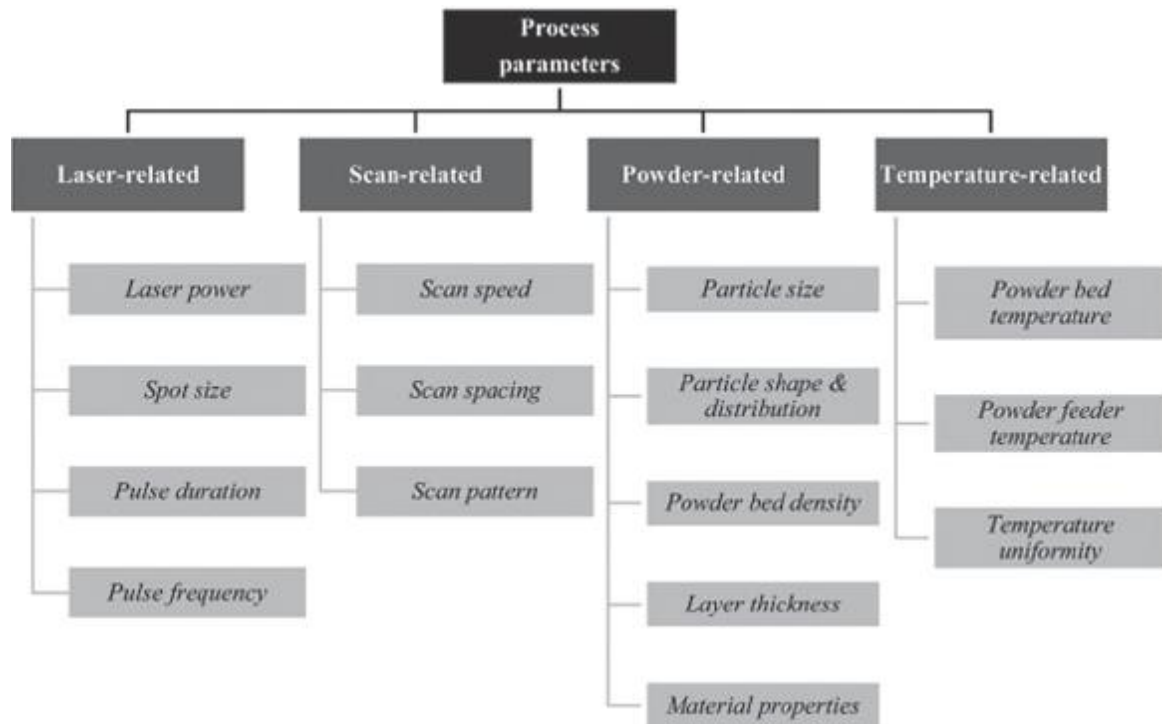


FIG1.5 OVERVIEW OF SLM PROCESS PARAMETERS [5]

1.2.1 SLM MANUFACTURING ISSUES

SLM manufacturing techniques have some issues that need to be given the necessary importance. First, the layer bonding defects, that occur due to insufficient heat input. In this case, the particles are not completely melted and are not consolidated with the bulk material. The result is that gas from the surrounding atmosphere is trapped in the material.

Furthermore, due to shrinkage, during solidification and cooling, the dimensional accuracy, especially that of the first layers or overhang areas, is diminished. In addition, stresses are induced during these phases, thus creating an object with residual stresses.

Balling effect is another issue of this technique. It is the result of instable melt pools. On one hand, single melt balls are formed due to the surface tension, that is overpowering the other forces. On the other hand, Plateau-Rayleigh instability leads to melt pool fragmentation for length-to-width ratios larger than 2.1:1 [6]

Finally, another effect occurring mainly with high-energy beams, is material transport. The maximum temperatures and evaporation rates increase and the confluence of melt pool lifetime, surface tension and evaporation pressure finally cause the material to accumulate on certain locations up to height greater than the layer thickness.

All the above defects together, form an uneven component surface after melting and solidification. If the defects do not occur, SLM-produced components achieve a flat and even top surface.

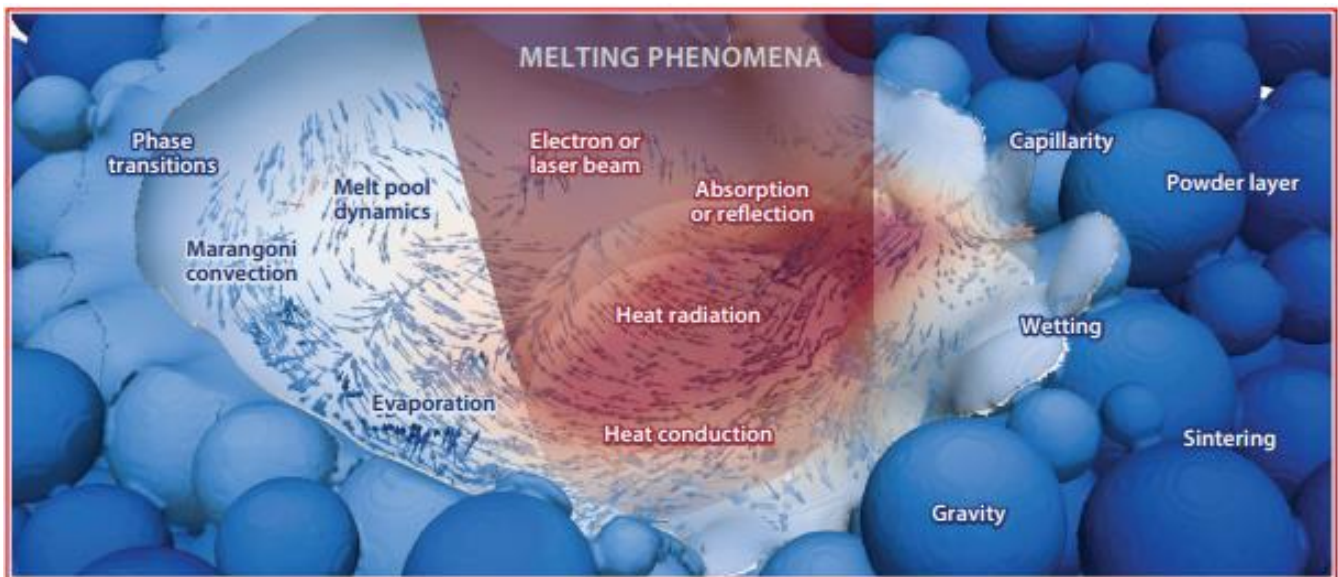


FIG. 1.6 PRINCIPLES OF THE SLM PROCESS[6]

1.3 ADVANTAGES AND DISADVANTAGES

Some advantages of this process, compared to other AM techniques and classical manufacturing techniques, are:

- High density and strength of the parts.
- Recycling of the powders used, leading to minimum waste of material.
- Parts with complicated 3D geometries can be created.
- Ability to process wide variety of metals and their alloys.
- No composite green part is produced. Thus, there is no need for binders or melt phases.

May the positive points of the process be enough to justify its emergence in many industries, though the drawbacks are not negligible. Below are shown some of them:

- Expensive, especially for parts not designed for manufacturing with this process.
- Limited geometric tolerances and dimensions that can be obtained.
- Rough surface finish of the parts.
- Post-process required, most of the time.

1.4 KEY FACTORS IN SLM TECHNOLOGY - MELT POOL

1.4.1 DOMINANT FORCES

Melt-pool of this type is already known from welding processes. The welding process can be implemented using an electric arc, electron beam or laser beam as a heat source. Below are shown the dominant forces that affect the weld pool:

- Buoyancy

Upward force exerted by a fluid that opposes the weight of an immersed object.

- Surface tension

This force is due to the tendency of the fluid surface to shrink to the minimum surface. This force decreases with increasing temperature.

- Electromagnetic forces

Also known as Lorentz force, it is the force caused by charged particles moving at a speed through an electric field.

- Marangoni force

This force is due to mass transfer along an interface between two fluids due to a gradient of the surface tension.

Below it can be seen the profile of a melt pool and its characteristic areas.

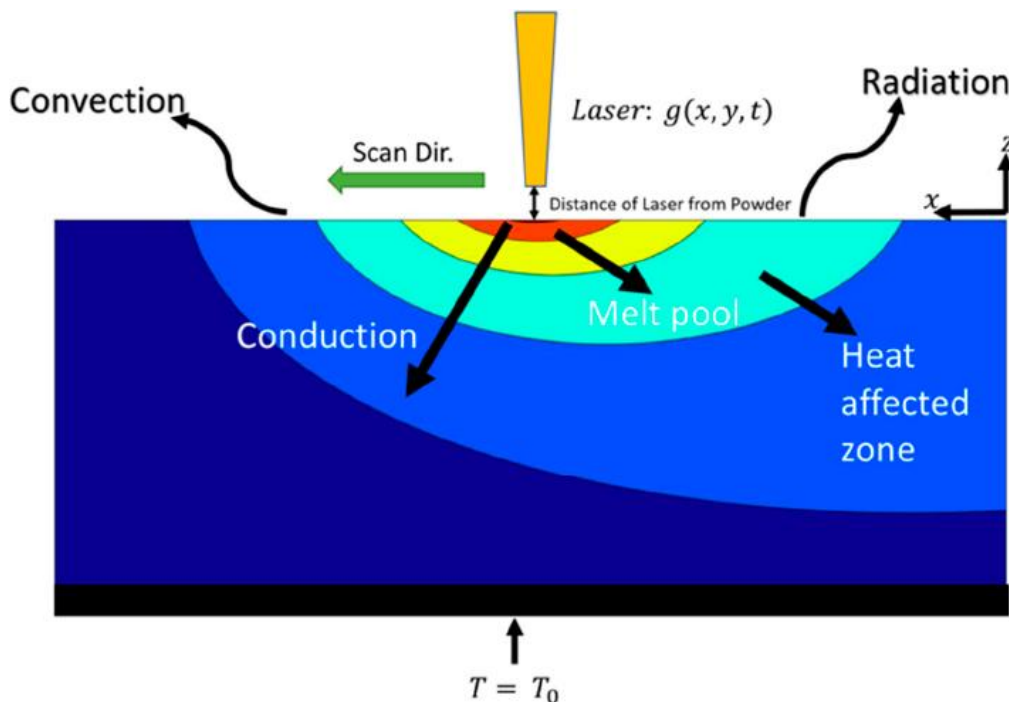


FIG 1.7 MELT POOL DURING LASER WELDING[7] FIG 1

A laser light heat source of Gaussian distribution can be noted heating the metal and forming a molten pool. Heat conduction occurs to the surrounding metal, and convection and radiation occur from the surface to the surrounding gas. Inert shielding gas (Argon, Helium etc.) is used to stop melt pool oxidation. Within the melt pool, the governing forces, mentioned above, are taking place. During laser melting, extreme temperatures can be created, exceeding the boiling point of the metal, thus metal evaporation is possible.

1.4.2 HEAT CONVECTION

The heat convection consists of two phenomena. The first is by random molecular movements (diffusion) and the second by the bulk of that fluid motion. The fluid motion is associated with the fact that, at any instant, massive numbers of molecules are moving collectively or as aggregates. Such motion, in a temperature gradient, contributes to heat transfer [8].

Below, it is visible the mechanism of heat transfer via convection. Where, x is the length of the surface, y is the thickness of the fluid layer, u is the fluid velocity, q is the heat flux, and T is the temperature.

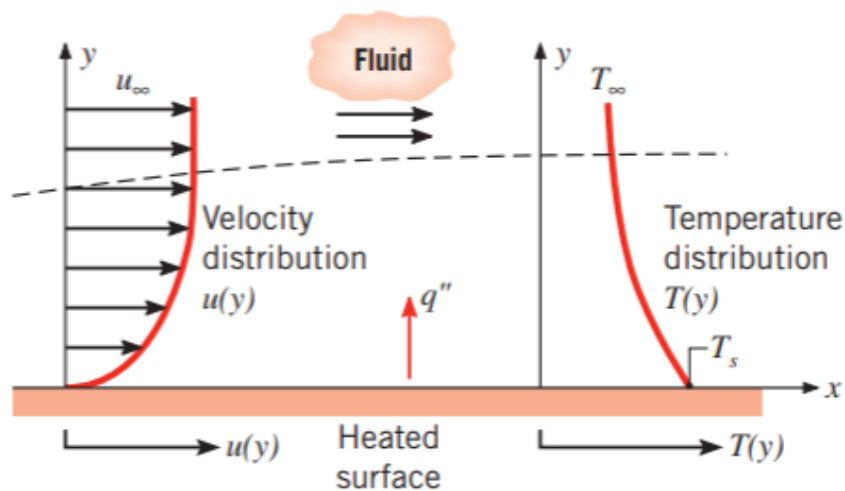


FIG 1.8 CONVECTION MECHANISM AND FLUID VELOCITY-TEMPERATURE PROFILES[8] PP 6

1.4.3 HEAT CONDUCTION

Conduction may be considered the transfer of energy from the more energetic to the less energetic particles of a substance due to interactions between the particles.

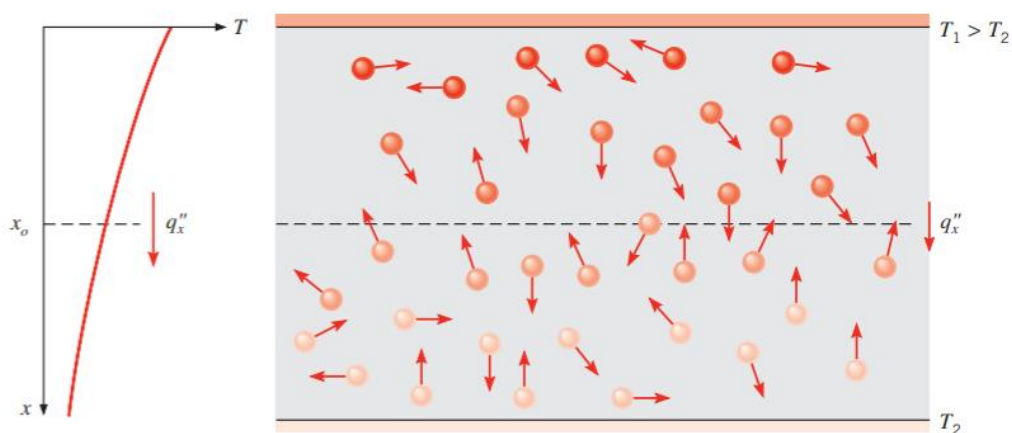


FIG 1.9 CONDUCTION HEAT TRANSFER MECHANISM[8] PP5-6

1.4.3 CONDUCTION MODEL VS THERMAL-FLUID MODEL

In literature, there have been developed and proposed many different models to simulate the SLM process. Heat transfer model is a simpler, yet effective way to determine melt pool characteristics, whereas thermal-fluid model is a more completed model to use in a more research manner but with a significant higher requirement in processing time.

Fluid flow calculations are essential in SLM models in order to predict the melt pool dimensions in cases where flow-related phenomena such as Marangoni flow are dominant. In the conduction melting mode the simulation results can be in good agreement with the experimental data without considering the flow related phenomena. The inclusion of Marangoni effect can lead to overestimation of the melt pool dimensions, when the effects of fluid flow are less significant. Therefore, there are various thermal models in the relevant literature, which have been shown to predict melt pool dimensions with high accuracy, as well as microstructure, onset of ball formation and residual stresses, and some researchers noted that in some cases melt pool dimensions can be predicted even by using simplified thermal models such as the Rosenthal equation [9]–[13].

Below, the melt pool profiles can be distinguished, modeled on conduction mode and Thermal-Fluid model, respectively.

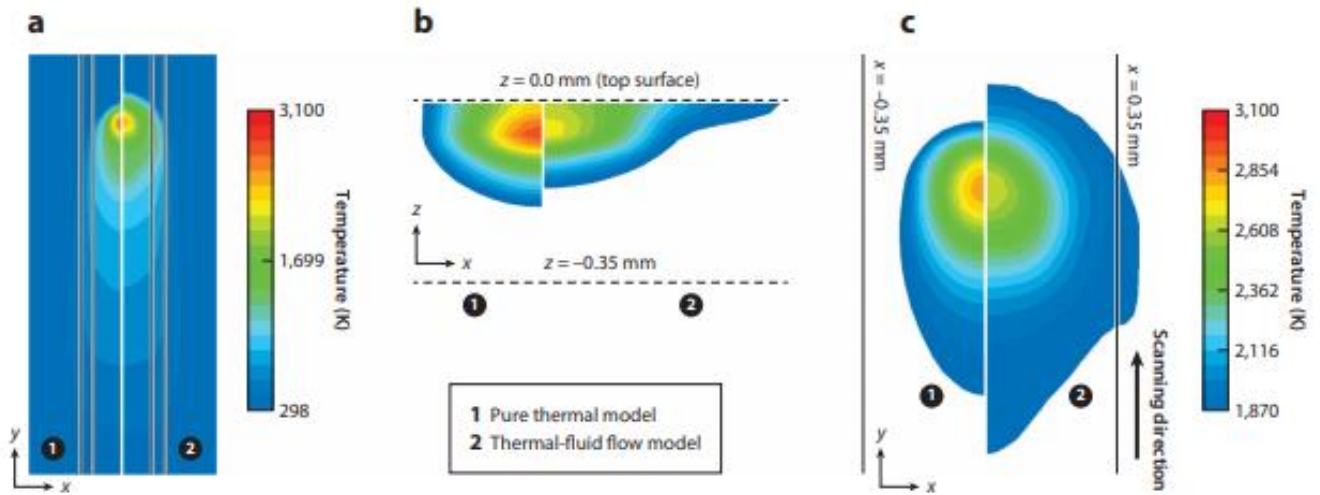


FIG. 1.10 MELT POOL PROFILE COMPARISON FOR THERMAL MODEL AND THERMAL-FLUID MODEL [6]

1.5 FINITE ELEMENT METHOD SOFTWARE

1.5.1 INTRODUCTION

Numerical techniques have emerged and advanced to satisfy the current needs of on many fields of engineering. One of them, is the Finite Element Method (FEM), which gives a piecewise approximation to the governing equations. Instead of solving the analytical equations, the solution region can be approximated by solving the equations for an assemblage of discrete elements (discretization). Simulations on complex shapes can be introduced, as the elements can take many forms and shapes [14].

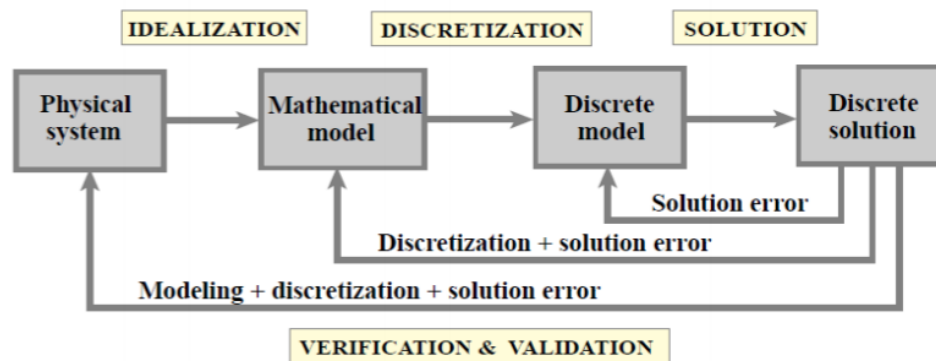


FIG 1.10 MODEL-BASED FEM FLOWCHART [14]

1.5.2 OPEN CODE SOFTWARE

Open code software is computer software under a license in which the copyright holder grants the rights to use, study and change the source code. This comes very handy in situations where the programming of a custom solver is unavoidable. Such software (aiming in CFD software) is:

CFD Software

- CODE_SATTURNE
- OPENFOAM
- GERRIS

Porous flow

- MODFLOW

FEM Software

- deal.II
- Elmer FEM
- FEniCS
- FreeFEM
- Kratos Multiphysics

Finally, one major advantage over commercially available software is the parallelization of code and the extensions available from the community. Especially, OpenFOAM, supports GPU acceleration, whereas well-known commercially available software does not.

1.5.3 ALTERNATIVE COMMERCIALY AVAILABLE SOFTWARE

Commercially available software is a computer software that is under a license in which the copyright holder does not allow any modification of the software or re-distribution of it. These software usually are more user friendly than the open code software and they are accompanied by a wide range of toolboxes and external modules to satisfy the customer needs. Some of them are listed below.

Company name	Product name	Web site
Hibbitt, Karlsson & Sorensen	ABAQUS	http://www.hks.com
Ansys, Incorporated	ANSYS	http://www.ansys.com
Structural Data Research Corp.	SDRC-Ideas	http://www.sdrc.com
Parametric Technology, Inc.	RASNA	http://www.ptc.com
MSC Software Corp.	MSC/NASTRAN	http://www.mscsoftware.com

FIG1.11 LEADING COMMERCIAL FEM SOFTWARE COMPANIES [14]

1.5.4 STRENGTH AND WEAKNESSES OF EACH SOLUTION

A table of advantages and disadvantages for the two types of software is presented here.

	Advantages	Disadvantages
Open Code	Technologically equivalent to commercial solutions	Often, not user-friendly
	Ability to create custom solvers	Sometimes need to learn other skills like programming
	Free	Frequently not so detailed documentation included
	Community support and variety of users code distributions	
Commercial	User-Friendly Interface	Not free of charge
	No need to learn programming	Cannot modify solvers
	Variety of extra modules and toolboxes	
	Exhaustive documentation	

TABLE 1.0 ADVANTAGES AND DISADVANTAGES OF OPEN CODE AND COMMERCIAL SOFTWARE

2. BASIC THEORY – STATE OF THE ART

OBJECTIVES

This chapter will familiarize reader with the governing equations behind FEM software. In addition, a brief explanation into some of the state-of-the-art SLM models will be presented.

WHY MODELING SINGLE TRACK

Studies show that single-track for SLM process is quite common and popular. Specifically, from 2016 to 2019 research papers on single-track simulations have increased by 350%.

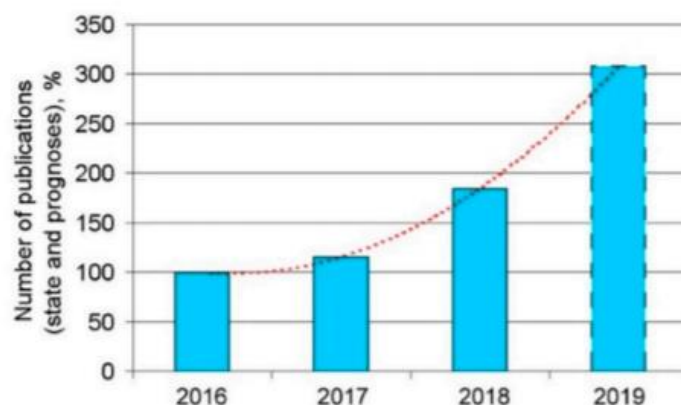


FIG. 2.1 INCREASING NUMBER OF RESEARCH ARTICLES IN SINGLE-TRACK SIMULATIONS FOR SLM PROCESS

Rather than being extremely time-effective, these studies are also very useful for researchers, as they can extract information and develop new models for successfully simulating the process. Single track studies not only can provide results with good accuracy for thermal-fluid phenomenon but they can also be used for simulating with success microstructure mechanisms [15].

2.1 GOVERNING EQUATIONS

The model created in this work is a simple conduction mode model, to investigate the differences of the two software. Thus, the governing equations are,

$$\rho C_p \frac{\partial T}{\partial t} - \nabla \cdot (k \nabla T) = \dot{Q} \quad \text{Eq. (2.1)}$$

where, ρ is the density in $[\text{kg/m}^3]$, C_p represents the specific heat $[\text{J/kgK}]$, k represents the thermal conductivity $[\text{W/mK}]$, and \dot{Q} represents the heat rate per unit volume (W/m^3) .

The Equation 2.1 is the time-dependent 3D Heat Transfer Conduction Mode Equation according to Fourier's Law [6]. Specifically, for this work the Gaussian distribution is modeled as a 2D free surface heat source, thus the right-side term \dot{Q} is equal to zero. The Equation 2.1 then, is written as,

$$\rho C_p \frac{\partial T}{\partial t} - \nabla \cdot (k \nabla T) = 0 \quad \text{Eq. (2.2)}$$

And,

$$k \nabla T = q_{\text{conv}} + q_{\text{rad}} + q_{\text{abl}} \quad \text{Eq. (2.3)}$$

In the right side of the equation the sum of the heat fluxes based on convection, radiation and vaporization of the material are presented. In this case, only the convection heat flux is modeled, thus q_{rad} and q_{abl} are equal to zero.

2.2 STATE OF THE ART

2.2.1 LASER BEAM MODELING

In literature the laser beam has been simulated as a moving heat flux mechanism, similar to what will be done in OpenFOAM software too. Specifically, C.H Fu et al. in the paper “3-DIMENSIONAL FINITE ELEMENT MODELING OF SELECTIVE LASER MELTING TI-6AL-4V ALLOY” has showed that using a DFLUX subroutine the laser beam can be implemented as a heat flux given by the following equation [16]:

$$F = \frac{AP}{\pi r^2} e^{\left(-\frac{2(x^2+y^2)}{r^2}\right)} \quad \text{Eq. (2.4)}$$

where F is the applied heat flux, A is the energy absorption coefficient, P is the laser power, and r is the laser spot radius on the top surface. This represents a Gaussian distribution for the laser beam heat flux and it is shown on the Figure 2.9 below,

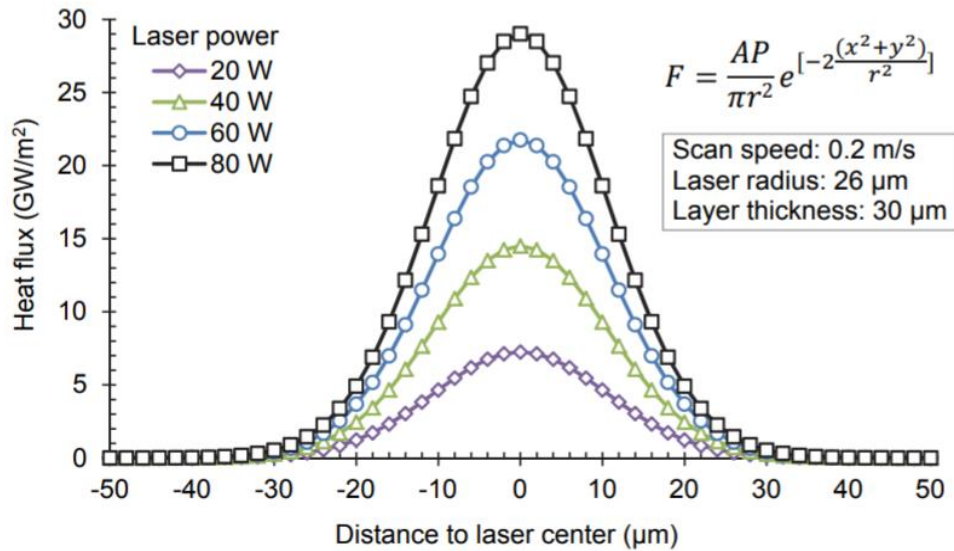


FIG. 2.2 LASER BEAM HEAT FLU GAUSSIAN DISTRIBUTION [16]

Furthermore, in literature, simulations have been accomplished with variable thermophysical values of materials depending on the Temperature [16].

Ti-6Al-4V Solid & Powder		Ti-6Al-4V Solid		Ti-6Al-4V Powder	
Specific heat	Temperature	Conductivity	Temperature	Conductivity	Temperature
J/kg·K	°C	W/m·K	°C	W/m·K	°C
580	20	7.20	26.85	0.2	20
610	205	8.15	100.00	19.4	1605
670	425	9.44	200.00	28.3	1655
760	650	13.32	500.00		
930	870	18.20	876.85		
936	1000	19.79	1000.00		
1016	1200	26.26	1500.00		
1095	1400	28.27	1655.00		
1126	1655	37.00	2126.00		
		42.00	2426.85		

TABLE 2.1 THERMOPHYSICAL VALUES OF TITANIUM ALLOY CHANGING WITH RESPECT TO TEMPERATURE

2.2.2 MELT POOL GEOMETRY

In addition, work has been done in the field of melt pool geometry calculation and prediction. In the following Figure 2.10, it is visible the main geometric characteristics of a melt pool. These characteristics are crucial to know, as many useful conclusions can be deduced, such as bonding reliability between two scanning lines [17].

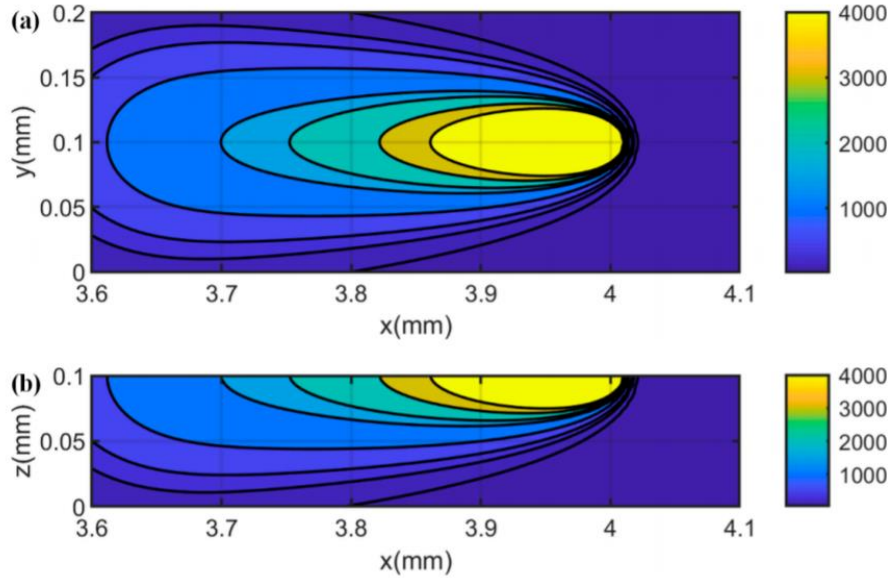


FIG. 2.3 PREDICTED TEMPERATURE DISTRIBUTION OVER A MELT POOL [18]

Having said the above, the melt pool geometric characteristics can be calculated and predicted via simulations. In this specific case that Jinqiang Ning et al. are investigating in the paper “Analytical Modeling of In-Process Temperature in Powder Bed Additive Manufacturing Considering Laser Power Absorption, Latent Heat, Scanning Strategy, and Powder Packing”, a useful graph plotting the molten pool dimensions depending on the scan time can be deduced [17],

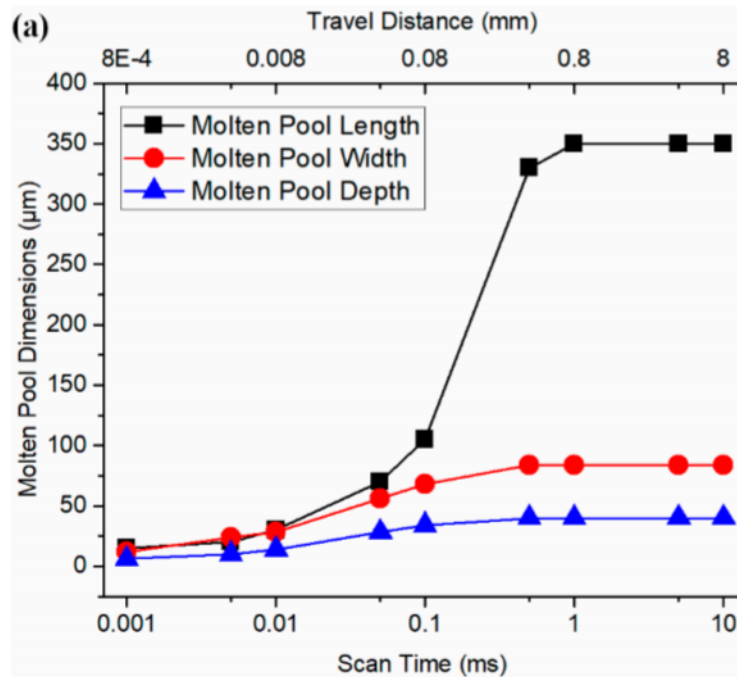


FIG. 2.4 MOLTEN POOL DIMENSIONS [17]

2.2.3 MESHING FOR SLM PROCESS SIMULATION

In literature many different types of mesh elements and mesh sizes have been tested for simulating the SLM process. In the paper “Simulation of metallic powder bed additive manufacturing processes with the finite element method: A critical review” there is a great explanation regarding this field. When simulating the SLM process a powder bed must be constructed and on it metallic particles (powder) should be deposited. The powder is never stacked perfectly thus, when the laser beam is striking the surface of the powder, powder particles of layers below can be affected from the beam. In order to simulate such a phenomenon a volumetric heat source and a mesh strategy like below, should be used [19],

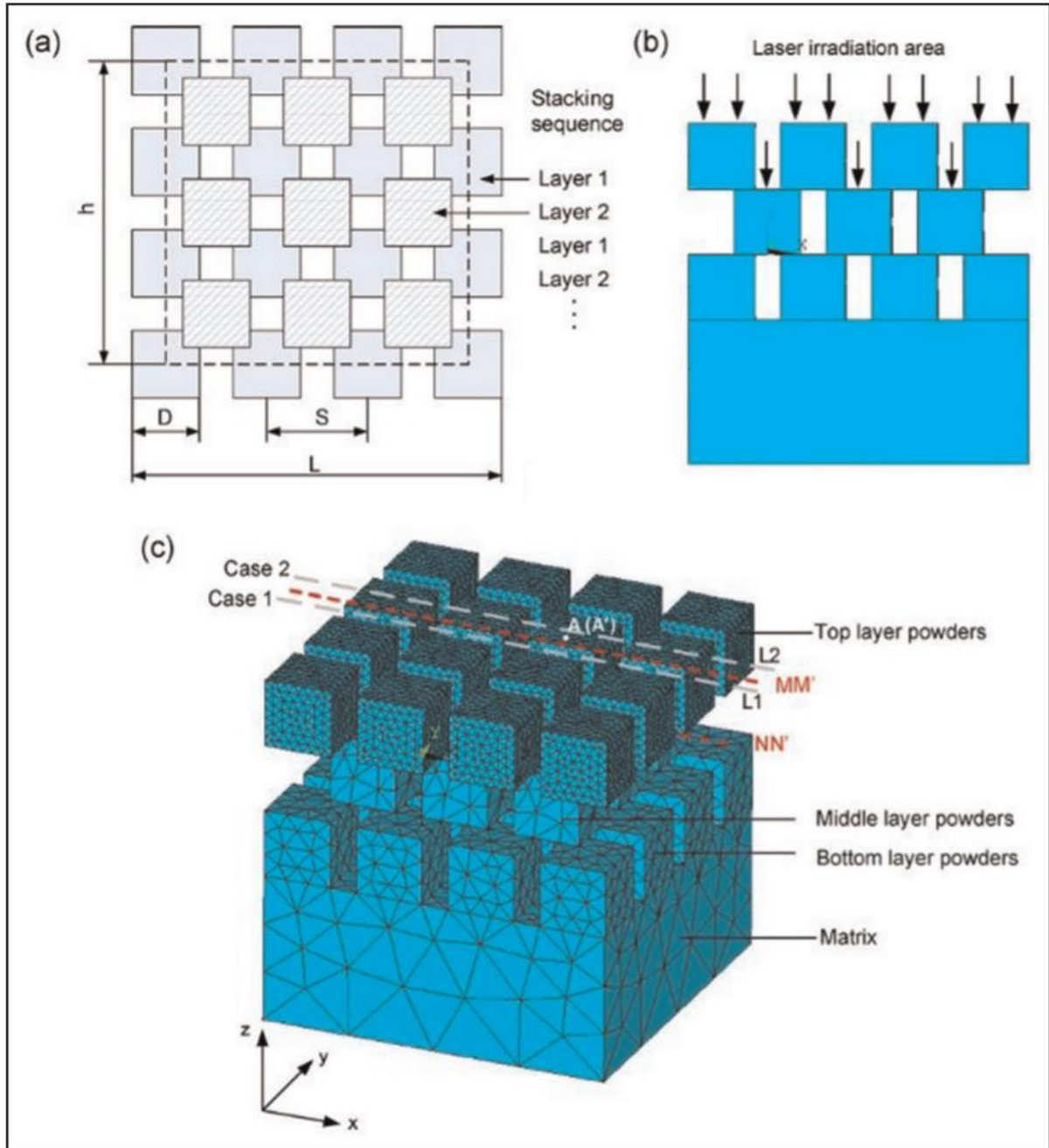


FIG. 2.5 (A) POWDER STACKING STRATEGY (B) LASER IRRADIATION REGION (C) MESHING FOR SIMULATION MODEL CONSIDERING POWDER [19]

2.2.1 ANALYSIS OF PROCESS DYNAMICS IN LASER WELDING

The need for analysis and development of the melt pool simulations is possible to come from other processes as well, such as the laser welding process. Using OpenFOAM as the main FEM software it is possible to create a multi physics simulation with adaptive mesh refinement and time stepping. Furthermore, is it possible to couple porosity physics and solidification phenomena [20].

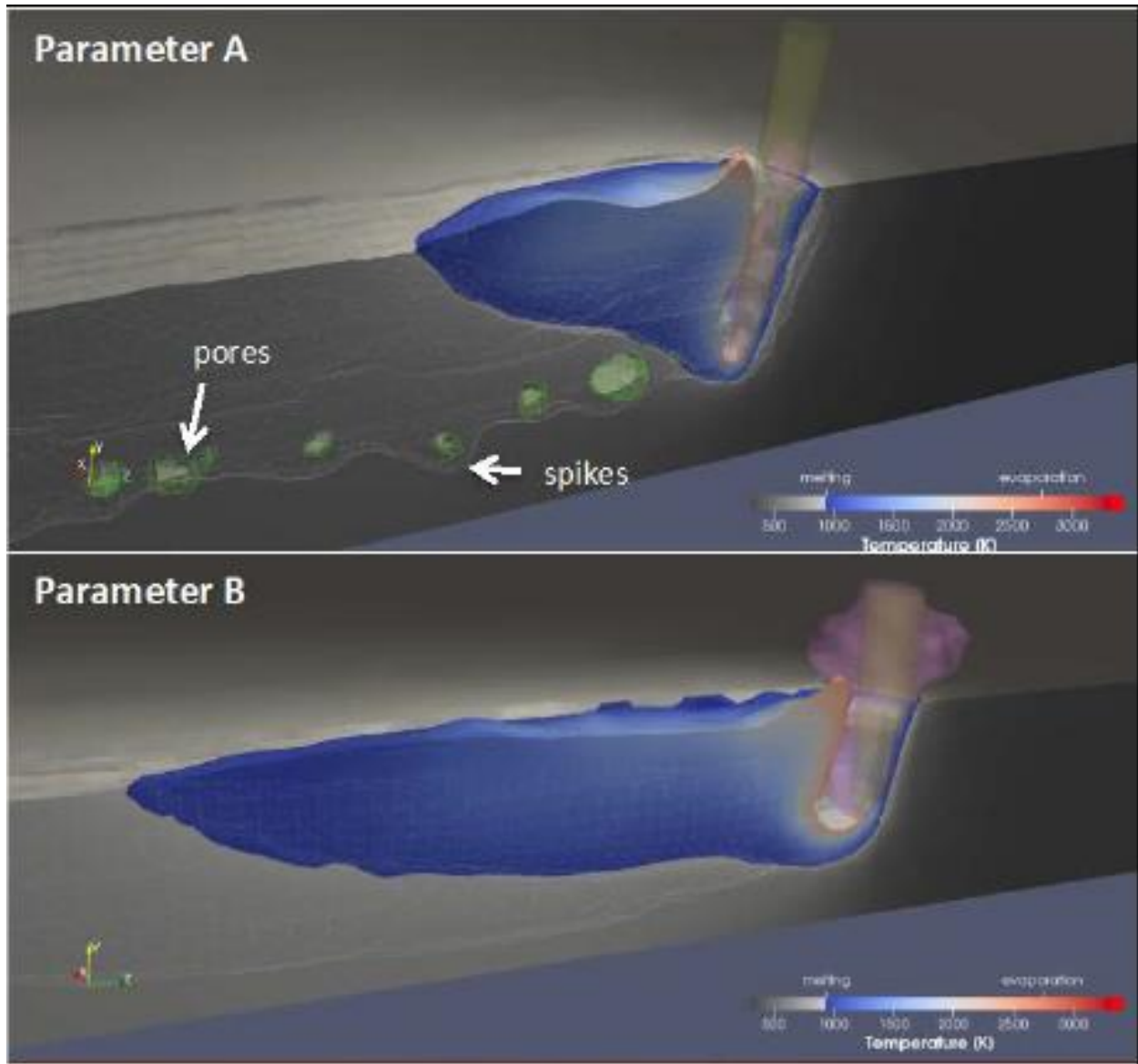


FIG. 2.6 MELT POOL FORMATION [20]

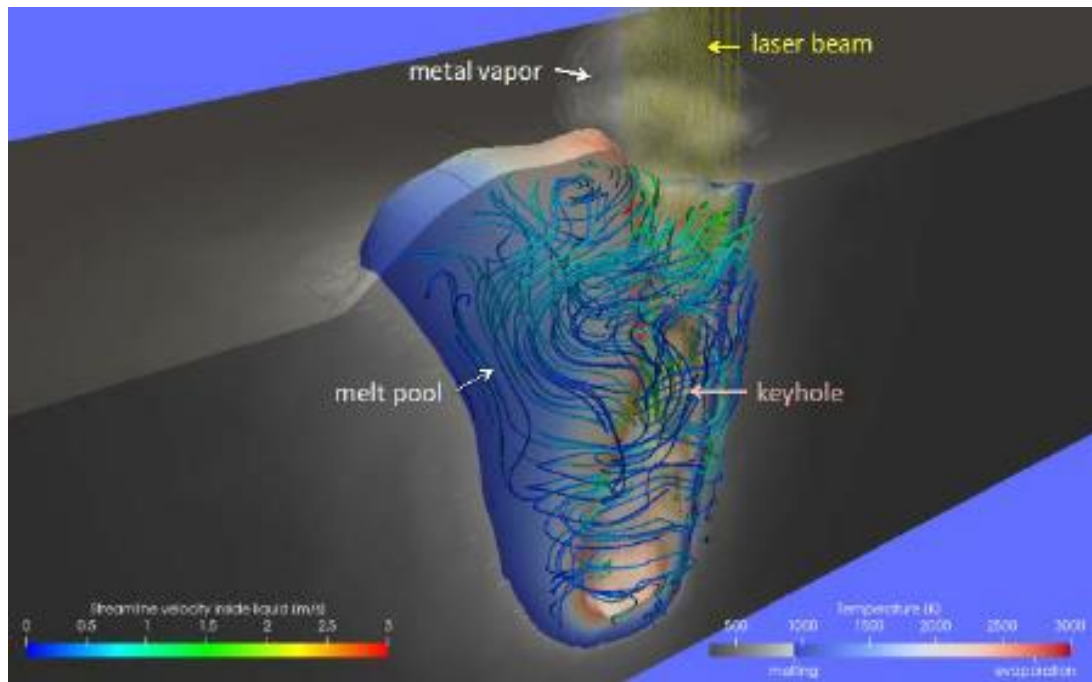


FIG. 2.7 MELT POOL FORMATION [20]

2.2.2 MESHFREE SIMULATIONS FOR ADDITIVE MANUFACTURING PROCESS OF METALS

Some types of simulation problems have not been able to scale well enough with hardware to solve them with conventional methods. Innovative approaches to problem solving must be taken in this area to radically change the simulation workflow. Using meshfree solvers it is possible to deal with some of the problems. Though, as a new it is not widely used and it has some disadvantages, such as the error from the experimental results [21].

Below it is visible the mesh method for SLM process simulation and a mesh free approach.

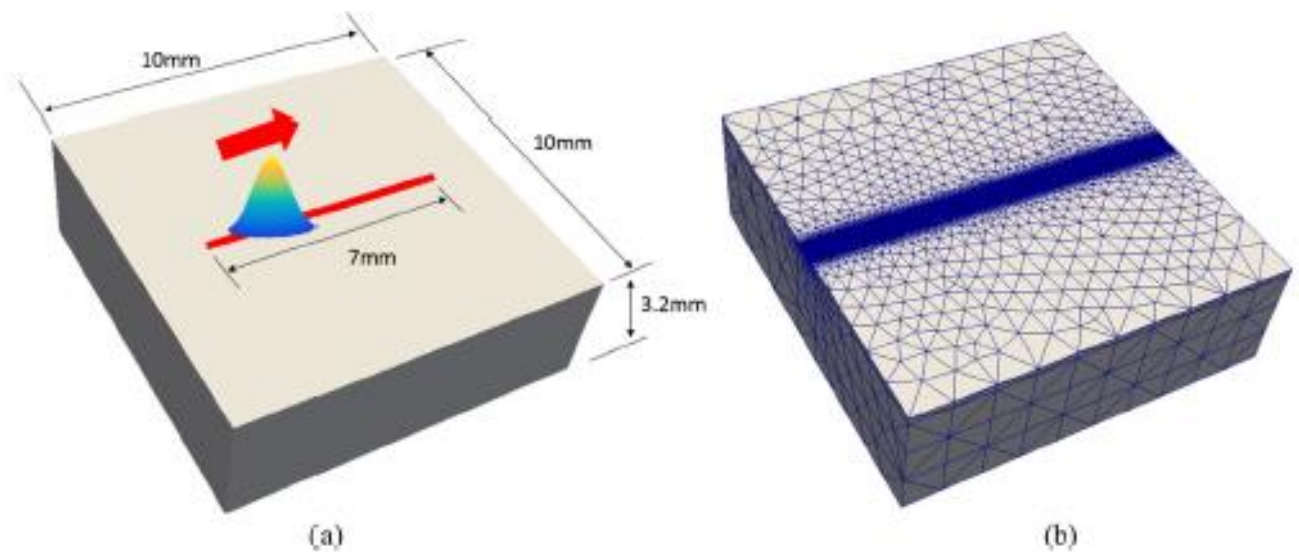


FIG 2.8 MESHING FOR SLM PROCESS [21]

The mesh is extra fine in the laser path, and this consumes many PC resources to solve the problem, thus making the runtime bigger.

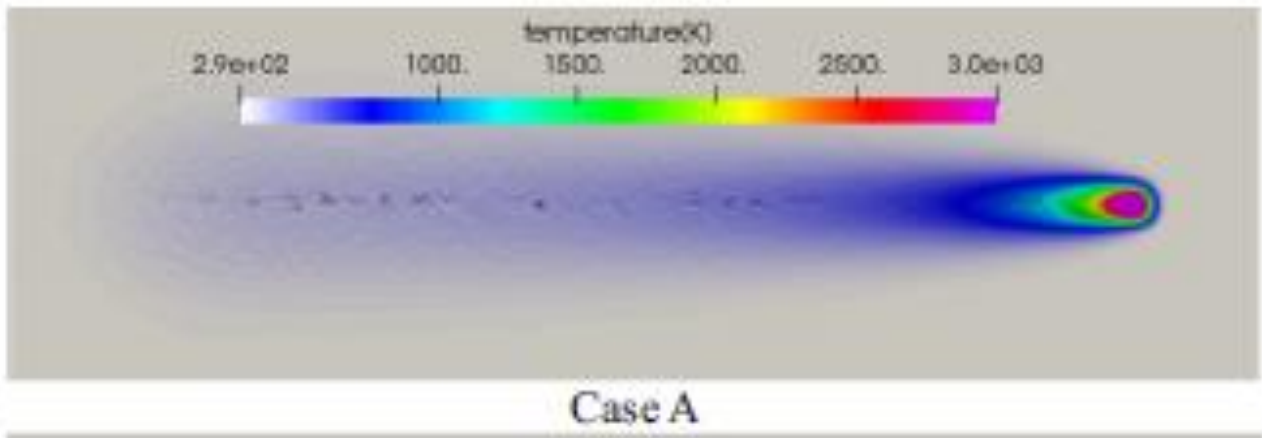


FIG 2.9 MESH FREE APPROACH AND RESULTS COMPARISON TO EXPERIMENTAL DATA [21]

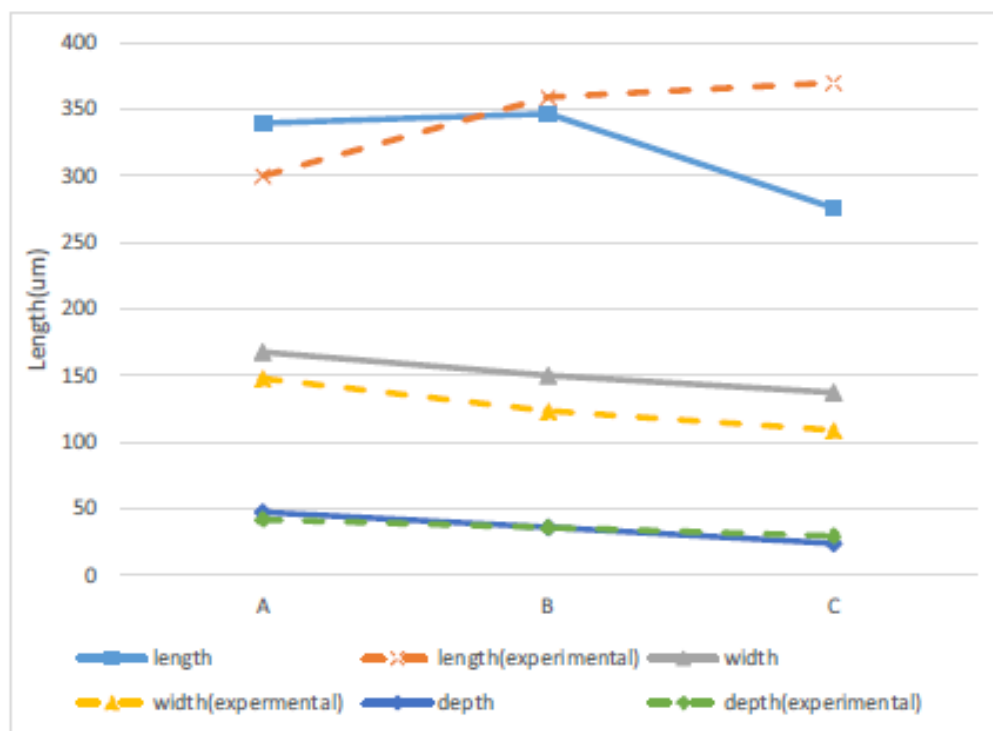


FIG 2.10 MESH FREE APPROACH AND RESULTS COMPARISON TO EXPERIMENTAL DATA [21]

2.2.3 PAPERS ON UNITE ALL THE PHYSICS

Finally, it is widely needed a universal model for additive manufacturing processes such as SLM process. This is well known from researchers all over the world and a big effort has been taken to conclude to such a model.

Fluid Dynamics, Heat Transfer, Optics, and a multi-scale approach are some of the things to be united in order to produce a universal model.



FIG 2.11 FLUID DYNAMICS OF MELT POOL [22]

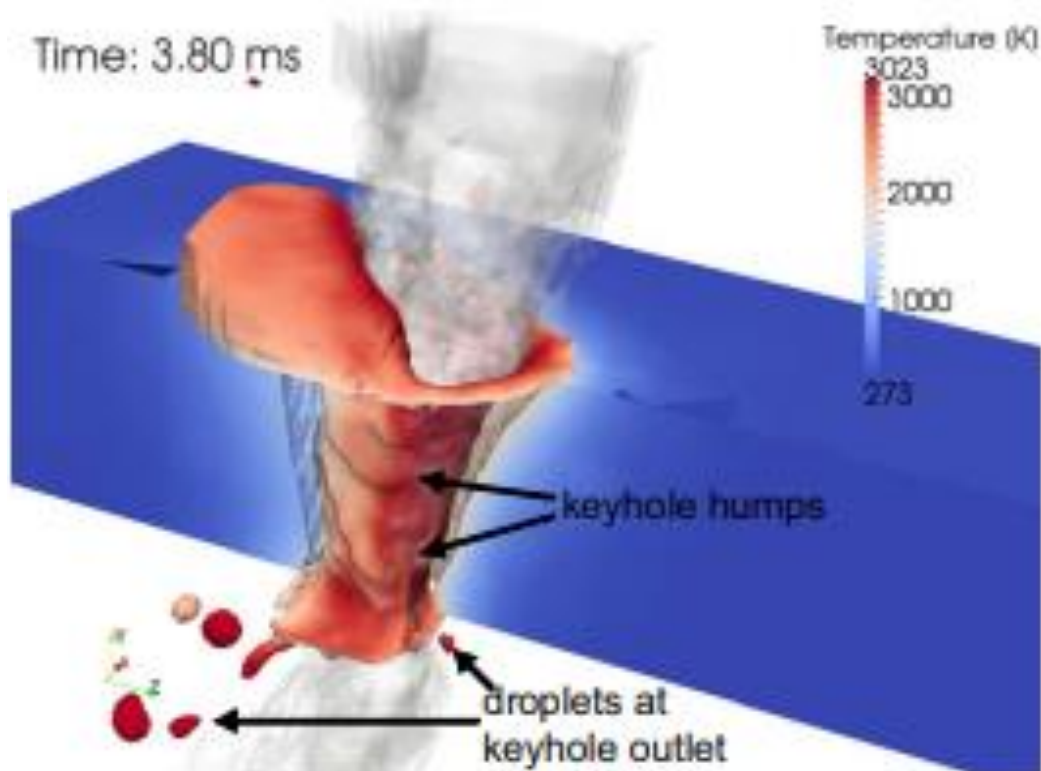


FIG 2.12 MATERIAL LOSS DURING LASER MELTING, DUE TO DROPLETS [22]

Specifically, Otto et al., from Vienna University of Technology have done great work simulating the mechanisms of Selective Laser Melting and similar processes. In the Figure 2.5, 2.6, 2.10 the keyhole formation is presented. In these papers the researchers coupled a thermal model with a fluid dynamics model to simulate thermofluidic phenomenon of the process. Also, a material loss model was introduced, by the researchers, as in SLM process some of the powder is lost during the process. This is also visible in Figure 2.11 where droplets at the keyhole outlet are present. This is a major mechanism of material loss during SLM process [20], [23].

Moreover, the researchers are trying to create, eagerly, a Multiphysics model for this process. The work that has been done in bibliography includes coupled models for porosity formation, thermal-fluid models, material loss models, solidifications and microstructure models for the SLM process. Furthermore, multi-scale simulations have been created in order to review mechanisms that appear in different scales such as in the micro-nano scale. For that reason, it was mandatory to create models that simulating phenomenon which occur in the femtosecond's timescale [22].

Last but not least, the idea of simulating models in a meshfree environment has emerged and it has found its way in the SLM process modeling. Such a method is extremely powerful in some cases. Nonetheless, as all the methods have their disadvantages so do the meshfree simulations. But as it is still not widely used, it can not be concluded if it is an effective method for simulating such a process or not [21].

Concluding, as said above the need for more complete models of the SLM process are mandatory in order to understand the mechanisms of it. Thus, researchers are constantly trying to develop and refine their theories and put them to the test via the simulation environments. However, these models need a lot of computing resources which are not available by everyone. Thus, in this work a simple, yet effective, thermal model was created to test the two software and show to the research community their options when concerning effective modeling of the SLM manufacturing technique.

2.2.4 BASIC FLUID DYNAMICS EQUATIONS FOR THERMAL-FLUID MODELING

Below it will be presented a basic FLUID DYNAMICS and HEAT TRANSFER Equations, that are used for making a more complete model for SLM process.

The Governing Equations are the equations that the main algorithm of FEM consists of. These can be split into three specific equations: Mass conservation, Momentum Conservation and Energy Conservation.

COMPUTATIONAL FLUID DYNAMICS (CFD)

This is an engineering field where fluid problems are solved numerically. These problems tend not to be solvable with analytical methods, thus a piecewise estimation of the solution is given.

The solution is given inside a domain called control volume (CV). Control Volume is a domain that encases the body of interest, including the surroundings. Here, the volume is stationary and the mass of fluid flows through that volume. Control mass is another approach in which the solution follows the matter.

FINITE VOLUME METHOD (FVM)

The control volume, mentioned above, is then spitted in discrete parts and are computed separately. This is called discretization and is needed for the Finite Volume Method (FVM). This method uses the conservation principles for mass. This can be seen in Equation (2.1), where m is mass, and the derivative of mass over time is equal to zero.

$$\frac{dm}{dt} = 0 \quad \text{Eq. (2.5)}$$

The Equation (2.1) has a second form, as it can be written as Newton's second law of motion, where v is the velocity of the matter and f the forces implied.

$$\frac{d(mv)}{dt} = \sum f \quad \text{Eq. (2.6)}$$

The above Equation 2.5 is written in the form of momentum and the derivative of the momentum over time is equal to the sum of forces f .

MASS CONSERVATION

The conservation of mass equation, also known as continuity equation, can be seen below.

$$\frac{\partial}{\partial t} \int_{\Omega} \rho d\Omega + \int_S \rho v \cdot n dS = 0 \quad \text{Eq. (2.7)}$$

Where ρ is the density, $[\text{kg/m}^3]$, v the velocity $[\text{m/s}]$, and n the surface normal vector. The CV is analyzed in two distinct parts, a volume integral over the enclosed volume Ω and a surface integral over the boundary surface S . The equations above, computes the entire mass of the CV.

Furthermore, the surface integral can be converted to a volume integral using Gauss' divergence theorem. Thus, the differential coordinate-free form of the Eq. (2.4) can be seen below.

$$\frac{\partial \rho}{\partial t} + \text{div}(\rho v) = 0 \quad \text{Eq. (2.8)}$$

The Eq. (2.4) can also be written as,

$$\frac{\partial \rho}{\partial t} + \frac{\partial(\rho u_x)}{\partial x} + \frac{\partial(\rho u_y)}{\partial y} + \frac{\partial(\rho u_z)}{\partial z} = 0 \quad \text{Eq. (2.9)}$$

In case of constant density, the Equation 2.5 becomes,

$$\frac{\partial u_j}{\partial x_j} = 0 \quad \text{Eq. (2.10)}$$

which is the matrix form of the Equation 2.5, and this form is commonly used by the solvers behind FEM software.

ENERGY CONSERVATION

Here it will be presented the temperature form of the energy conservation equation. In Equation 2.7 it is visible that e is the internal energy in $[m^2kg/s^2]$, q_k is the conductive heat flux leaving the control volume in the integral form of Equation 2.7, and τ_{ij} is the viscous stress.

$$\frac{\partial}{\partial t}(\rho e) + \frac{\partial}{\partial x_j}(\rho e u_j) = -p \frac{\partial u_k}{\partial x_k} + \tau_{ij} \frac{\partial u_i}{\partial x_j} - \frac{\partial q_k}{\partial x_k} \quad \text{Eq. (2.11)}$$

For incompressible flows, the second term of the right-hand side of the Equation 2.7 is equal to zero. In addition, the first term, that contains the divergence the velocity, of on the right-hand side of the Equation 2.7 is also equal to zero. This results from the continuity equation. So, the new simplified form of the Equation 2.7 is,

$$\frac{\partial}{\partial t}(\rho e) + \frac{\partial}{\partial x_j}(\rho e u_j) = - \frac{\partial q_k}{\partial x_k} \quad \text{Eq. (2.12)}$$

Using the term,

$$\rho [(\bar{e} + e')(\bar{u}_j + u'_j)] \quad \text{Eq. (2.13)}$$

Thus, it is possible to decompose the convection term. Also, e' denotes a residual quantity of internal energy. The Equation 2.8 can be averaged and the resolved or mean internal energy equation derives:

$$\frac{\partial}{\partial t}(\rho \bar{e}) + \frac{\partial}{\partial x_j}(\rho \bar{e} \bar{u}_j) = - \frac{\partial q_{t_k}}{\partial x_k} - \frac{\partial \bar{q}_k}{\partial x_k} \quad \text{Eq. (2.14)}$$

The q_{t_k} term, is the turbulent heat flux, which is,

$$q_{t_k} = \overline{\rho \bar{e} u'_k} + \overline{\rho e' u_k} + \overline{\rho e' u'_k} \quad \text{Eq. (2.15)}$$

The heat transfer conduction mode equation is listed below,

$$\bar{q}_k = -k \frac{\partial \bar{T}}{\partial x_k} \quad \text{Eq. (2.16)}$$

Using the above equation, an analogy for the turbulent heat flux equation can be made,

$$\bar{q}_{t_k} = -k_t \frac{\partial \bar{T}}{\partial x_k} \quad \text{Eq. (2.17)}$$

If the density ρ is set to constant $\rho = \rho_0$, viscosity to $\mu = \mu_0$ and $e = c_p T$, Equation 2.14 is formed,

$$\frac{\partial \bar{T}}{\partial t} + \frac{\partial}{\partial x_j} (\bar{T} \bar{u}_j) = \frac{\partial}{\partial x_k} \left[\left(\frac{\nu_t}{Pr_t} + \frac{\nu_0}{Pr} \right) \frac{\partial \bar{T}}{\partial x_k} \right] \quad \text{Eq. (2.18)}$$

where the Prandtl number is $Pr = \frac{c_p \mu_0}{k}$ and $Pr_t = \frac{c_p \mu_t}{k_t}$. Based on turbulent and laminar kinematic viscosities and the Prandtl values, the heat transfer coefficient can be formed,

$$k_{eff} = \frac{\nu_t}{Pr_t} + \frac{\nu_0}{Pr} \quad \text{Eq. (2.19)}$$

Using the above equation on Equation 2.14, the temperature equation is derived [24],

$$\frac{\partial \bar{T}}{\partial t} + \frac{\partial}{\partial x_j} (\bar{T} \bar{u}_j) - \frac{\partial}{\partial x_k} \left(K_{eff} \frac{\partial \bar{T}}{\partial x_k} \right) = 0 \quad \text{Eq. (2.20)}$$

VOLUME OF FLUID (VOF)

Well known and commonly used method for simulating the interaction between fluid and other phases, is the Volume of Fluid (VoF) method. Here phase fractions α_{phase} imply and an additional equation must be solved,

$$\frac{\partial \alpha_{phase}}{\partial t} + \frac{\partial (\alpha_{phase} u_j)}{\partial x_j} = 0 \quad \text{Eq. (2.21)}$$

The above equation is applied to distinguish the interphase between the two phases. In Equation 2.18 $\frac{\partial \alpha_{phase}}{\partial t}$ is the partial time derivative of the dimensionless phase fraction and $\frac{\partial (\alpha_{phase} u_j)}{\partial x_j}$ is the position derivative of the velocity vector.

PRANDTL NUMBER

The Prandtl number is the ratio of the momentum diffusivity ν to the thermal diffusivity and can be seen in the below equation,

$$Pr = \frac{\text{momentum diffusivity}}{\text{thermal diffusivity}} = \frac{c_p \cdot \mu}{k} = \frac{\nu}{a} \quad \text{Eq. (2.22)}$$

Where ν is the momentum diffusivity or kinematic viscosity in $\left[\frac{m^2}{s} \right]$, a is the thermal diffusivity in $\left[\frac{m^2}{s} \right]$, μ is the dynamic viscosity in $[Pa \cdot s]$, k is the thermal conductivity in $\left[\frac{W}{m \cdot K} \right]$, c_p is the specific heat in $\left[\frac{J}{kg \cdot K} \right]$.

2.2.5 ANSYS AM MODULE

Another, new, method of simulating the SLM process is the AM module of the Ansys Software. It has a high-level and a low-level analysis. That means, it can qualify parts for printing and/or collect data for management of the process. Low-level means that it can simulate the process single bead to extract useful information about material and porosity formation. It can also simulate process on a whole part to calculate residual stresses and shrinkage to compensate the error in the geometry file (STL). Finally, it can analyze the geometry of the file and it can predict failure during printing [25].



FIG. 2.9 ANSYS AM MODULE CAPABILITIES

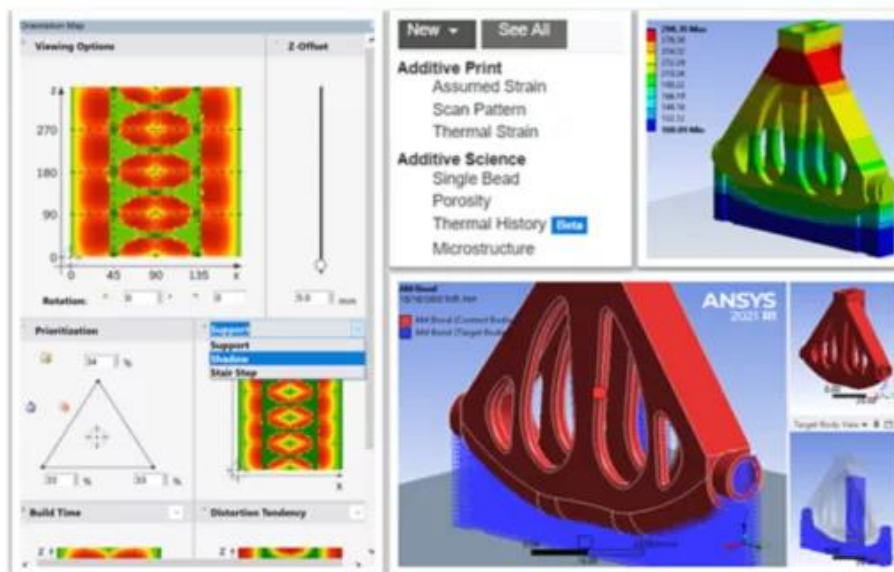


FIG. 2.10 GRAPHIC USER INTERFACE OF ANSYS AM MODULE

3. MODEL ASSUMPTION AND MATERIAL PROPERTIES

3.1 MODEL ASSUMPTION WHEN SIMULATING THE SLM PROCESS

Many factors are involved in this AM process, so limitations and compromises had to be introduced as assumptions in this project to create a functioning model. Therefore, the assumptions are shown below.

- There is no solidification modeling in this project.
- Fluid dynamics of melt pool were not modeled in this work.
- No pores model. The porosity was not implemented in this model as this would mean a full reprogramming of some solvers to object pressure differences in the melt pool and create pores.
- Material loss model was not included in this work.
- A 2D Gaussian distribution was implemented for the laser beam.
- In conduction mode there is no keyhole formation thus, the reflection mechanism is of minor importance. Thus, there was no laser secondary reflection modeling in the laser beam.
- Forces that are created by plasma interaction with the melt pool are not implemented in this model, nor plasma shielding.
- The heat flux from the laser beam was modeled as Gaussian-distributed heat flux and was given directly on the top of the bulk material.
- The simulation did not consider latent heat loss at the phase transition.
- The laser spot was assumed to have a circular shape.
- The convective heat transfer coefficient between the bulk material and the environment was assumed to be constant and independent of temperature.

3.2 MATERIAL PROPERTIES

The material used is pure Aluminum. The COMSOL library has the thermophysical values change in respect of the temperature changes. But for simplicity manner, constant values will be used.

Aluminum properties	Value	Unit
Density ρ	2702	kg/m ³
Heat Transfer Coefficient for heating h	150	W/m ² /K
Thermal Conductivity k	10	W/mK
Material thermal diffusivity DT	8e-05	m ² /s

TABLE 3.1 MATERIAL PROPERTIES OF ALUMINUM

4. MODEL DEVELOPEMENT USING OPENFOAM

OBJECTIVES

In this chapter a brief introduction to modeling with OpenFOAM will be presented. After reading the chapter, reader, will be familiarized with OpenFOAM modelling workflow.

4.1 MODEL

For simple Heat Transfer the LaplacianFoam solver was used. In addition, the problem of introducing laser on OpenFOAM was solved by importing it as a convection boundary condition (BC) with accompanying Gaussian distributed laser beam. It was compiled as a free-standing library into the OpenFOAM pre-existing library and then implemented in a standard solver [26].

4.1.1 LAPLACIAN SOLVER

LaplacianFoam solver: This is a basic solver for heat transfer. It can simulate both steady state and transient problems. The solver evolves a scalar, T , using the equation:

$$\frac{\partial}{\partial t}(T) - \nabla \cdot (D_T \nabla T) = S_T \quad \text{Eq. (4.1)}$$

which is like the governing Equation 2.1 that was described in Chapter 2. The D_T term is the thermal diffusivity coefficient like the k term used in Equation 2.3 [27].

Finite volume schemes: In this file all numerical schemes are specified. The subcategories of the schemes are,

- Time scheme: The first- and second-time derivatives, $\frac{\partial}{\partial t}$ and $\frac{\partial^2}{\partial t^2}$.
- Grad schemes: The gradient, ∇ .
- Laplacian schemes: The Laplacian, ∇^2 .

It is worth noting that, using first order schemes, the solution will be less accurate, but it will need less processing time than the second order solutions.

4.1.2 LASER BC

The laser beam is modeled as a Gaussian distributed heat source and the Equation that describes it is,

$$f_{Gauss}(x, y) = \frac{1}{2\pi\sigma_x\sigma_y\sqrt{1-\rho_{shape}^2}} \exp\left[-\frac{1}{2(1-\rho_{shape}^2)}\left(\frac{x^2}{\sigma_x^2} + \frac{y^2}{\sigma_y^2} - \frac{2\rho_{shape}xy}{\sigma_x\sigma_y}\right)\right] \quad \text{Eq. (4.2)}$$

Where σ [m] is representing the standard deviation of the Gaussian distribution laser beam, the x, y [m] are representing the two orientations of the laser beam plane and ρ_{shape} [-] the correlation factor.

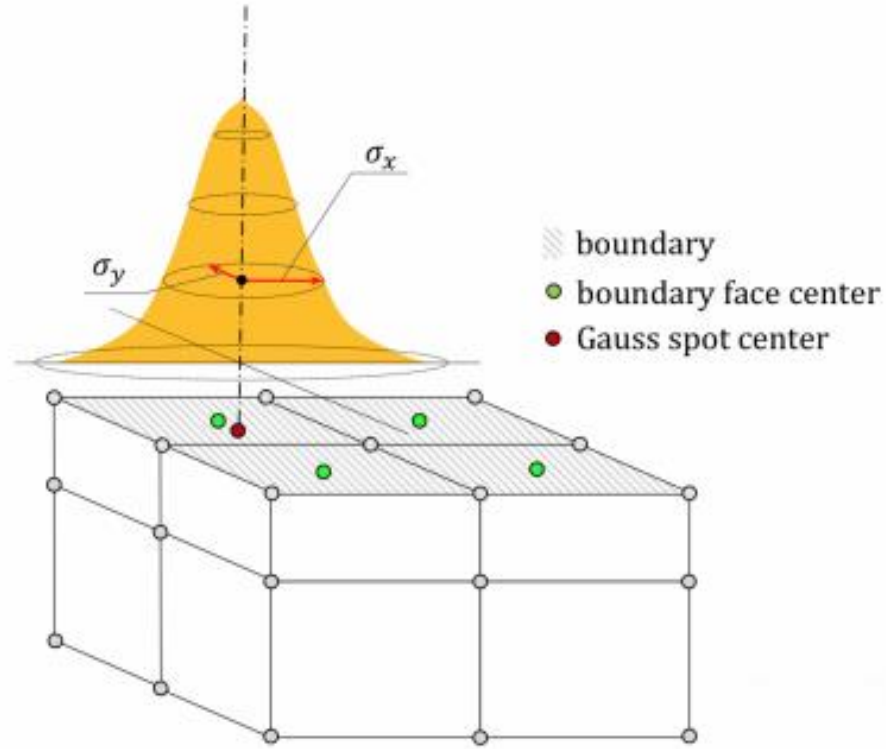


FIG 2.1 GAUSSIAN DISTRIBUTION HEAT BEAM [26]

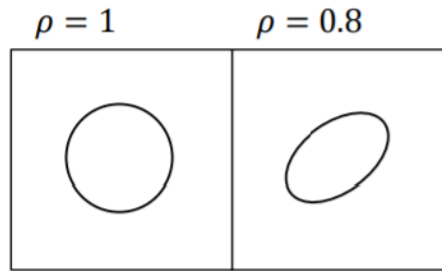


FIG. 2.2 CORRELATION FACTOR ρ

The above figure shows the heat beam striking the meshed volume. The red dot shows where the center of the beam strikes down on the surface and the green dots represent the center points of the boundary face mesh. The boundaries are indicated by grey shading on the top faces.

The x and y -coordinates used in code are differences between the position of the spot center of the Gaussian beam, $x_{\text{spotCentre}}$, and the center point of the boundary face center, x_{Face} , as seen in Equation 2.5,

$$x = x_{\text{spotCentre}} - x_{\text{Face}} \quad \text{Eq. (4.3)}$$

Similarly for y coordinate the Equations is,

$$y = y_{\text{spotCentre}} - y_{\text{Face}} \quad \text{Eq. (4.4)}$$

4.1.3 CONVECTIVE BC

A convective boundary condition was implemented to mimic the cooling on the surface and in this case the conduction boundary conditions were swapped for convective boundary conditions.

To be able to calculate a convective boundary condition, the difference between the surface temperature and the surrounding, ambient, temperature had to be evaluated and used. A flux was then established in the direction of the lower temperature. The temperature, T , is evaluated in $[K]$, the distance between the cell center and the center point of the cell face, δ , is measured in $[m]$. The thermal conductivity, k , is measured in $\left[\frac{W}{mK}\right]$, the heat transfer coefficient h is implemented in $\left[\frac{W}{m^2K}\right]$ and the heat flux \dot{q} , has the unit $\left[\frac{W}{m^2}\right]$.

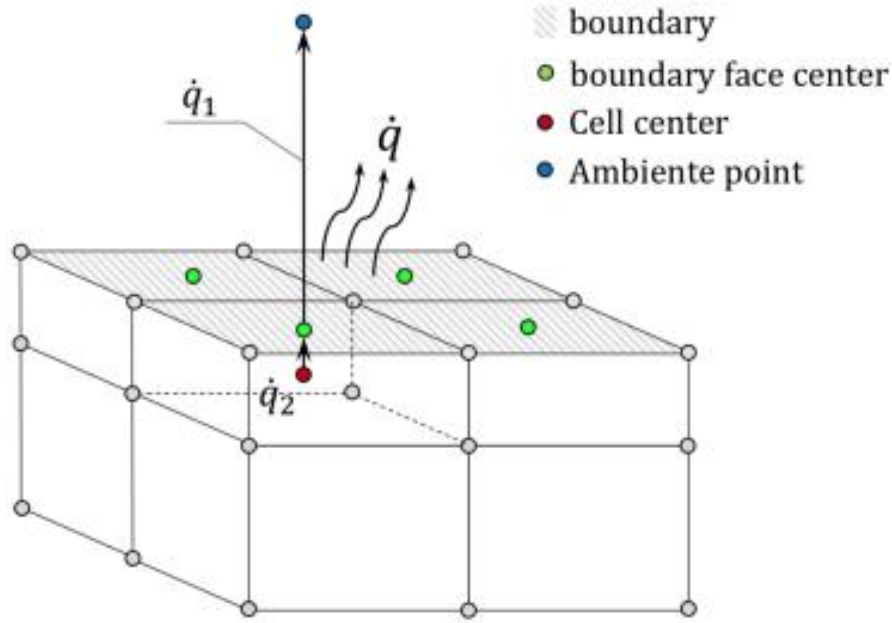


FIG. 2.3 CONVERSION OF A CONVECTIVE BOUNDARY CONDITION INTO A DISCRETE MESH

Below the Equation 4.5 shows that the heat on the material, measured on the right side of the equation must be equal to what is measured on the other side of the boundary interface, in this case outside the metal.

$$h \cdot (T_{Face} - T_{Amb}) = k \cdot \frac{T_{Cell} - T_{Face}}{\delta} \quad \text{Eq. (4.5)}$$

In addition, applying energy conservation on either side of the boundary, the heat fluxes should be equal.

$$\dot{q}_1 = \dot{q}_2 \quad \text{Eq. (4.6)}$$

where, the dot over the q term means the surface normal vector. Thus, the heat flow on the outside of the boundary is,

$$-\dot{q}_1 = h \cdot (T_{Face} - T_{Amb}) \quad \text{Eq. (4.7)}$$

Last but not least, the heat flow in the material is formed by the Equation 4.8 below,

$$-q_2 = k \cdot \frac{\partial T}{\partial n} = k \cdot \frac{T_{Cell} - T_{Face}}{\delta} \quad \text{Eq. (4.8)}$$

4.1.4 MATHEMATICAL TREATMENT OF THE BOUNDARY FACES IN OPENFOAM

The mathematical treatment of the boundary faces is seen below where $\delta^* = \frac{1}{\delta}$,

$$T_{Face} = f \cdot valueExpression + (1-f) \cdot (T_{cell} + gradExpr \cdot \delta^*) \quad \text{Eq. (4.9)}$$

The above is a general expression where f and $(1-f)$, need to be evaluated. $valueExpression$ and $gradExpr$ are numerical values, in this case T_{Amb} and T_{cell} respectively.

If the function f is defined as the convective boundary condition, that is described in Equation 2.7, the Equation 2.11 gives the solution,

$$T_{Face} = \frac{h}{k \cdot \left(\frac{h}{k} + \frac{1}{\delta} \right)} \cdot T_{Amb} + \frac{1}{\delta \cdot \left(\frac{h}{k} + \frac{1}{\delta} \right)} \cdot T_{Cell} \quad \text{Eq. (4.10)}$$

Subsequently, the values of f and $(1-f)$ are equal to,

$$f = \frac{h}{k \cdot \left(\frac{h}{k} + \frac{1}{\delta} \right)} \quad \text{Eq. (4.11)}$$

$$(1-f) = \frac{1}{\delta \cdot \left(\frac{h}{k} + \frac{1}{\delta} \right)} \quad \text{Eq. (4.12)}$$

4.1.4 MATHEMATICAL TREATMENT OF THE LASER IN OPENFOAM

The heat transfer produced by the laser source is calculated by the Equation 2.15,

$$Q = h \cdot A \cdot \Delta T \quad \text{Eq. (4.13)}$$

The heat from the middle of the cells was translated to the cell faces by conduction in the material, as seen below,

$$Q = \frac{k}{\delta} \cdot A \cdot (T_{Cell} - T_{Face}) \quad \text{Eq. (4.14)}$$

If $\delta^* = \frac{1}{\delta}$ then the Equation 2.16 can be written,

$$(T_{Cell} - T_{Face}) \cdot \delta^* = \frac{Q \cdot f_{Gauss}}{k} \quad \text{Eq. (4.15)}$$

4.1.5 MATHEMATICAL TREATMENT OF THE FINAL BOUNDARY CONDITION

The implementation of the Equation 2.17 in the C++ code can be done using the form below,

$$T_{Face} = f \cdot T_{Amb} + (1-f) \cdot \left(T_{Cell} + \frac{Q \cdot f_{Gauss}}{k} \right) \quad \text{Eq. (4.16)}$$

As seen above, Equation 2.17 is the $gradExpr$ term in Equation 2.18.

THERMAL DIFFUSIVITY

The ratio of the thermal conductivity to the volumetric heat capacity is called thermal diffusivity and it is described by the equation below,

$$DT = \frac{k}{\rho c_p} \quad \text{Eq. (2.21)}$$

where, k is thermal conductivity in $\left[\frac{W}{m \cdot K} \right]$, c_p is the specific heat capacity in $\left[\frac{J}{kg \cdot K} \right]$, ρ is the density in $\left[\frac{kg}{m^3} \right]$ and $\rho \cdot c_p$ is the volumetric heat capacity in $\left[\frac{J}{m^3 K} \right]$

4.2 OPENFOAM INTERFACE

Open-source Field Operation and Manipulation is a complex C++ FEM library able to solve most of the CFD related problems, but also structural problems, too. It is released and developed primarily by OpenCFD Ltd since 2004. There is no Graphical User Interface (GUI), and therefore it can be run from terminal. Below, the OpenFOAM structure is visible,

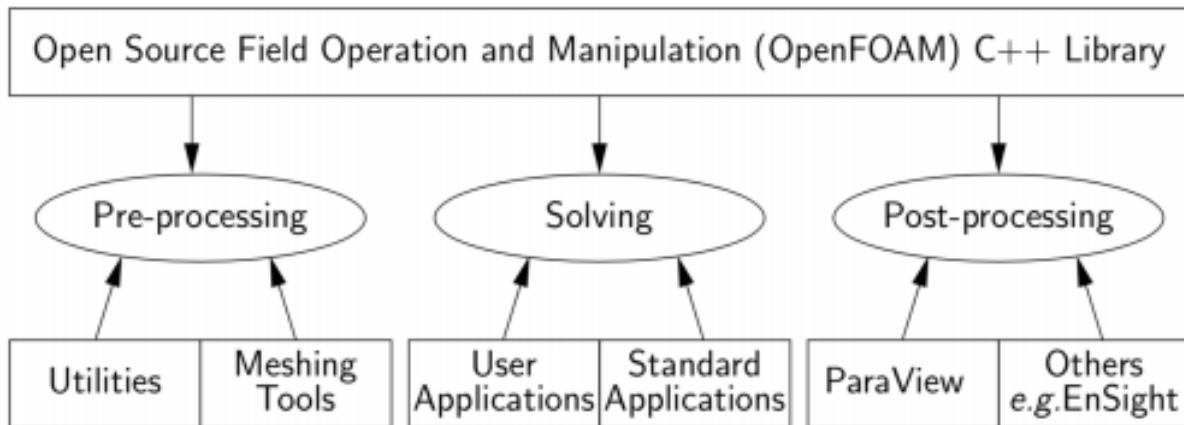


FIG. 4.1 OPENFOAM STRUCTURE [28]

As viewed in the Figure 4.1, pre-processing can be performed on CAD programs or by writing scripts to create a mesh directly in OpenFOAM. Post-processing is mostly done in ParaView, for a graphic interpretation of the output files from OpenFOAM [28]

An overview of the directory structure is shown in Figure 4.2. The <case> is the main folder and it should be renamed as the user wish. There are three major subfolders, system, constant and time directories subfolders.

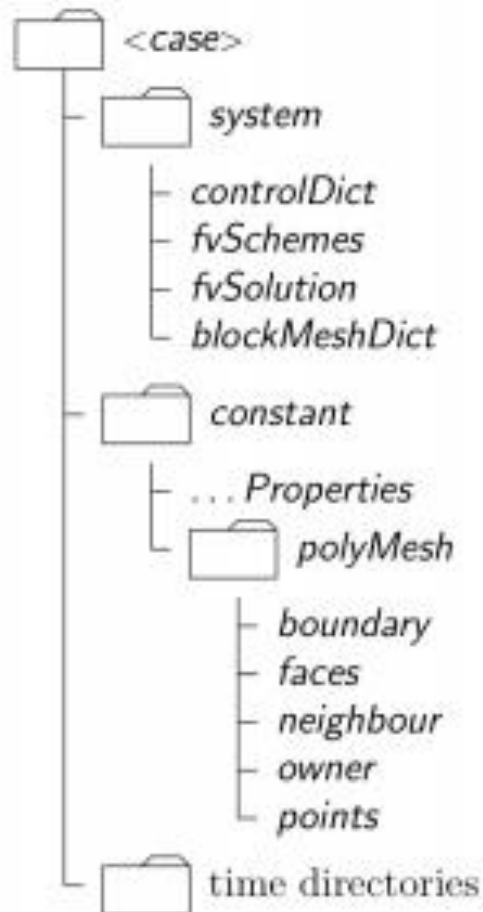


FIG. 4.2 <CASE> DIRECTORY STRUCTURE[28]

4.1.1 SYSTEM DIRECTORY

The System Directory contains many different files such as blockMesh, if the mesh is being created in OpenFOAM, setFields the model contains separate conditions in subdomains of the geometry. Though, there are three files that are mandatory to be present for the case to be able to run. These are,

ControlDict: Holds all the parameters for the program, like the solver, the start and stop time, the time step, the output format, and the number of output files.

fvSchemes: Contains the numerical schemes of the model.

fvSolution: Contains the solution and algorithm controls.

In case of parallelization the system dictionary contains the decompose parallel dictionary, which is used for subdividing the geometry for parallel processing of the simulation[28].

4.1.2 CONSTANT DIRECTORY

In this directory the properties files and polyMesh files are included.

Properties files are files that contain turbulence, phase, and thermo-physical properties of the fluid.

polyMesh folder contains all information about the mesh.

4.1.3 TIME DIRECTORIES

The time directory contains the solution at the discrete time steps. The initial and boundary conditions are included on the zero folder. It is possible to run a simulation from a later time step. In this case, the selected time step becomes the initial one [28].

4.2 MESH IN OPENFOAM

In OpenFOAM, the mesh is structured by cells, thus the desired geometry is built up. To describe it, five files are needed: boundary, faces, points, neighbor, and owner. The sides are included in the polyMesh folder under the constant directory. All cells must be of hexahedral type; thus, they are composed of eight corners (vertexes) and six surfaces (faces).

Note: There is the ability to convert a hexahedral into a tetrahedral but this is applicable only for cylinders [28].

4.2.1 POINTS

In order to define 3-dimensional locations in space, points are used. This location can be pinpointed by a vector in units of meters. The point file is consisting of a list and each point refer to a label. The position in the list corresponds to the label given, starting from zero. The above list, though, cannot contain points that share identical positions or points that are not part of any surface [28].

4.2.2 FACES

An ordered list of points, that are referred to by their label, consist of a surface. Two neighboring points are connected to each other by an edge; thus, they create the circumference of the face. Faces, like points, are consisted of a list that represents the corresponding label given to the face.

The direction of the normal vector is defined by the right-hand rule, when looking towards a face. If the numbering of the points follows an anti-clockwise path, the normal vector points towards you.

Internal Faces: These are the faces that connect two cells together. Therefore, these can be no more than two.

Boundary faces: When one or more sides coincide with the boundary of the domain, boundary faces are used. Therefore, a boundary face is addressed only by a one cell and a boundary patch[28].

4.2.3 CELLS

The Cells file consists of an ordered list of faces. All cells must be contiguous, convex, and closed.

Contiguous: Contiguous means that the cells may not overlap one another and that they must completely cover the computational domain.

Convex: Cells must keep their center inside the cell.

Closed: All cells must be both geometrically and topologically closed.

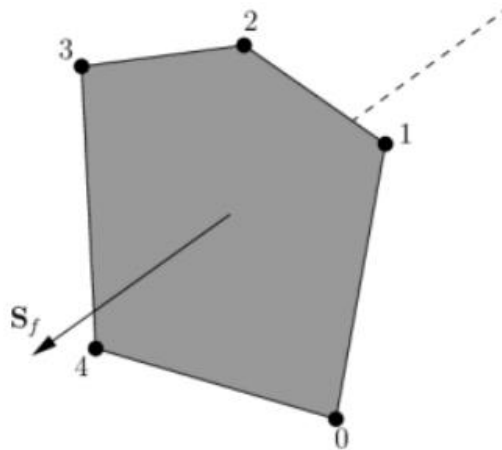


FIG. 4.3 FACE IN OPENFOAM [28]

On figure 4.3 a face is presented. The cornering numbers are the points, and the surface is the face. Following the right-hand rule, the surface normal points in the direction of S_f in the figure.

Below, hexahedral cells are visible. The left figure numbers the corner vertexes, the middle figure depicts the face areas of the cell and the right most figure, the boundary edges of the cell[28].

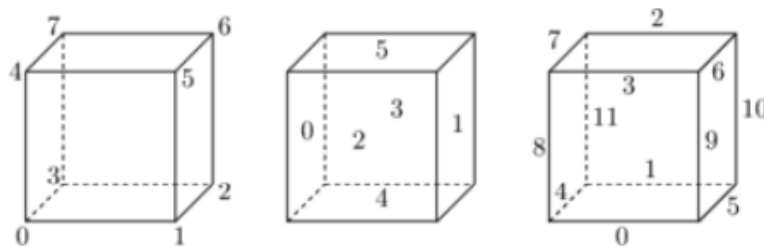


FIG. 4.4 HEXAHEDRAL CELL IN OPENFOAM

4.2.4 PATCHES

Specific face labels around the mesh edges are included in the patch's lists. Thus, these lists only contain boundary faces. Naming the patches, is the user's work to do. Commonly used names are inlet, outlet, top, bottom, depending upon what is to be simulated[28].

4.2.5 BOUNDARY

Patches that are being associated with specific boundary conditions are called boundaries. The boundary edge must be closed. That means, the sum of the boundary face area vectors is zero[28].

4.2.6 DIMENSIONS IN OPENFOAM

In OpenFOAM Parameter dimensions mean physical dimensions with respect to the SI unit system, shown below,

$$SI [kg\ m\ s\ K\ mol\ A\ cd]$$

If the unit is present, a number is given to that position in the bracket. Furthermore, whether the unit is present in the numerator or the de-numerator of the dimension, the number is positive or negative, respectively.

For example, the velocity is calculated in $\left[\frac{m}{s} \right]$ so the dimensions vector will be,
dimensions $[0\ 1\ -1\ 0\ 0\ 0\ 0]$

4.3 MESH GEOMETRY

A 3-Dimensional mesh is created for this work. The mesh is a rectangular box. The mesh was created in OpenFOAM. The dimensions are,

Dimensions of Box [mm]	X	Y	Z
	10	10	10

TABLE 4.1 GEOMETRY DIMENSIONS

The mesh stats are,

Mesh stats

```
points:          28611
faces:           78500
internal faces:  71500
cells:           25000
faces per cell:   6
boundary patches: 3
point zones:      0
face zones:       0
cell zones:       0
```

Which means, the mesh is constructed of 25000 hexahedral cells in total.

A top view of the mesh geometry is shown here,

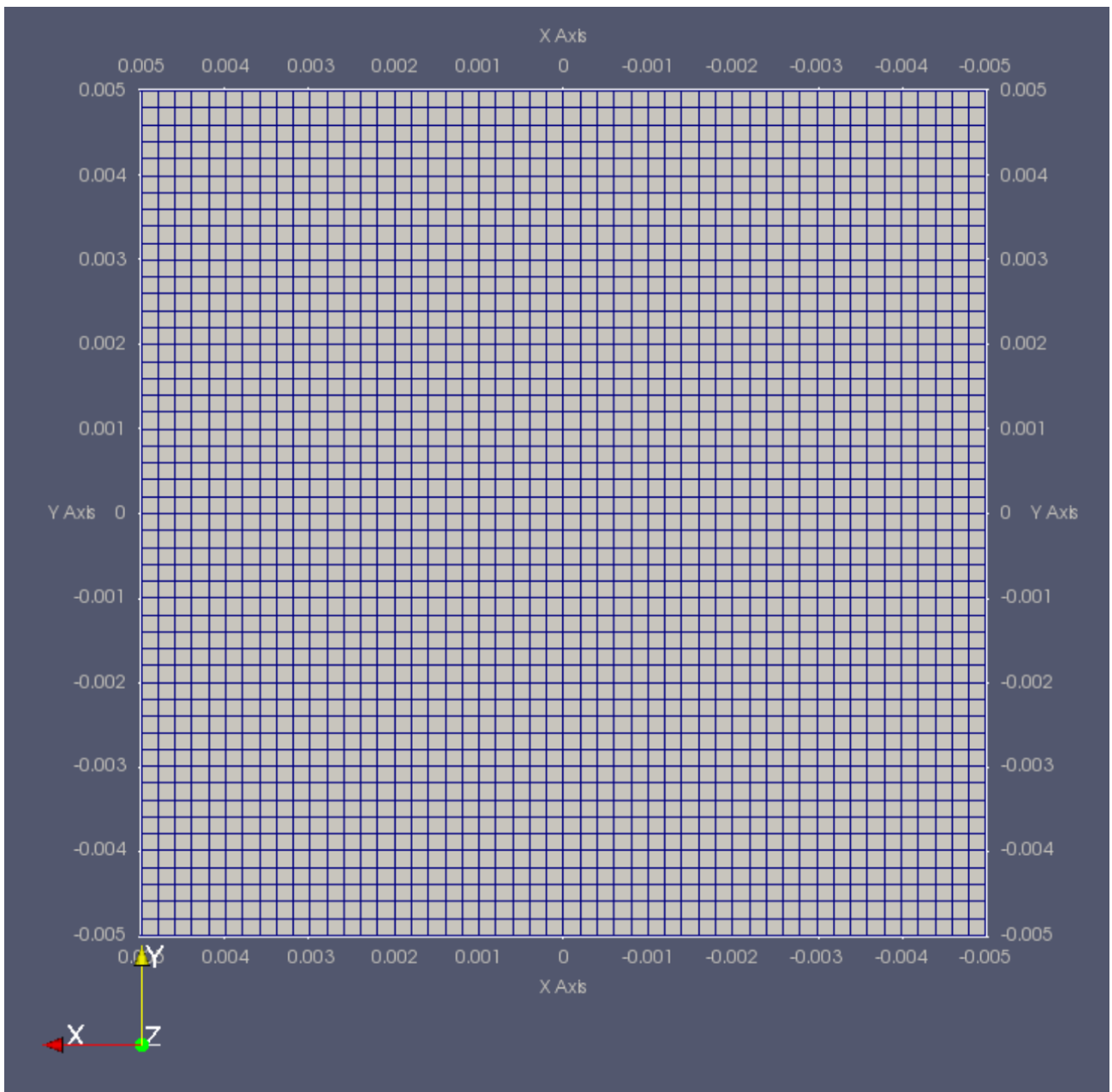


FIG. 4.5 TOP VIEW OF MESH

4.4 SYSTEM, CONSTANT AND ZERO DIRECTORIES DURING SIMULATION

4.4.1 SYSTEM FOLDER

Systems directory consists of control dictionary, finite volume schemes, finite volume solutions, the block mesh and the decompose parallel dictionary.

Control Dictionary: The solver is specified here. In this case laplacianFoam solver. The time was set 0.2 [s] and the time step to 0.01 [s].

Constant directory: The *polymesh* folder is contained in the constant directory. This folder has the mesh specifications. It is possible to import a mesh file (.msh) in OpenFOAM, by using commands like *fluentMeshToFoam* in order to convert the mesh file to a OpenFOAM mesh. Last but not least, in case the gravity is needed, it can be defined in the constant file.

Zero directory: In this directory all the boundary and initial conditions are specified.

Velocity file: Here an initial velocity of zero is given.

Temperature file: The temperature boundary and initial conditions are found in the zero directory. The initial temperature was set to a uniform value of 293 Kelvin. If there are non-uniform list of scalar temperatures the following script on the upper patch is applied.

PatchName

```
{  
    type fixedValue;  
    value nonuniform List<scalar>  
    (  
        temperature list of values  
    );  
}
```

In this case, which the laser beam is introduced, a convective boundary condition was applied to all surfaces, where the edges and bottom patches were given a heat transfer coefficient of $h = 50 \left[\frac{J}{msK} \right]$.

The laser beam specifications are included in the boundary condition. The laser beam theoretical absorbed power is 350 [W]. The beam σ_x , σ_y are equal to 0.0015 [m]. And the moving speed of the laser in the one axis is 0.05 [m/s].

The thermal conductivity is specified in this area too, $k = 25 \left[\frac{W}{mK} \right]$.

4.4.2 COMPILING THE laserConvectionBC

The modeling of the laser beam is given by a discrete library, that was downloaded and compiled to be added to the solver used. The files were compiled using the *wmake* command in the terminal. Using the library as shown in APPENDIX A, by adding the following line in the end of the file *ControlDict*

libs ("liblaserConvectionBC.so");

This enables the library to be used for this specific case, thus making possible for the boundary condition to be written into the temperature file.

4.4.3 THE HEAT TRANSFER COEFFICIENT AND MATERIALS CONDUCTIVITY

The heat transfer coefficient, h , is measured in SI units $\left[\frac{W}{m^2 K} \right]$. Heat is transferred to the surrounding material, otherwise the buildup of heat energy escalates. This is approximated by a convective boundary condition. The Equation used is visible below,

$$\frac{q}{A} = h \Delta T \quad \text{Eq. 4.17}$$

Material conductivity is,

$$k = 25 \left[\frac{W}{mK} \right] \quad \text{Eq. 4.18}$$

And it is used in the Equation 2.3.

4.4.4 PARALLELIZATION

In OpenFOAM is possible to run simulations in parallel. In order to do that the *decomposeParDict* must be implemented. This is done by decomposing simulation in subdomains, usually equal to the number of the available cores of the computer. So, an example of such implementation is,

```
mpirun -np 6 laplacianFoam -parallel
```

Which decompose the case in 6 distinct parts, for the CPU to process it. After that, it is mandatory that the case is reconstructed for the post-process in ParaView.

4.4.5 ParaView

In order to post process, the simulation in OpenFOAM, an extra software is needed. ParaView is used as a viewer software to visualize the results of the simulations.

The code of *ControlDict* code is quoted in Appendix A

5. MODEL DEVELOPMENT USING COMSOL

OBJECTIVES

In this chapter an introduction to modeling with COMSOL will be conferred. In the end of the chapter, reader, will be familiarized with COMSOL modelling workflow.

5.1 COMSOL

COMSOL is a commercially available FEM software with a Graphical User Interface (GUI). It is an all-in-one software as it provides Model builder to create 2-3D models and post-processing built-in software for viewing and editing results.

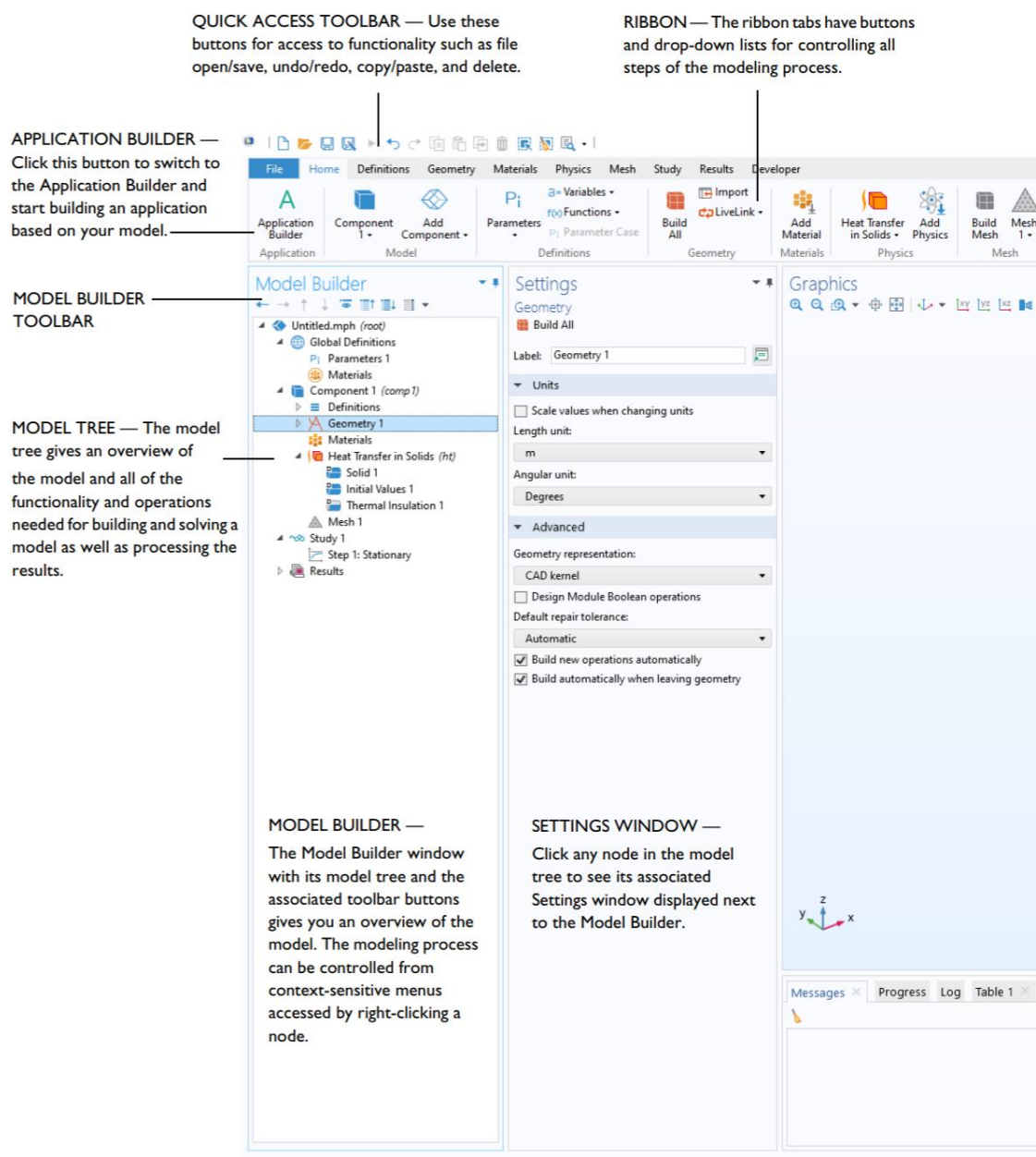


FIG. 5.1 COMSOL MULTIPHYSICS GRAPHICAL USER INTERFACE [29]

In the Figure 5.1, it can be seen all the basic information for the COMSOL's user interface. The interface consists of seven distinct parts.

Ribbon tabs: The buttons and drop-down lists control all the steps of the modelling process.

Quick Access toolbar: Here the use of buttons, for access to functionality such as file open/save, undo/redo, copy/paste, and delete, is available.

Application builder: Clicking this button will switch to the Application Builder and start building an application based on the current model.

Model Builder Toolbar

Model Tree: The model tree gives an overview of the model and all the functionality and operations needed for building and solving a model as well as processing the results.

Model Builder: The Model Builder window with its model tree and the associated toolbar buttons gives an overview of the model. The modeling process can be controlled from context-sensitive menus accessed by right-clicking a node.

Setting Window: Click any node in the model tree to see its associated Settings window displayed next to the Model Builder.

5.1.1 FILES:

In COMSOL, a single file is created for each case with file extension “.mph”. This file contains all the information about model, meshing, physics, study and results. Its size is depending on the mesh size and the computed solution.

5.2 WORKFLOW

The workflow is very intuitive thanks to the graphical environment of COMSOL. The Ribbon Tabs shows the basic steps to complete a simulation.

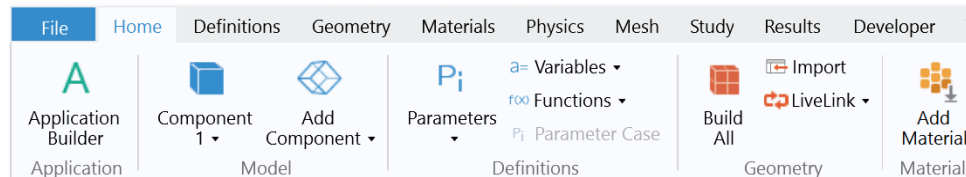


FIG 5.2 COMSOL RIBBON TAB

The first step is to start from the Definitions Tab where all the parameters of the study are defined. After that, the geometry is imported or created inside the COMSOL. In addition, the material is specified in the Material Tab. In the Physics Tab, the kind of simulation is determined. It is possible to choose from a variety of physics and Multiphysics in COMSOL. After choosing the desired Physics, the Mesh is created, where it is possible to change the Mesh size and shape depending on the needs of simulation. Finally, in the Study Tab should be selected the type of study (Time dependent etc.). After the Study is over, the visualization and post-processing of the results can be done in the Results Tab.

5.2.1 GEOMETRY AND MESHING

In the Geometry Tab it is possible to import a geometry file or create a 2-3D geometry in the integrated CAD-like Model Builder. The integrated model builder offers a variety of shapes like blocks, cylindrical shapes, and features known from CAD Software like Extrude, Revolve, Sweep commands.

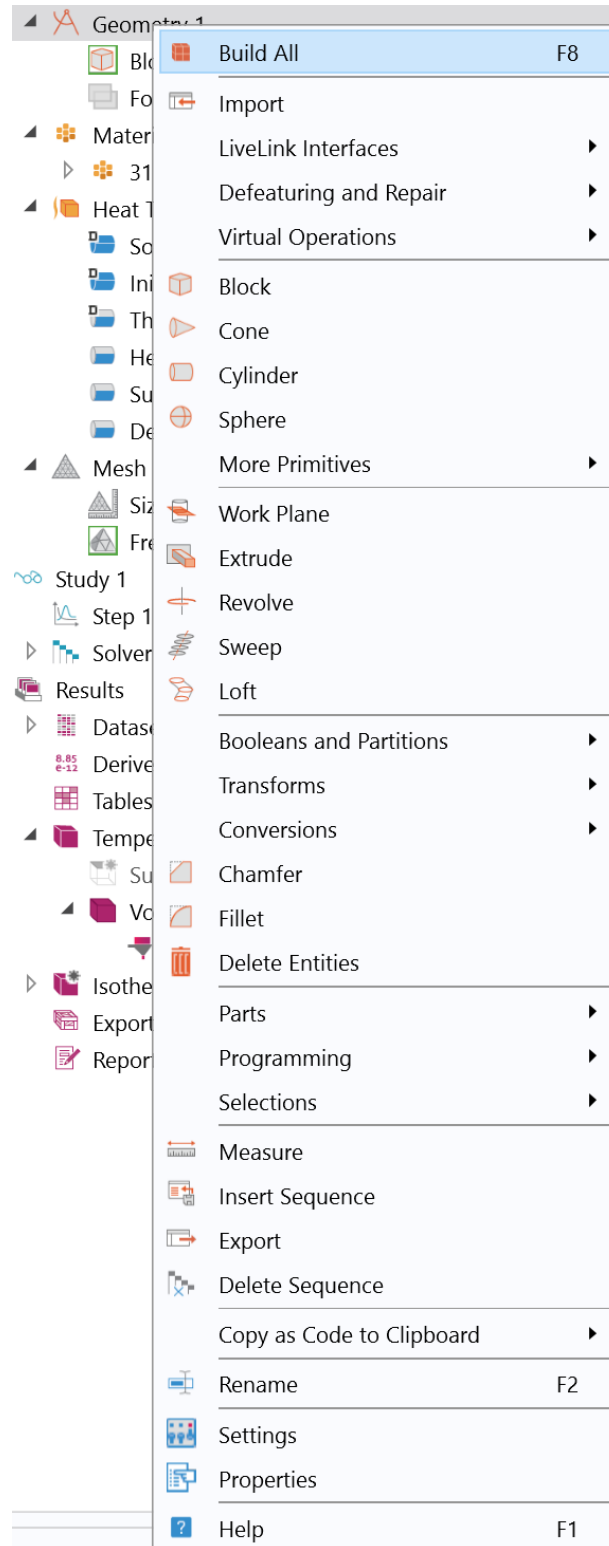


FIG. 5.3 COMSOL GEOMETRY TAB OVERVIEW

After a geometry has been imported or created in the software, the meshing should be created. The mesh tab has all the features needed in order to create the suitable mesh for each case.

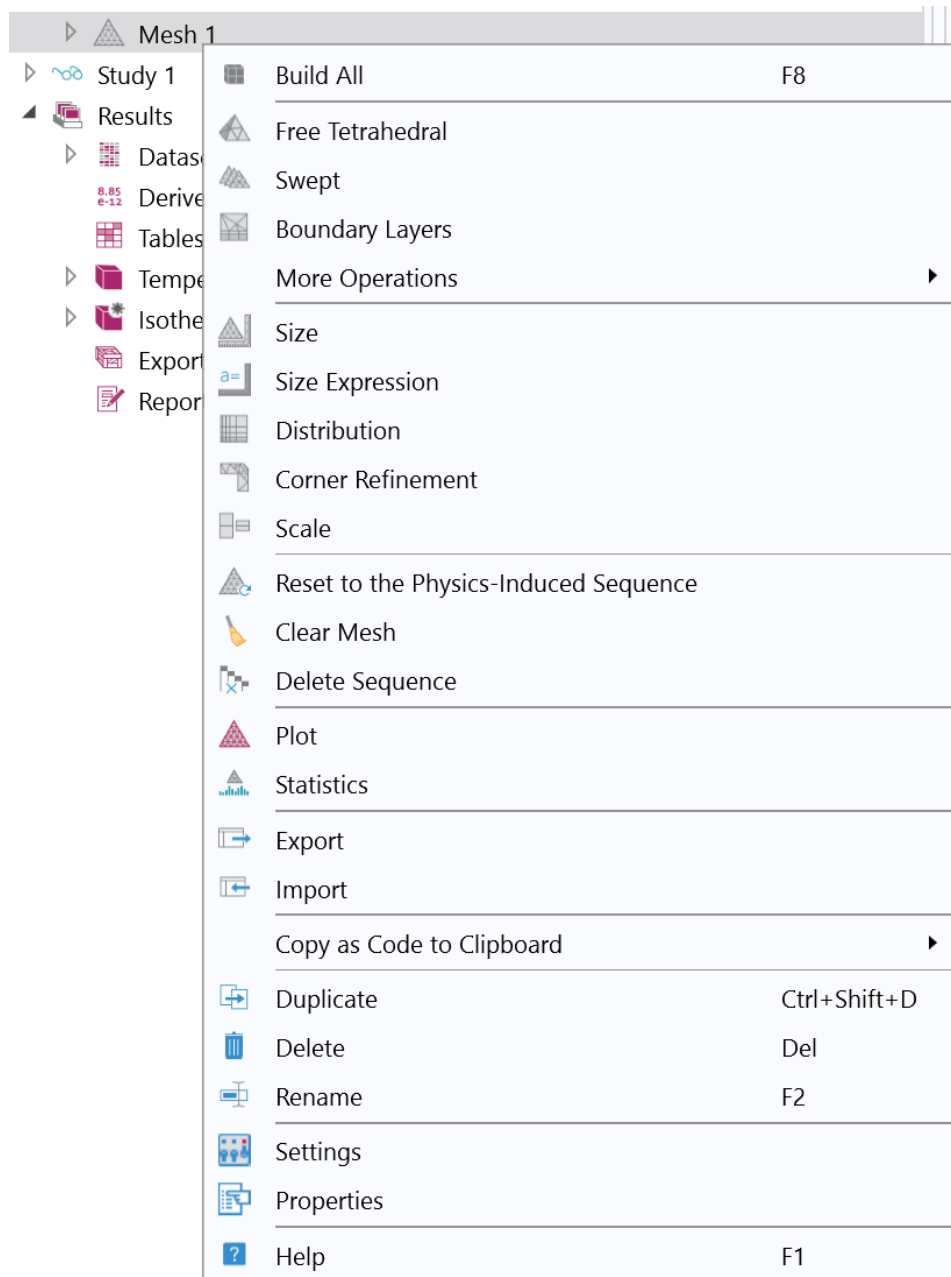


FIG. 5.4 COMSOL MESH TAB OVERVIEW

In this case, a hexahedral mesh is needed as this type of mesh was used in OpenFOAM case, too. Unfortunately, COMSOL does not possess a direct way of using Hexahedral mesh. Instead, an indirect way of creating this type of mesh is shown below,

Using the Mesh Tab, navigating to Boundary drop list, selection of a Free Quad button is visible. Free Quad is a way to generate unstructured quadrilateral mesh. In the Settings Tab of the Free Quad command, the *Geometric entity_level* is set to Boundary and the user should, now, select a face of the geometry that this mesh will apply to, in this case the upper face.

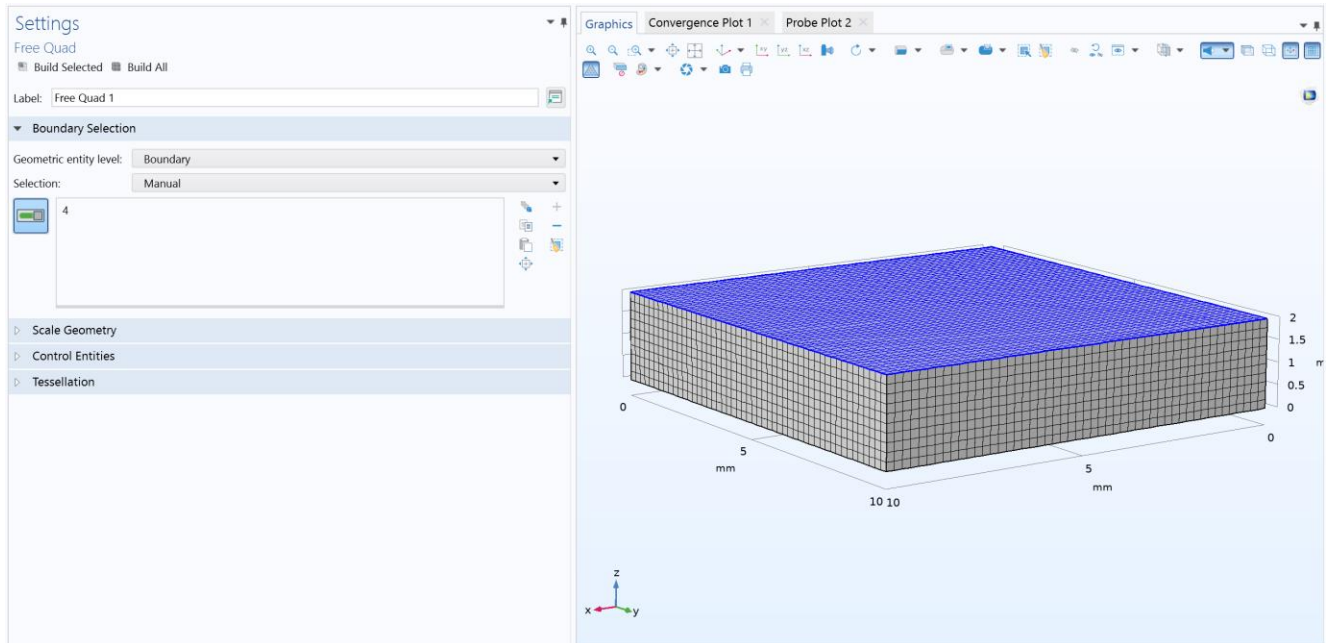


FIG. 5.5 FREE QUAD SETTINGS TAB

After the above steps are over, the user should choose the swept command to extend these elements to the other side of the geometry, in this case the downside. The result of the mesh is shown in the Figure 5.5. The mesh generated consists of 25000 hexahedral cells in total.

5.2.2 MATERIALS

In the Materials Tab the user can select from a variety of materials from the COMSOL's built-in library. Also, the user can import material library or can create a material with custom properties like unisotropy.

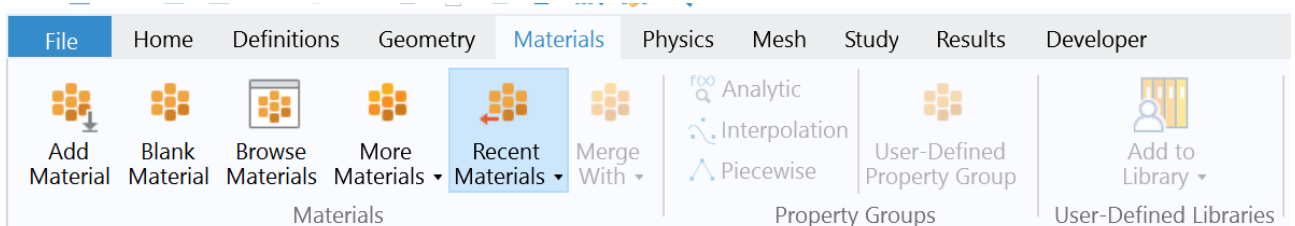


FIG. 5.6 MATERIAL TAB OVERVIEW

5.2.3 PHYSICS

To choose the physics of the simulation, the user should navigate to the Physics tab and select the desired module for the case developed. There are available single-physics modules and multi-physics modules on COMSOL. In this specific case the module below was used,

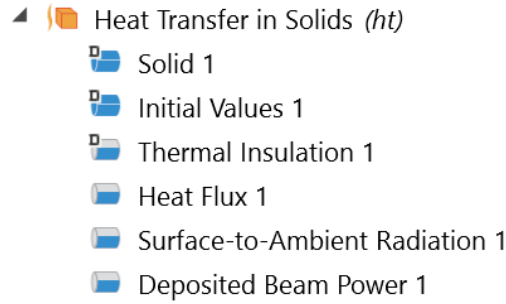


FIG. 5.7 HEAT TRANSFER IN SOLIDS

As seen on Figure 5.7, the *Heat Transfer in Solids* Physics was used. Using this type of physics, it is possible to simulate heat Conduction, heat Convection on boundaries and laser beam.

Governing Equation:

$$\rho C_p \frac{\partial T}{\partial t} + \rho C_p \mathbf{u} \cdot \nabla T + \nabla \cdot \mathbf{q} = Q + Q_{\text{ted}}$$

$$\mathbf{q} = -k \nabla T$$

Eq. 5.1

The Equation 5.1 is the COMSOL's form of Equation 2.1.

Laser Beam:

In COMSOL the laser beam is easily simulated by using the *Deposited Beam Power* option that is included in the *Heat Transfer in Solid* Physics. The parameters of the beam are specified in the Settings Tab as shown below,

FIG. 5.8 DEPOSITED BEAM POWER SETTINGS

The Laser Beam distribution is Gaussian and is described by the Equation 5.2,

$$f(\mathbf{O}, \mathbf{e}) = \frac{1}{2\pi\sigma^2} \exp\left(-\frac{d^2}{2\sigma^2}\right), \quad d = \frac{\|\mathbf{e} \times (\mathbf{x} - \mathbf{O})\|}{\|\mathbf{e}\|}$$

Eq. 5.2

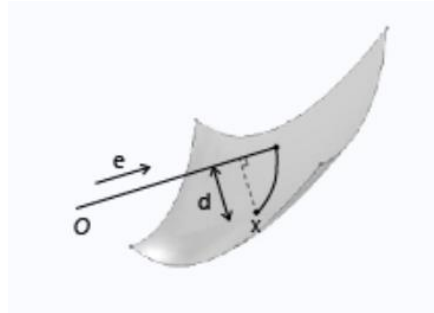


FIG. 5.8 LASER BEAM DISTRIBUTION

This is like what is used in the *LaserConvectionBC* algorithm shown in Equation 2.4.

Controlling the Laser Beam path is possible through the *Beam origin point*. In this case, a global parameter “speed” was defined in the *Parameters Tab*, which specify the laser beam speed across one axis. Then, this parameter was used in the *Beam origin point* and specifically in the y-axis direction to create a linear movement in the y-axis. Using more complicated formulas it is possible to create more complicated shapes and thus, create a scan pattern.

5.2.4 STUDY

Finally, when the simulation is almost ready to run, the user needs to specify what type of study will be running. This is possible from the *Study Tab* where the options below are given,

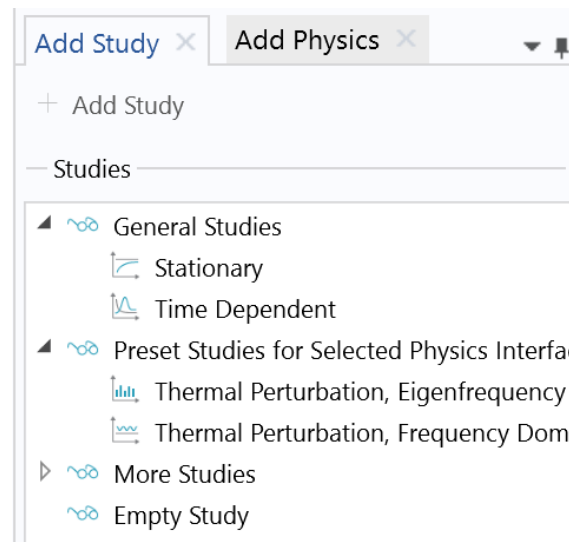


FIG. 5.8 COMSOL ADD STUDY PANEL OVERVIEW

Here the *Time Dependent Study* was chosen with settings,

The screenshot displays the 'Settings' window for a 'Time Dependent' study. The 'Study Settings' section includes a 'Time unit' set to 's', 'Output times' set to 'range(0,0.001,0.1)', and 'Tolerance' set to 'Physics controlled'. The 'Results While Solving' section has 'Plot' checked, 'Plot group' set to 'Temperature (ht)', 'Update at' set to 'Times stored in output', 'Probes' set to 'All', and 'Update at' set to 'Time steps taken by solver'. The 'Physics and Variables Selection' section shows 'Modify model configuration for study step' unchecked. A table lists the 'Physics interface' as 'Heat Transfer in Solids (ht)', 'Solve for' as 'Discretization' (checked), and 'Physics settings' as 'Physics settings'. At the bottom, there are expandable sections for 'Values of Dependent Variables', 'Mesh Selection', 'Adaptation', and 'Study Extensions'.

Physics and Variables Selection		
<input type="checkbox"/> Modify model configuration for study step		
Physics interface	Solve for	Discretization
Heat Transfer in Solids (ht)	<input checked="" type="checkbox"/>	Physics settings

FIG. 5.9 TIME DEPENDENT STUDY SETTINGS TAB

As shown in the Figure 5.9 the time was set from 0 to 0.1 sec with time step 0.001. These values were selected because in the *Deposited Beam Power* settings the laser beam speed was set to 1000 [mm/s]. Also, the current geometry has a length of 100 mm, which means that the laser beam will scan the hole length of the block in 0.1 sec. Thus, the simulation time was chosen as shown in the Figure 5.9.

5.2.5 ADDITIONAL FEATURES

ADAPTIVE MESHING

In COMSOL, it is possible to use adaptive meshing. This is done through the *Study Settings Tab* -> *Adaptation Drop List*. Adaptive meshing is creating a coarse mesh at first in order to distinguish the areas which errors are occurred. After that, a refinement of the mesh in these areas is done for the simulation to run smoothly.

AUXILLIARY SWEEP

This is a feature that *Time Dependent Study Solver* is possessing. This features let the user run the simulation iteratively for many different parameter values. For example, if the user wanted to run the simulation for *laserpower* equal to 100 [W], 200[W], 350 [W] in one row, then the usage of auxiliary sweep is highly recommended.

LINEAR SYSTEM SOLVERS

In COMSOL, the following linear system solvers are included:

MUMPS: The MUMPS solver works on general systems of the form $Ax = b$ and uses several reordering algorithms to minimize the fill-in by permuting the columns. MUMPS can be used to solve problems on distributed memory architectures by using MPI. The code is written in Fortran 90. Further, details about MUMPS can be found in [30].

PARDISO: The PARDISO solver works on systems of the form $Ax = b$. The solver algorithms are based on a Level-3 BLAS update, and exploit pipelining parallelism with a combination of left-looking and right-looking supernode techniques. PARDISO is multi-threaded on platforms that support multi-threading. If you clear the Parallel Direct Sparse Solver for Clusters check box, or if you run PARDISO in the out-of-core mode, the solver settings are changed to corresponding MUMPS settings. The code is written in C and Fortran. COMSOL Multiphysics uses the PARDISO version developed by Olaf Schenk and collaborators [23], included with Intel® MKL [30].

SPOOLES: The SPOOLES solver works on systems of the form $Ax = b$, using the multi-frontal method and direct LU factorization of the sparse matrix A . If the matrix A is symmetric or Hermitian, the solver uses an LDLT version of the algorithm, which saves half the memory. SPOOLES uses several reordering algorithms to minimize fill-in by permuting the columns. SPOOLES supports multi-threading on platforms that support multi-threading, and it also supports solving on distributed memory architectures through using MPI. The code is written in C. COMSOL uses SPOOLES version 2.2, developed by Cleve Ashcraft and collaborators [30].

DENSE MATRIX SOLVER: The dense matrix solver works on systems of the form $Ax = b$. The dense matrix solver uses LAPACK for multi-threaded solves and ScaLAPACK for distributed memory architectures. This solver is mainly useful for cases where the system matrices are densely populated, including boundary element (BEM) models [30].

5.3 UNITS IN COMSOL

In COMSOL, the selection of Units is done in the CASE Setting Tab as shown below,

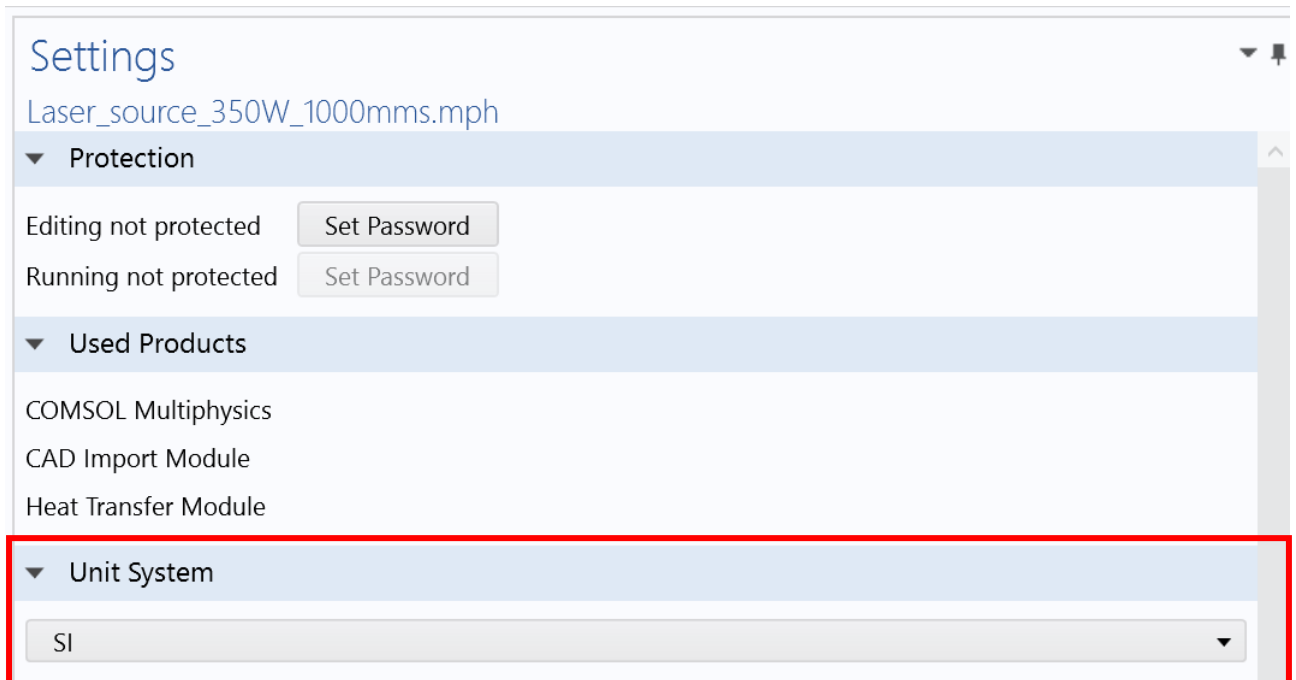


FIG. 5.10 UNIT SYSTEM SELECTION

Is possible to select between a variety of Unit Systems,

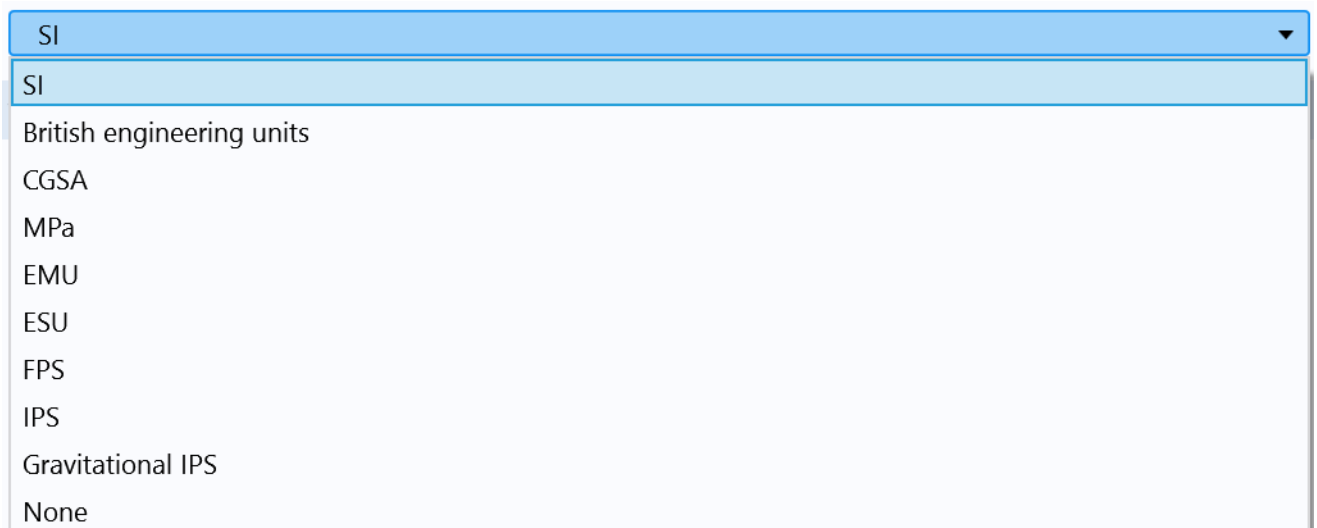


FIG. 5.11 UNIT SYSTEMS

Furthermore, if the user desire to write the values in different units from the SI, for example write the velocity in [mm/s] instead of [m/s], it can be done directly on the cell where the value is entered by including the desired units like in the figure below,



FIG. 5.12 IMPORT UNIT SUBDIVISION DIRECTLY IN VALUE'S CELL

6. RESULTS AND COMPARISON OF THE SOFTWARE

OBJECTIVES

In this chapter the results of the two software will be presented and compared. Also, a brief comparison will be presented for the two software in means of Processing time, Resources management and features.

COMPUTER CHARACTERISTICS

Device name DESKTOP-K11I1SC

Processor Intel(R) Xeon(R) E-2176M CPU @ 2.70GHz 2.71 GHz

Installed RAM 32.0 GB (31.8 GB usable)

System type 64-bit operating system, x64-based processor

PROCESSOR

Xeon E-2176M is a 6-core, 12-threads mobile processor (designed for laptop-notebook use) with a clock speed of 2.70GHz and Intel turbo boost of 4.40Ghz. In this case the Intel turbo boost function is disabled. It also possesses 12 MB Intel® Smart Cache and a bus speed of 8GT/s.

MEMORY

32768 MBytes of Dual-Channel DDR4 Random-Access Memory (RAM), clocked at 2666 MHz.

SYSTEM TYPE

The Windows 10 Pro 64bit operating system was used to run COMSOL and the Windows Linux Subsystem with Ubuntu 18.04 LTS was installed in order to run OpenFOAM on a Linux environment. The 64bit system's integer supports up to **9.22e+18** cells, faces, points in the mesh whereas the 32bit system supports up to **2.147e+09** cells, faces or points in a mesh [31].

6.1 MESH

Both software have the option to import or directly create a mesh for a geometry locally. In openFOAM it is done through some integrated mesh converters such as,

fluentMeshToFoam

Reads a Fluent.msh mesh file, working for both 2-D and 3-D cases.

starToFoam

reads STAR-CD/PROSTAR mesh files.

gambitToFoam

reads a GAMBIT.neu neutral file.

ideasToFoam

reads an I-DEAS mesh written in ANSYS.ans format.

cfx4ToFoam

reads a CFX mesh written in .geo format.

Furthermore, it is possible to import a STL file and convert it to mesh with the *snappyHexMesh* command. The results of the meshing are showed below,

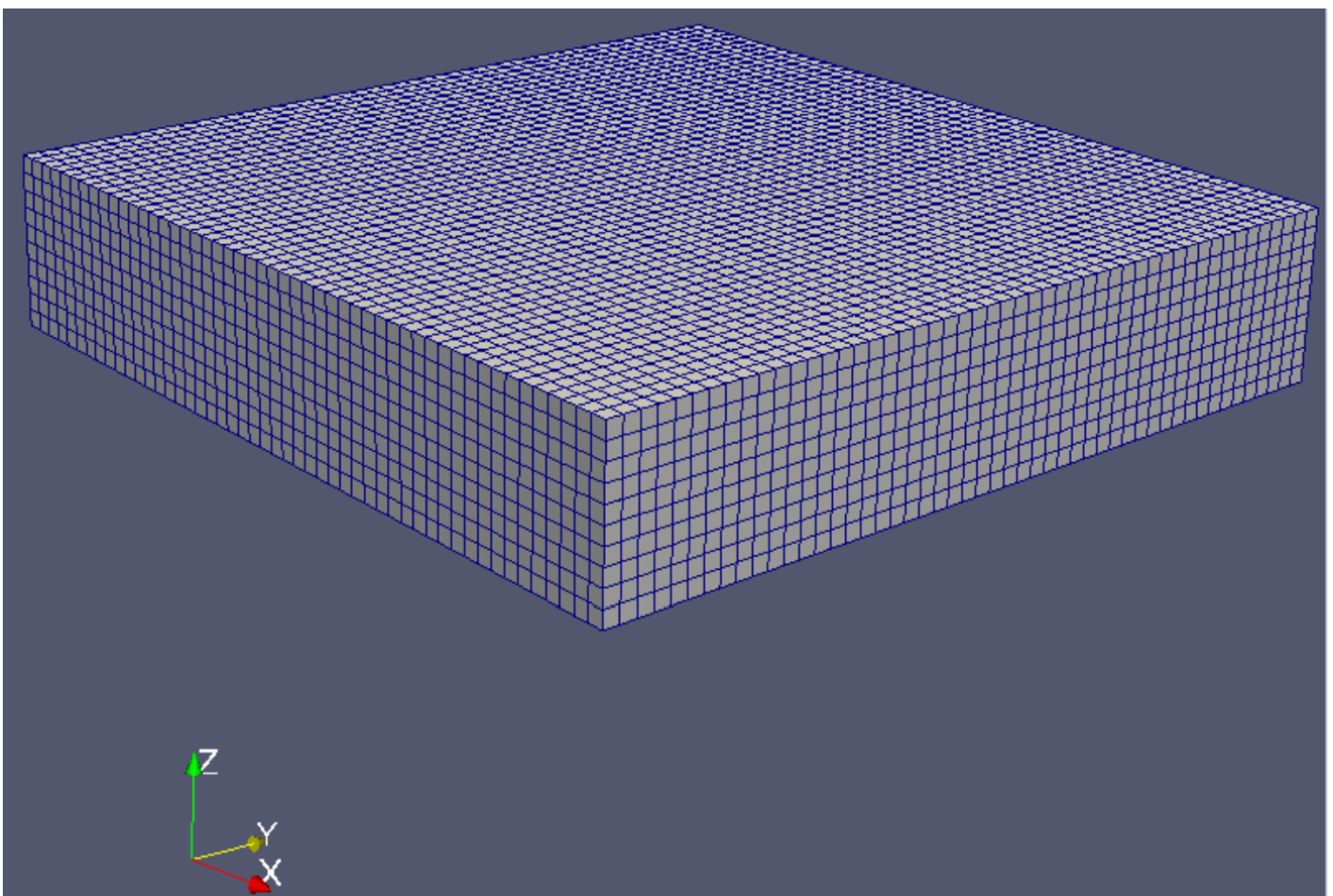


FIG. 6.1 MESH IN OPENFOAM

In COMSOL, this is done through the Geometry and Mesh Tabs mentioned in Chapter 5 and with a predefined extremely fine element size.

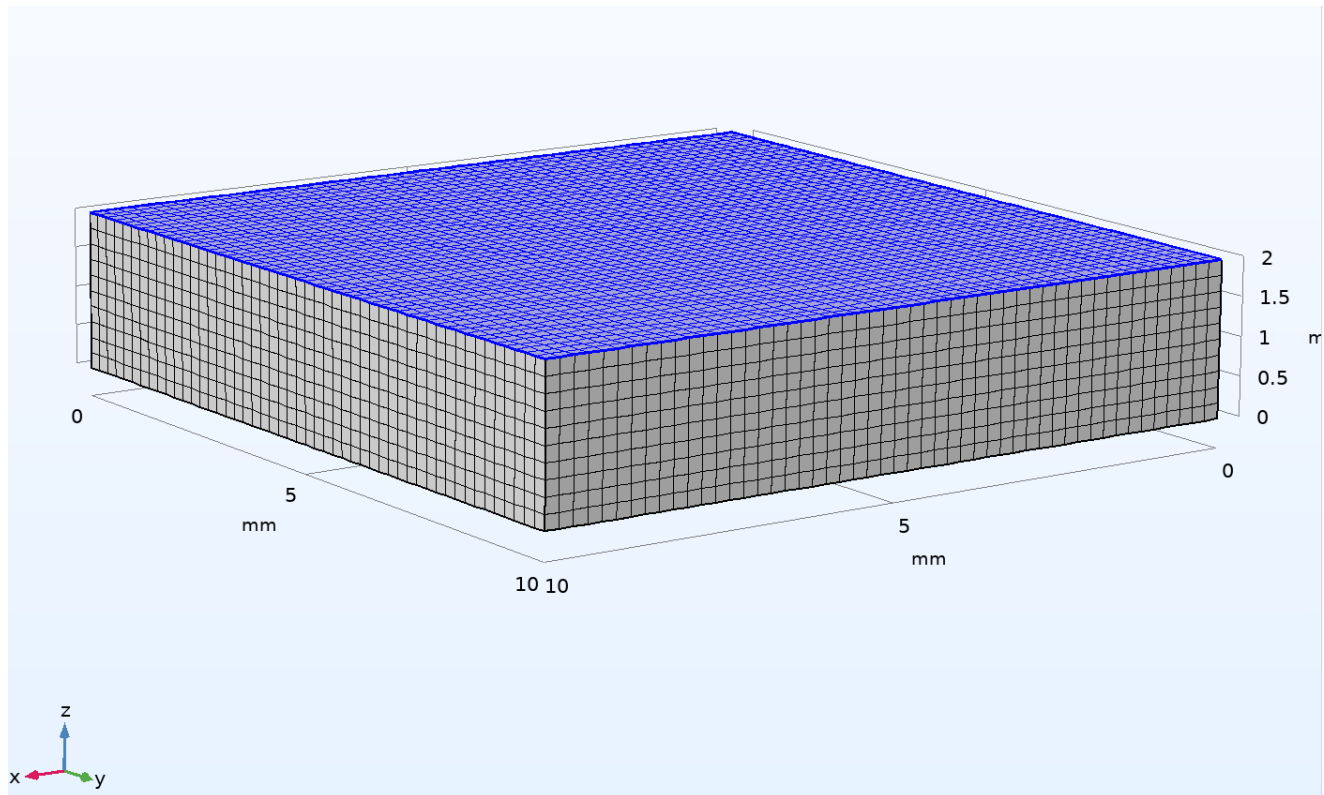


FIG. 6.2 MESH IN OPENFOAM

The mesh stats in both programs are,

Mesh Stats	OpenFOAM	COMSOL
Type	Hexahedral	Hexahedral
Total Elements	25000	25000

TABLE 6.1 MESH STATS

It is important for the mesh to be of same size for a correct comparison of the results in Chapter 6.2.

6.2 MELT POOL GEOMETRY

The thermophysical and solver settings of the two simulations are:

Thermophysical Values	OpenFOAM	COMSOL
Thermal Conductivity	Constant	Constant
Density	Constant	Constant
Specific Heat	Constant	Constant

TABLE 6.2 THERMOPHYSICAL VALUES SETTINGS FOR THE TWO SOFTWARE

And the solver settings are,

Solver Settings	OpenFOAM	COMSOL
Precision	6 digits	5 digits
Tolerance	0.01	0.01

TABLE 6.3 SOLVER SETTINGS VALUES SETTINGS FOR THE TWO SOFTWARE

It is worth noting that the thermophysical values are kept constant. This will make the results to be far from realistic ones but in this case, it is not a major problem as the simulation are done with comparison as the primary purpose. The COMSOL software's Material libraries have these values change with the change of temperature. Unfortunately, OpenFOAM does not have a materials library at all. This means that the user must import the material's thermophysical values in respect to Temperature change in order to have realistic results.

In addition, it is important noting that for the simulation to be comparable, the same environment settings must be implemented on both cases. The settings are shown below,

Case settings	OpenFOAM	COMSOL
Initial Temperature [K]	293.15	293.15
Laser Power [W]	350	350
Laser Speed [mm/s]	50	50
Laser Beam σ [m]	0.0015	0.0015

TABLE 6.4 CASE ENVIRONMENT VARIABLES

Here, it is appropriate to say that there was no power reduce coefficient included on *Laser Power*. This coefficient is simulating the primary reflection of the material and is implemented by multiplying *Laser Power* with the power reduce coefficient which is taking values from 0 to 1.

The results from the OpenFOAM laser case are shown below,

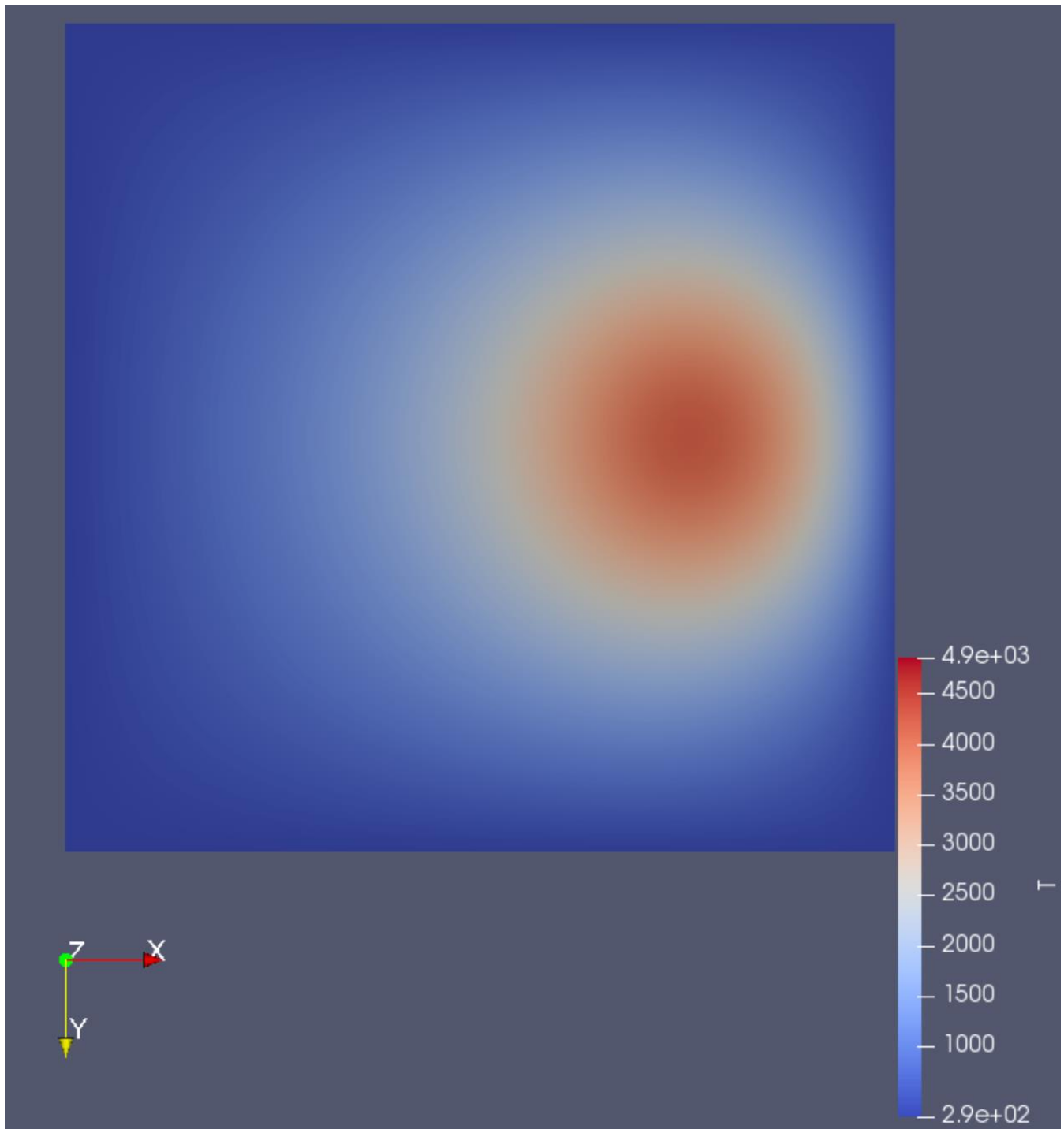


FIG. 6.3 LASER MELTING CASE IN OPENFOAM. START TIME 0s, END TIME 0.2s, STEP 0.01s.

In the Figure 6.3 it is visible that the beam is travelling on the positive direction of the X-axis. The maximum Temperature is 4850K.

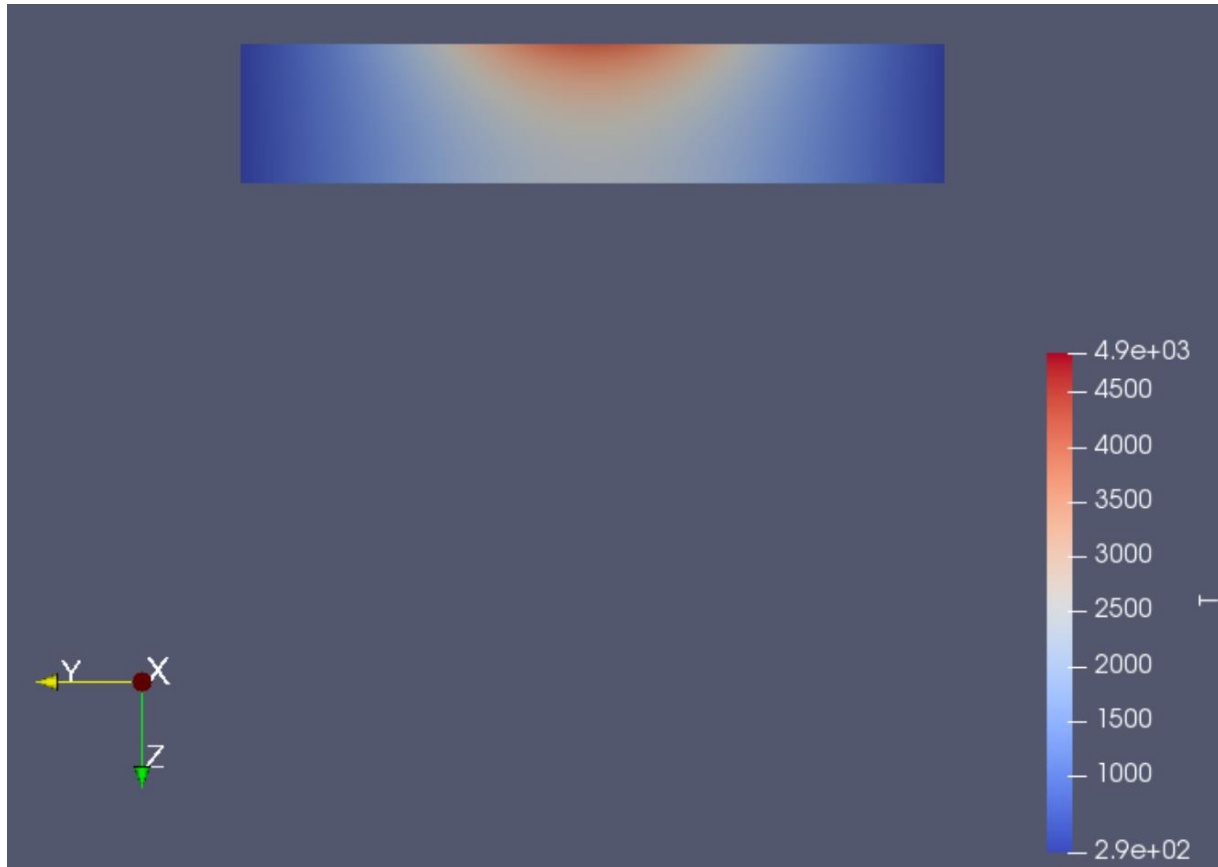


FIG. 6.4 SECTION VIEW ON SIMULATION RESULTS ON PLANE YZ

The profile of the Temperature in conduction mode is similar to other profiles analyzed in bibliography.

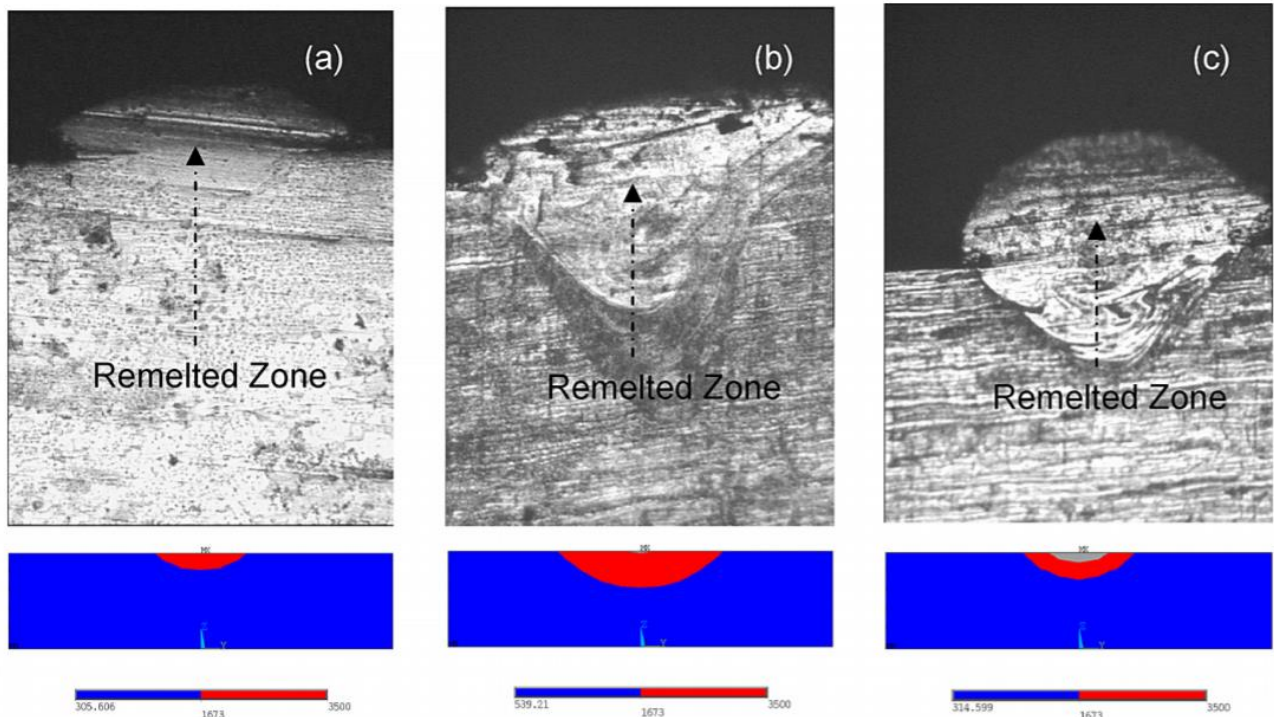


FIG. 6.5 THE MICROGRAPH OF SINGLE TRACK FORMATION OF SS 316L POWDER ON SS 316L SUBSTRATE (A) P 150W; V 12 M/MIN; D 300 M; (B) P 200W; V 2.4 M/MIN; D 500 M; (C) P 200W; V 8.4 M/MIN; D 300 M [32].

Here a threshold value was implemented in the results and a volume was generated with temperature $T > 2000$,

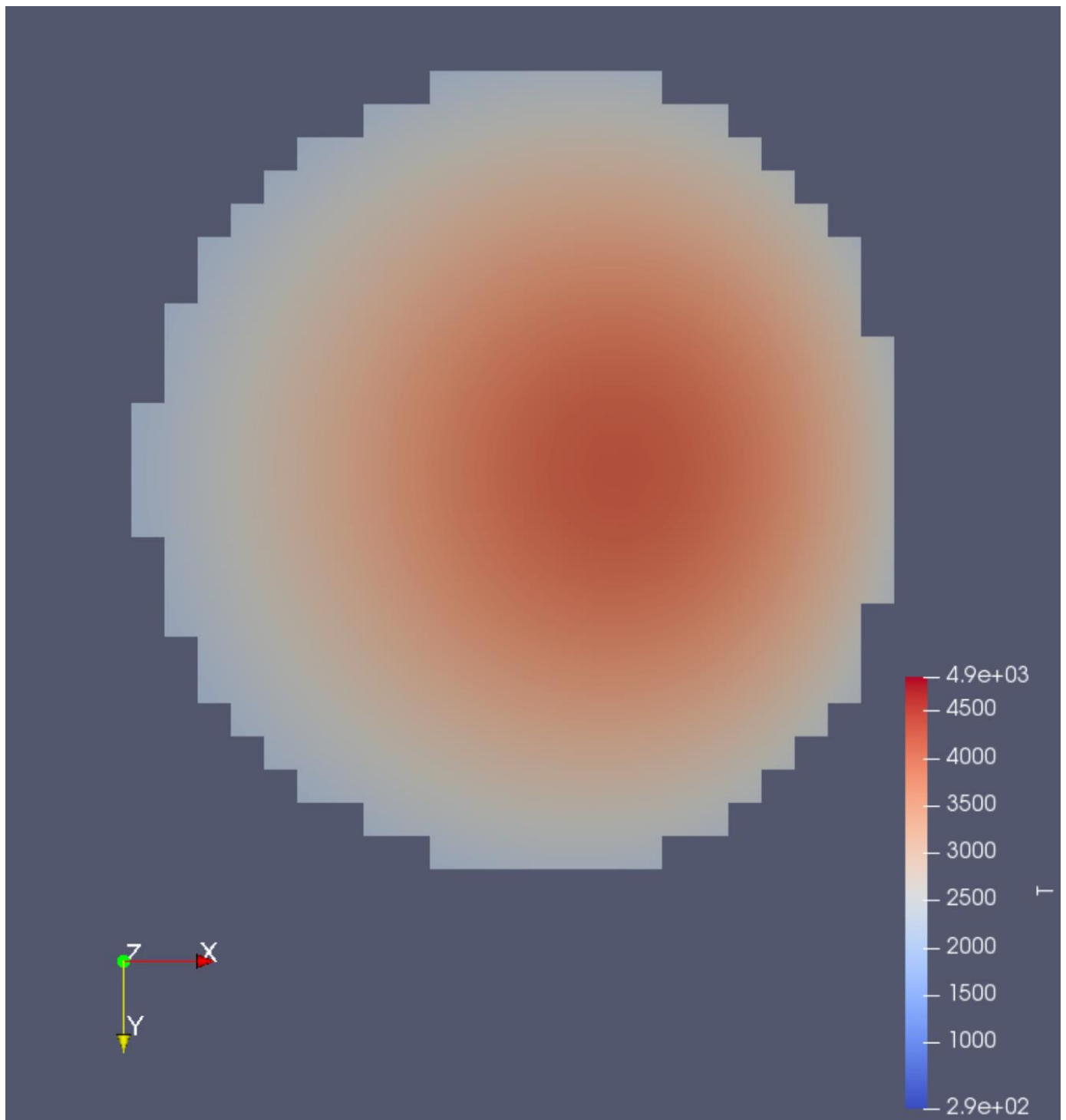


FIG. 6.7 THRESHOLDED VOLUME FOR $T > 2000\text{K}$, TOP VIEW

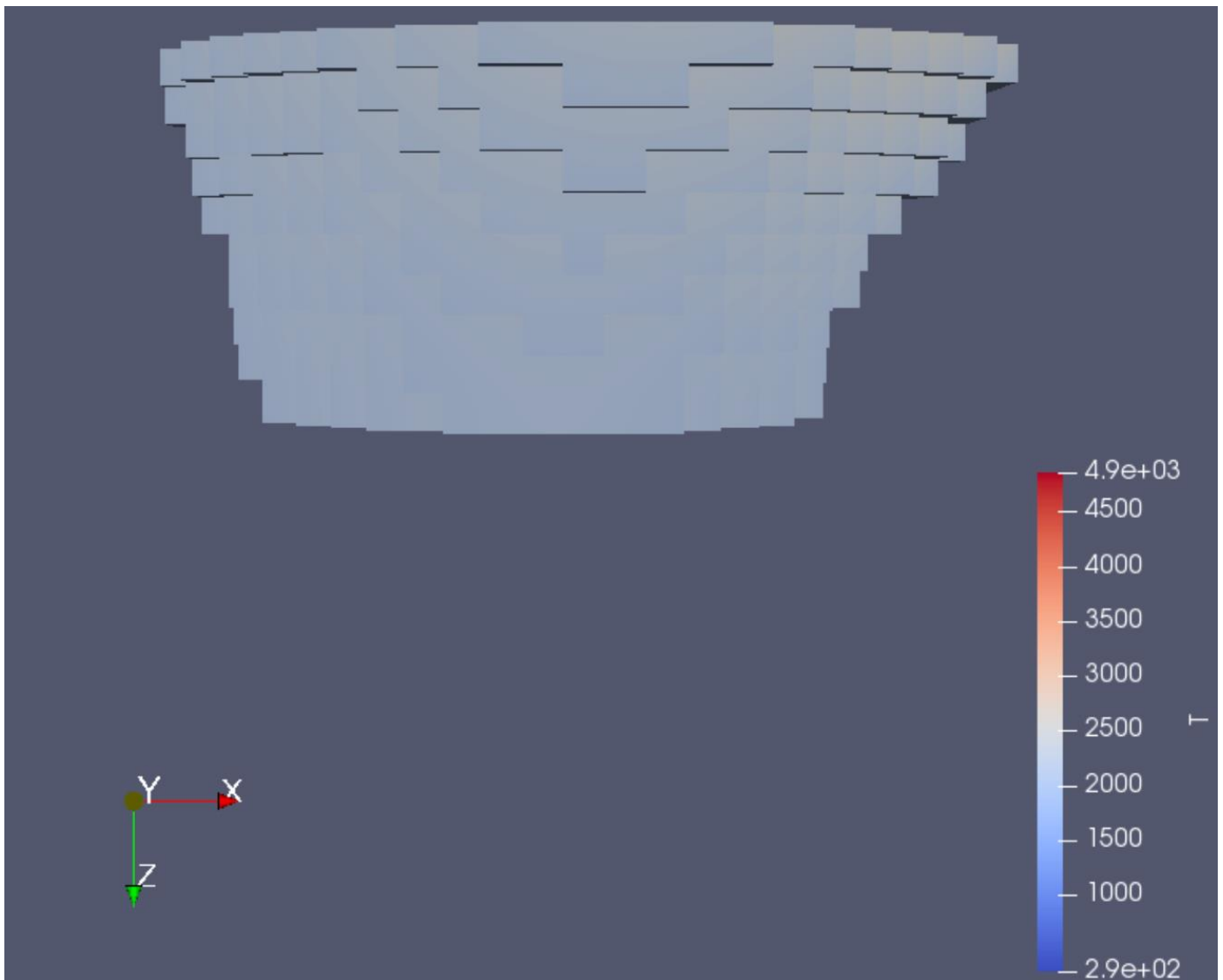


FIG. 6.8 THRESHOLDED VOLUME FOR $T > 2000\text{K}$, SIDE VIEW

The volume of this shape is computed by the Paraview post-processor, and it is equal to $2.31 \times 10^{-8} \text{ m}^3$. There is no extrapolation implemented in cells, thus the volume is calculated as the sum of each cell volume. This is easily implemented with the *Integrate Variables Filter*.

And the results from COMSOL are shown below,

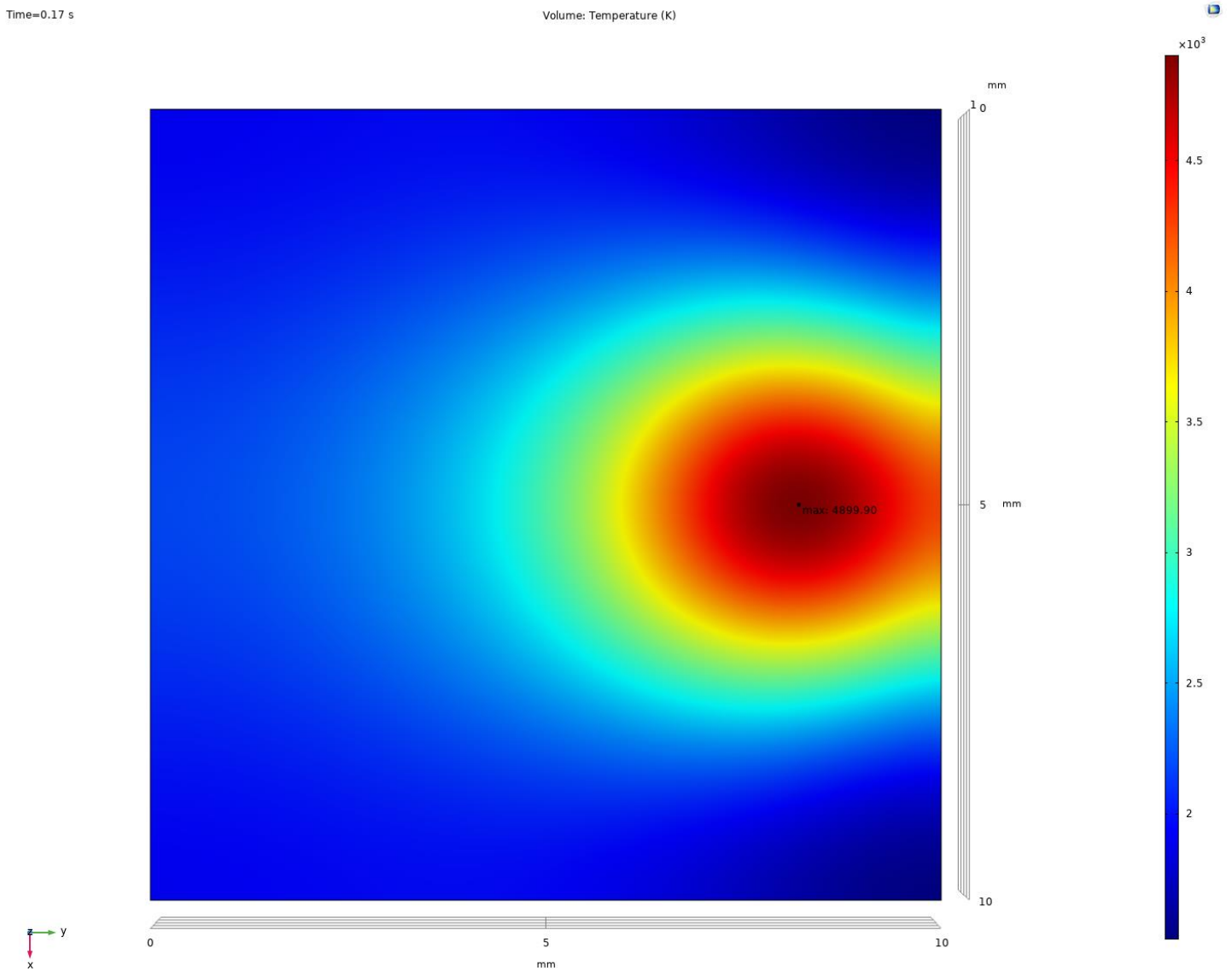


FIG. 6.9 SINGLE TRACK RESULTS FROM COMSOL SIMULATION

In the Figure 6.9 it is visible that the beam is travelling on the positive direction of the X-axis. The maximum Temperature is 4900K.

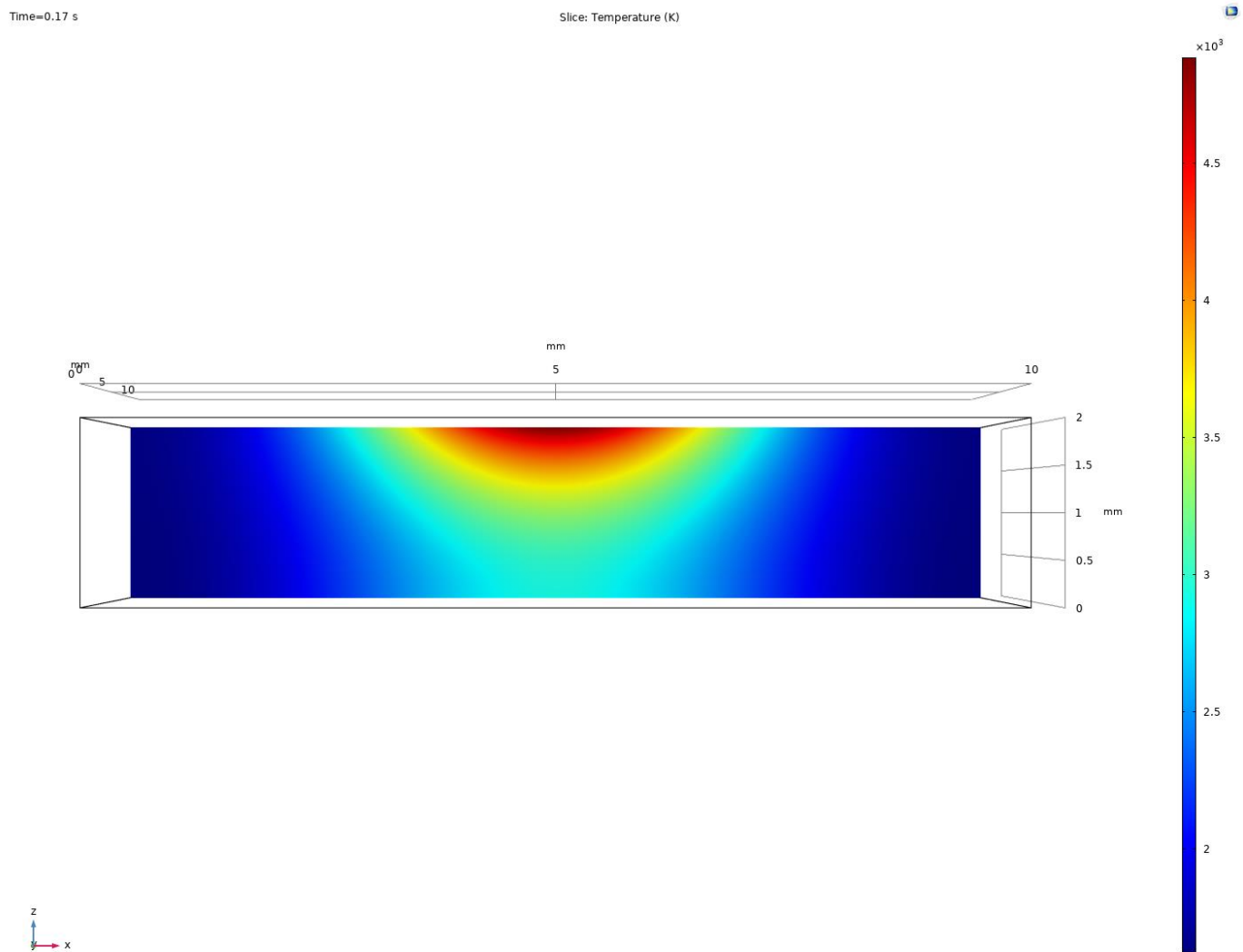
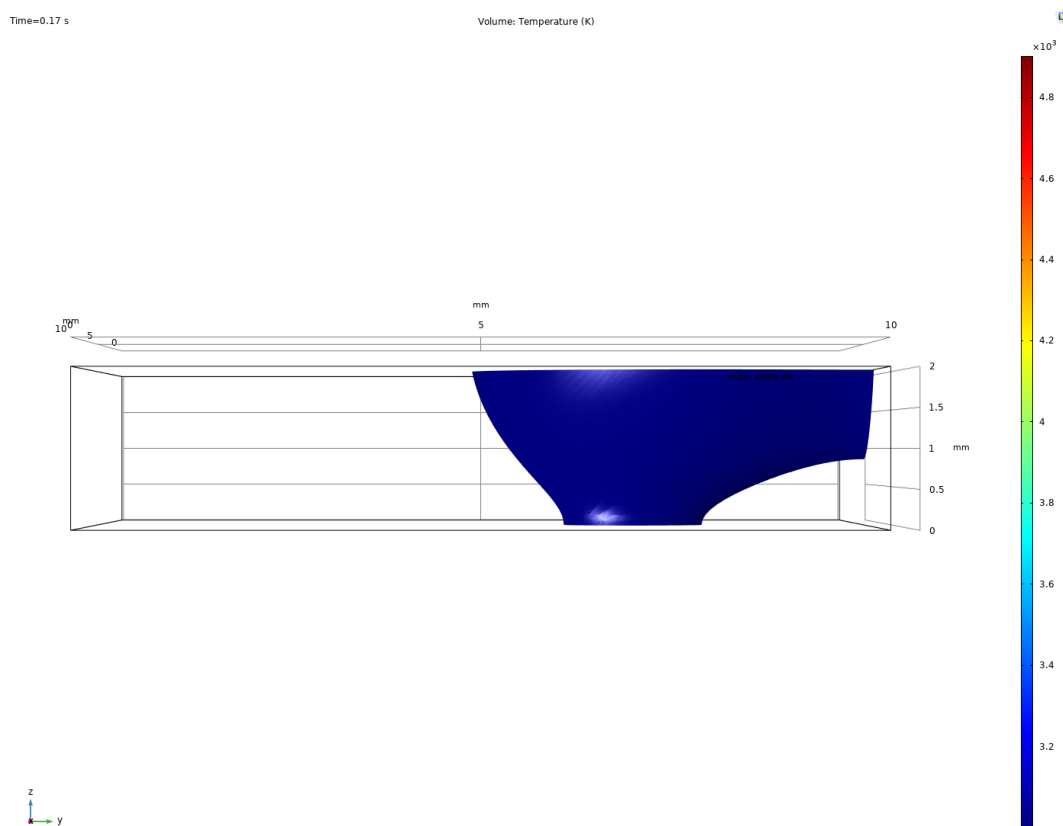
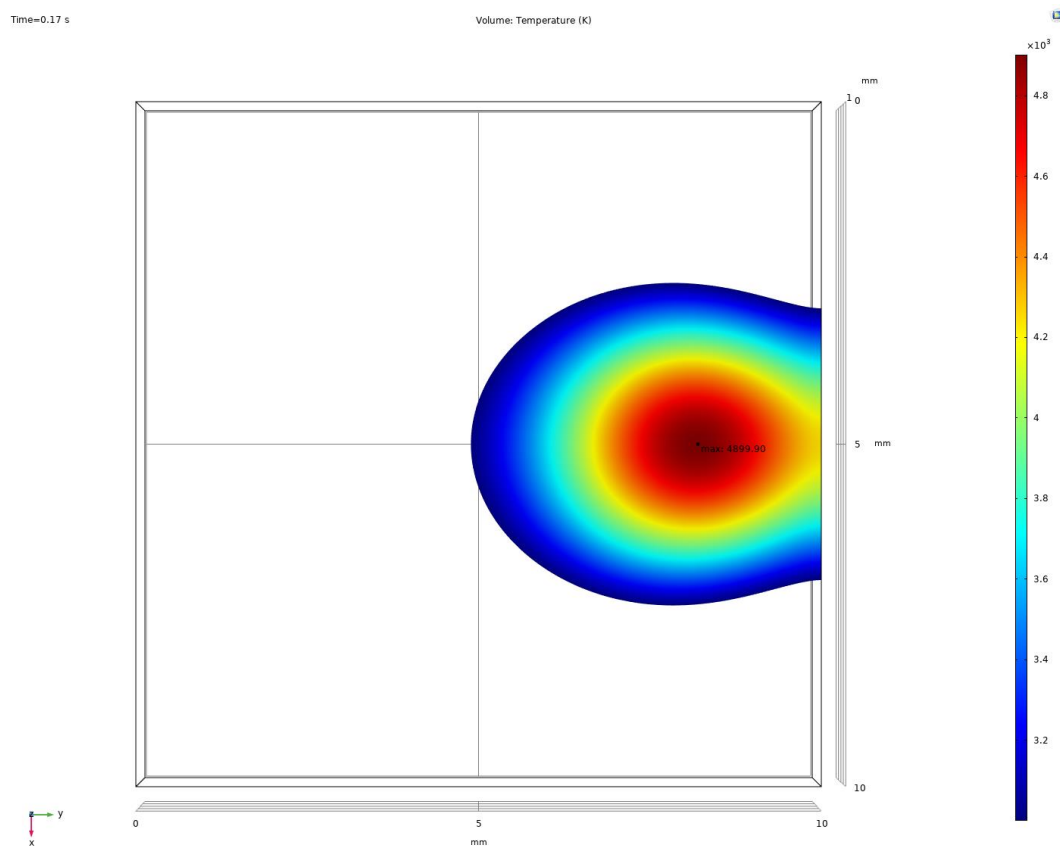


FIG. 6.10 SECTION VIEW OF COMSOL'S SIMULATION RESULTS ON PLANE YZ

The profile of the Temperature in conduction mode is similar to other profiles analyzed in bibliography as shown in Figure 6.5.



The criterion, chosen, for evaluating the results of the two software is the calculation of the generated volume from the threshold value filter ($T > 2000\text{K}$), which are visible in Figure 6.7 and 6.12. This is a common and easily implemented method for the two software unlike the measurement of melt pool manually, which could result in random error. The calculated volumes are shown below,

Volumes	OpenFOAM	COMSOL
	2.3168e-08	2.1062e-08

TABLE 6.5 CALCULATED THRESHOLDED VOLUME VALUES FOR THE TWO SOFTWARE

Because the implemented model is not a complicated one, the results should be remarkably similar to each other. So, the differences of the two software are concluded here,

The maximum Temperature on OpenFOAM is 4850K whereas on COMSOL is 4900K. This results in a 1.2% difference between them. And the filtered volume on OpenFOAM is 2.3168e-08 whereas on COMSOL is 2.1062e-08, resulting in a 9.1% difference between them.

Comparison of results	OpenFOAM	COMSOL	Difference
Temperature [K]	4850	4900	1.2%
Calculated filtered volume [m^3]	2.3168e-08	2.1062e-08	9.1%

TABLE 6.6 DIFFERENCES OF THE TWO SOFTWARE

Finally, the same method was iteratively executed for 2 more case with laser speed equal to $2 \times \text{laser speed}$ and $10 \times \text{laser speed}$:

Comparison of results	OpenFOAM	COMSOL	Difference
Temperature [K], $2 \times \text{laser speed}$	3292	3356	1.9%
Filtered Volume [m^3], $2 \times \text{laser speed}$	4.832e-09	3.9337e-09	18.6%
Temperature [K], $10 \times \text{laser speed}$	2080	1998	3.9%
Filtered Volume [m^3], $10 \times \text{laser speed}$	3.84e-10	4.8422e-10	20.7%

FIG. 6.7 RESULTS FOR CASES: A) $2 \times \text{LASERSPEED}$; B) $10 \times \text{LASERSPEED}$

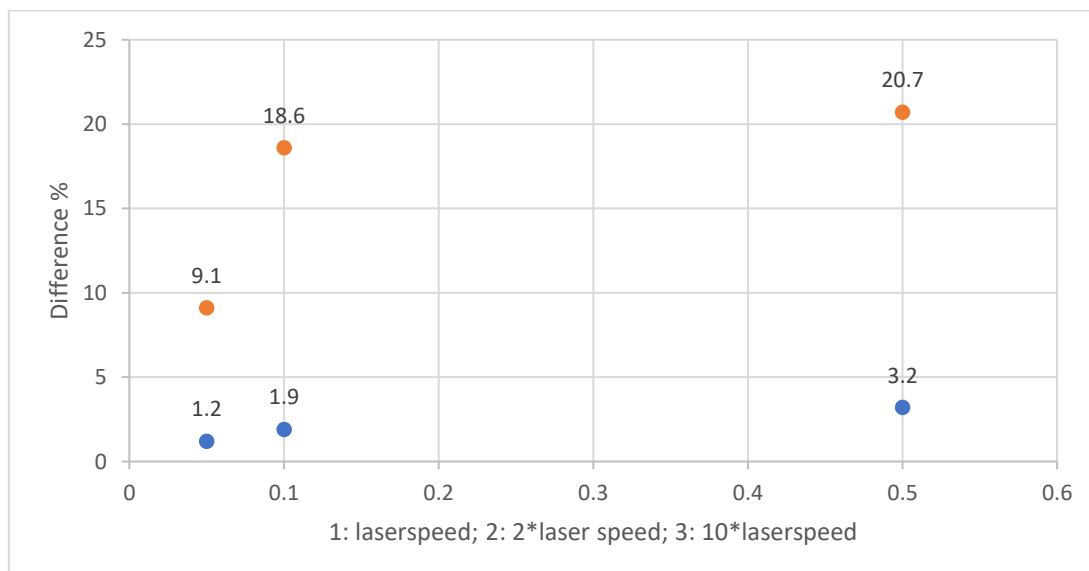


FIG. 6.13 GRAPH SHOWING THE DIFFERENCES IN RESPECT TO LASER SPEED CHANGE

From the Graph presented in Figure 6.13 it is observed that the difference between the *temperature* and the *laserspeed* is growing to one extent and then it shows similar shape to a $\log(x)$.

Below, will be presented the differences in the same values for each program,

X-Values	OpenFOAM Temperature [K]	COMSOL Temperature [K]	OpenFOAM Filtered Volume [e-08m ³]	COMSOL Filtered Volume [m ³]
0.05	4850-4850=0	4900-4900=0	0	0
0.1	4850-3292=1558	4900-3356=1544	2.3168-0.4832=1.8336	2.1062-0.39337=1.71283
0.5	4850-2080=2770	4900-1998=2902	2.3168-0.0384=2.2784	2.1062-0.048422=2.057778

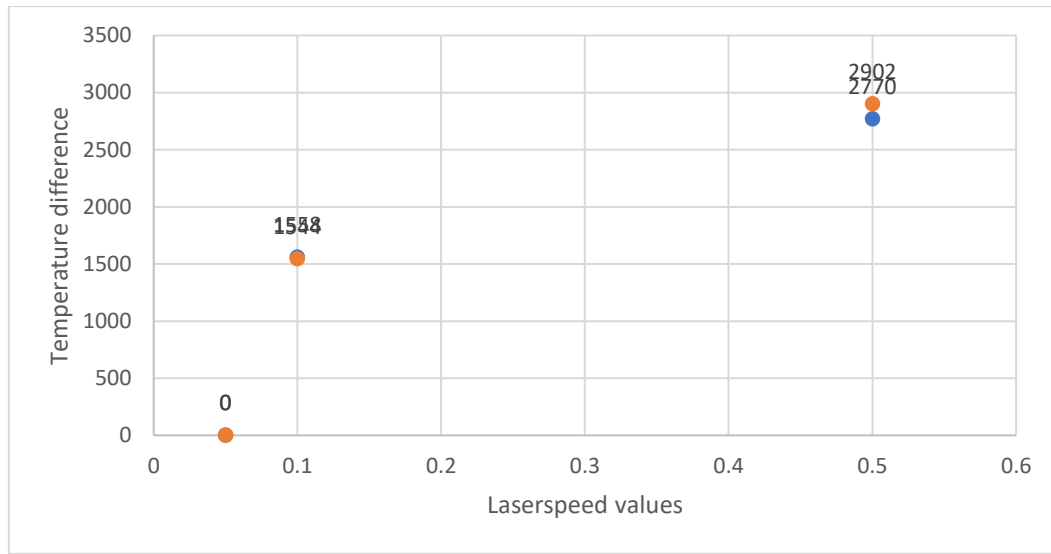


FIG. 6.14 GRAPH SHOWING THE TEMPERATURE DIFFERENCE BETWEEN EACH VALUES OF THE TWO SOFTWARE

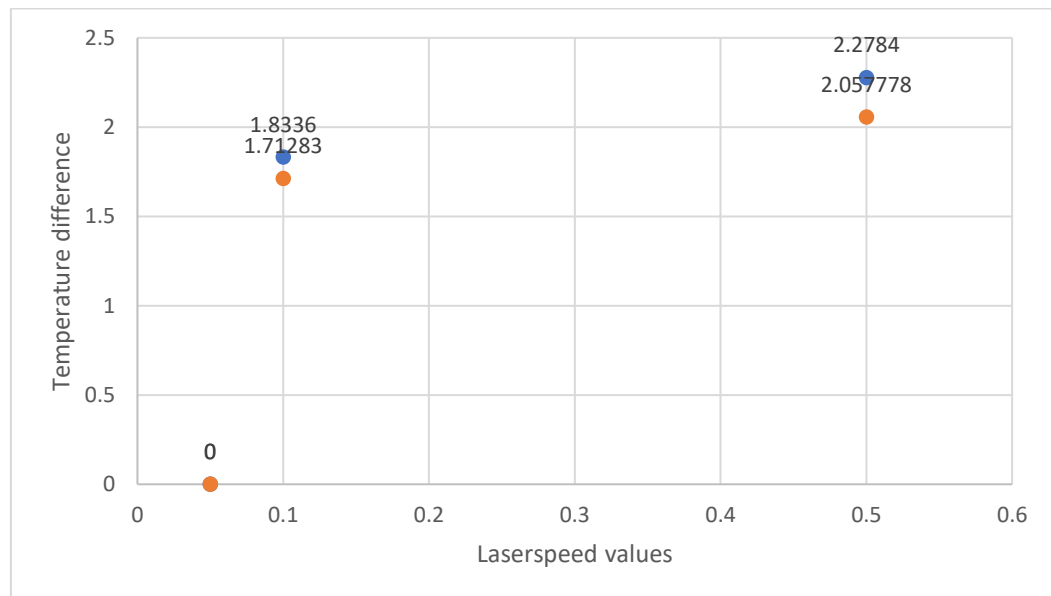


FIG. 6.15 GRAPH SHOWING THE FILTERED VOLUME DIFFERENCE BETWEEN EACH VALUES OF THE TWO SOFTWARE

These graphs were included as a way to observe why there are these differences in the Figure 6.13.

6.3 PROCESSING TIME, COMPUTER RESOURCES MANAGEMENT AND PARALLELIZATION

The processing time for the two software is,

Processing time	OpenFOAM	COMSOL
Wall clock time [s]	22	423

TABLE 6.6 SIMULATION RUNTIME VALUES FOR THE TWO SOFTWARE

OpenFOAM can use both physical and logical processing units unlike COMSOL which is able to use only the physical cores. Moreover, OpenFOAM currently supports GPU Acceleration capabilities whereas COMSOL do not. COMSOL also states this at the simulation log file shown at Figure 6.14.

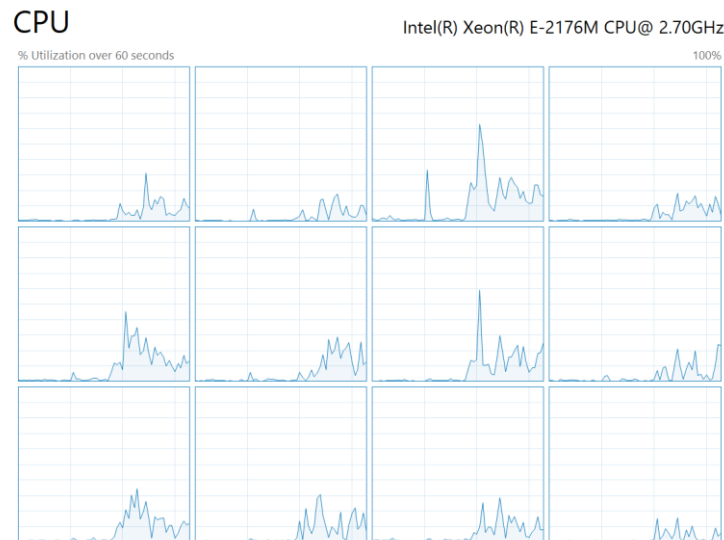


FIG. 6.14 OPENFOAM UTILIZING 12 LOGICAL PROCESSORS AT THE SAME TIME

Running on Intel64 Family 6 Model 158 Stepping 10, GenuineIntel.
Using 1 socket with 6 cores in total on DESKTOP-K11I1SC.
Available memory: 32.54 GB.

FIG. 6.14 PART OF COMSOL'S SIMULATION LOG FILE.

Below the terminal log is presented after running the **time ./Allrun** command, which runs the case and counts the processing time.

```
real    0m22.169s
user    0m11.969s
sys     0m5.047s
```


The means of the above different types of time are presented here,

- **Real** is wall clock time - time from start to finish of the call. This is all elapsed time including time slices used by other processes and time the process spends blocked (for example if it is waiting for I/O to complete).
- **User** is the amount of CPU time spent in user-mode code (outside the kernel) *within* the process. This is only actual CPU time used in executing the process. Other processes and time the process spends blocked do not count towards this figure.
- **Sys** is the amount of CPU time spent in the kernel within the process. This means executing CPU time spent in system calls *within the kernel*, as opposed to library code, which is still running in user-space. Like 'user', this is only CPU time used by the process. See below for a brief description of kernel mode (also known as 'supervisor' mode) and the system call mechanism.

Thus, Real refers to actual elapsed time; User and Sys refer to CPU time used *only by the process* [33]. To compare the results to COMSOL the real time will be used.

For COMSOL, the solution log file was exported and a part of it is presented below,

Running on Intel64 Family 6 Model 158 Stepping 10, GenuineIntel.

Using 1 socket with 6 cores in total on DESKTOP-K11I1SC.

Available memory: 32.54 GB.

Time: 1 s.

Physical memory: 1.84 GB

Virtual memory: 2.23 GB

**----- Compile Equations: Time Dependent in Study 1/Solution 1 (sol1) -----
----->**

**<----- Dependent Variables 1 in Study 1/Solution 1 (sol1) -----
-----**

Physical memory: 1.85 GB

Virtual memory: 2.24 GB

**.
.
.**

Time-stepping completed.

Solution time: 423 s. (7 minutes, 3 seconds)

Physical memory: 4.93 GB

Virtual memory: 5.56 GB

It is worth noting that, in COMSOL, each time the simulation runs, the processing time differs on a small extent. This is due to the solver implementation to choose a relatively different value for iterative algorithm initialization.

For example, the above Simulation was executed in COMSOL several times and the results of the processing time are,

COMSOL SOLUTION	RUNTIME [s]
1	462
2	434
3	402
4	576
5	423

TABLE 6.7 COMSOL RUNTIME VALUES AFTER SEVERAL EXECUTIONS

7. CONCLUSIONS

OBJECTIVES

In this chapter, some final conclusions regarding these two software will be deduced.

First of all, the results in Chapter 6.2 show a growing difference between the two software, as the laser speed is increasing. Probably this can be corrected by calibrating the OpenFOAM solvers, that are manually set up for more steps to be calculated.

At the end of this work, it is mandatory to say that both software have their advantages and disadvantages. They are both reliable when used appropriately. If a simulation needs to run multiple times with changing values on meshing, solver or parameters then OpenFOAM is very flexible software to make it work as desired in the cost of much more time for setting up the code. If the GPU Acceleration and extremely robust powerful optimization algorithms is mandatory for the simulation, then again OpenFOAM is the way to go. Though, if the user wants to experiment with different solvers in a short time and get results quickly in an intuitive graphical user interface, then the COMSOL is the suitable program.

In some cases, the equations a solver is computing need to change. This is easily done in OpenFOAM as the solvers are open and written in C++. Unfortunately, in COMSOL something like this is not feasible as the program is not open code. This “feature” of OpenFOAM makes it possible for the community to contribute on this code and, thus create a large capacity of third-party solvers and libraries able to do extremely complicated tasks such as Topology Optimization which COMSOL does not include yet.

The two-software address different audience. The COMSOL is a commercially available software used by big manufacturers and research labs. OpenFOAM is an open-code software used by researchers and manufacturers on a smaller scale and mainly for Research and Development (RnD) as it is highly customizable as said in chapter 6.4. To use OpenFOAM, knowledge of Linux systems and coding in C++ is highly recommended, thus it has a smaller audience unlike COMSOL which has a GUI environment which is very intuitive to learn.

Both programs possess features that are extremely useful. COMSOL, includes a material library which has a large dataset of materials and their thermophysical properties in respect to Temperature change. Furthermore, in COMSOL a mirror plane can be introduced in a simulation which is very useful as the solution is running only for the half geometry, thus reducing the runtime further. On the other hand, OpenFOAM, can be highly customizable as said in the Chapter 6.4 and many third-party libraries and solvers are available from researcher, thus making it an immensely powerful tool.

Thus, in the following table the similarities and differences of the tested software are summarized,

	Similarities	Differences
OpenFOAM-COMSOL	Ability to implement multiphysics models	User Interface is a lot different in these two software and depending on the user, it can be easy or difficult to learn
	Powerful and effective solvers	Material Library
	Widely used, community support	Customization differences as the COMSOL is not easily customizable
		Meshing as OpenFOAM does not support all kind of elements

TABLE 7.1 SIMILARITIES AND DIFFERENCES OF OPENFOAM AND COMSOL

8. FUTURE WORK

Objectives

This chapter is dedicated in the potential of the current work for future additions. The information below, will create motivation and set some remarkably interesting point for future developing of the current work.

8.1 MODELING AND COUPLING OF FLUID DYNAMICS AND PHASE CHANGE

A more complete model would be one with thermal and fluid coupling. This can be done via the *icoReactingMultiphaseInterFoam* solver. This solver can handle simulations with multiple phases. Better described, the solver, first, solves the continuity and momentum equations for two fluids and then uses the Volume of Fluid approach to solve the phase-fraction based interphase equation for the interface between the fluid boundaries. This problem can be mathematically described by the equations shown in the Chapter 2.5.4.

8.2 MODELING OF ELECTROMAGNETIC FORCES DUE TO PLASMA INTERACTION

During Selective Laser Melting process, electromagnetic forces are present (Lorentz forces) due to plasma generation. This phenomenon could be coupled with the above thermal-fluid model and produce a more complicated and completed model.

8.3 COMPARING THERMAL, FLUID, ELECTROMAGNETIC MODELS TO DETERMINE IF IT HAS ANY EFFECT ON THE RESULTS

The above cases should be tested for their impact on the overall results. This should be done on a statistical manner. The models tested should be the thermal model, the thermal-fluid model and the thermal-fluid-electromagnetic model. Some characteristics and advantages for each model should be presented.

8.4 COMPARISON BETWEEN DIFFERENT MESH SIZES

Here a comparison between different mesh sizes should be done. This is vital as the processing time is decreasing a lot. Using Richardson extrapolation estimation method, it is possible to determine the error between two different mesh sizes and evaluate them with processing time as a criterion.

The Richardson extrapolation estimation method I used for estimating the error which occurs due to discretization.

First, a representative height for the cell, mesh or grid size must be defined. In 3-Dimensional cases this is defined in Equation 4.1,

$$height = \left[\frac{1}{N} \sum_{i=1}^N (\Delta V_i) \right]^{\frac{1}{3}} \quad \text{Eq. 8.1}$$

Where *height* is a cell height taken by averaging the volumes.

The extrapolated temperature is calculated by the Equation 4.2,

$$T_{ext}^{i+1,i} = \frac{(r_{i+1,i}^p T_1 - T_2)}{(r_{i+1,i}^p - 1)} \quad \text{Eq. 8.2}$$

The term *p* in Equation 4.3 is defined by the Equation 4.3 below,

$$p = \frac{1}{\left(\ln(r_{i+1,i}) \right)} \cdot \left[\ln \left| \frac{\varepsilon_{i+2,i+1}}{\varepsilon_{i+1,i}} \right| + q(p) \right] \quad \text{Eq. 8.3}$$

Where ε term is described as,

$$\varepsilon_{i+2,i+1} = T_{i+2} - T_{i+1} \quad \text{Eq. 8.4}$$

And,

$$q(p) = \ln \left(\frac{r_{i+1,i}^p - s}{r_{i+2,i+1}^p - s} \right) \quad \text{Eq. 8.5}$$

Finally, the s term that is present in the Equation 4.5 can be defined as follows,

$$s = \operatorname{sgn} \left(\frac{\varepsilon_{i+2,i+1}}{\varepsilon_{i+1,i}} \right) \quad \text{Eq. 8.6}$$

This method can be used to estimate the error between two varied sizes of mesh, which is shown in [34].

8.5 PLASMA SHIELDING COUPLING (BEAM ENERGY LOSS)

During SLM process the metal is changing phases from solid to liquid, thus creating the melt pool. Though as the power of the laser beam is focused on a small area, it is common to change phase from solid to gas on an instant. During this state of the process, plasma is generated, and a drop of laser beam power is introduced as the plasma is “shielding” the powder. This problem can be modeled as a simple power loss of the beam, which will not be as precise as a more sophisticated modeling.

8.6 TOWARDS AN OPEN-SOURCE AM SOFTWARE TOOLKIT, BASED ON OPENFOAM OPEN-CODE SOFTWARE

In order to evolve the SLM process, more researchers should be able to have access to free software to experiment with their ideas. Having said that, this work is possible to set the start line for the development of an open-source software based on OpenFOAM and open code software, that will be able to perform multiple types of simulations such as, thermal history simulation, residual stresses etc. Many other features can be introduced, such as an adaptive set for SLM process parameters, depending on the object’s geometry. This will facilitate researchers and enthusiasts to enter this field of research and evolve it with their innovative ideas.

APPENDIX A

ControlDict

```
1  /*-----*- C++ -*-*/
2  | ===== |
3  | \ \ / F i e l d | OpenFOAM: The Open Source CFD Toolbox |
4  | \ \ / O p e r a t i o n | Version: 4.0 |
5  | \ \ / A n d | Web: www.OpenFOAM.org |
6  | \ \ / M a n i p u l a t i o n | |
7  /*-----*/
8  FoamFile
9  {
10     version      2.0;
11     format        ascii;
12     class         dictionary;
13     location      "system";
14     object        controlDict;
15 }
16 // *****
17
18 application      laplacianFoam;
19
20 startFrom        latestTime;
21
22 startTime        0;
23
24 stopAt           endTime;
25
26 endTime          1;
27
28 deltaT           0.01;
29
30 writeControl      runtime;
31
32 writeInterval     0.01;
33
34 purgeWrite        0;
35
36 writeFormat       ascii;
37
38 writePrecision    6;
39
40 writeCompression off;
41
42 timeFormat        general;
43
44 timePrecision     6;
45
46 runtimeModifiable true;
47
48 libs ( "liblaserConvectionBC.so" );
49 // *****
```

Bibliography

- [1] D. Deradajat and T. Minshall, "Decision trees for implementing rapid manufacturing for mass customisation," *CIRP Journal of Manufacturing Science and Technology*, vol. 23, pp. 156–171, Mar. 2018.
- [2] T. S. Srivatsan and T. S. Sudarshan, *Additive manufacturing: innovations, advances, and applications*. CRC Press, 2015.
- [3] Y. Rupinder and S. J. P. Davim, "MANUFACTURING DESIGN AND TECHNOLOGY SERIES ADDITIVE MANUFACTURING APPLICATIONS AND INNOVATIONS."
- [4] S. M. Thompson, L. Bian, N. Shamsaei, and A. Yadollahi, "An overview of Direct Laser Deposition for additive manufacturing; Part I: Transport phenomena, modeling and diagnostics," *Additive Manufacturing*, vol. 8, pp. 36–62, Oct. 2015.
- [5] M. Srivastava, S. Rathee, S. Maheshwari, and T. K. Kundra, "Additive Manufacturing; Fundamentals and Advancements."
- [6] M. Markl and C. Körner, "Multiscale modeling of powder bed-based additive manufacturing," *Annu. Rev. Mater. Res.*, vol. 46, no. 1, pp. 93–123, Jul. 2016.
- [7] E. Mirkoohi, J. Ning, P. Bocchini, O. Fergani, K.-N. Chiang, and S. Liang, "Thermal Modeling of Temperature Distribution in Metal Additive Manufacturing Considering Effects of Build Layers, Latent Heat, and Temperature-Sensitivity of Material Properties," *JMMP*, vol. 2, no. 3, p. 63, Sep. 2018.
- [8] "Theodore L. Bergman, Adrienne S. Lavine, Frank P. Incropera, David P. DeWitt - Fundamentals of Heat and Mass Transfer, Seventh Edition' ' -John Wiley & Sons, Inc. (2011).pdf."
- [9] Y. S. Lee and W. Zhang, "Modeling of heat transfer, fluid flow and solidification microstructure of nickel-base superalloy fabricated by laser powder bed fusion," *Additive Manufacturing*, vol. 12, pp. 178–188, Oct. 2016.
- [10] C. Bruna-Rosso, A. G. Demir, and B. Previtali, "Selective laser melting finite element modeling: Validation with high-speed imaging and lack of fusion defects prediction," *Mater. Des.*, vol. 156, pp. 143–153, Oct. 2018.
- [11] T.-N. Le and Y.-L. Lo, "Effects of sulfur concentration and Marangoni convection on melt-pool formation in transition mode of selective laser melting process," *Mater. Des.*, vol. 179, p. 107866, Oct. 2019.
- [12] M. Tang, P. C. Pistorius, and J. L. Beuth, "Prediction of lack-of-fusion porosity for powder bed fusion," *Additive Manufacturing*, vol. 14, pp. 39–48, Mar. 2017.
- [13] J. Metelkova, Y. Kinds, K. Kempen, C. de Formanoir, A. Witvrouw, and B. Van Hooreweder, "On the influence of laser defocusing in Selective Laser Melting of 316L," *Additive Manufacturing*, vol. 23, pp. 161–169, Oct. 2018.
- [14] V. JAGOTA, A. SETHI, and K. KUMAR, "Finite Element Method: An Overview."
- [15] J. Patalas-Maliszewska, E. Feldshtein, O. Devojno, M. Śliwa, M. Kardapolava, and N. Lutsko, "Single Tracks as a Key Factor in Additive Manufacturing Technology-Analysis of Research Trends and Metal Deposition Behavior.," *Materials (Basel)*, vol. 13, no. 5, Mar. 2020.

- [16] C. H. Fu and Y. B. Guo, "3-DIMENSIONAL FINITE ELEMENT MODELING OF SELECTIVE LASER MELTING TI-6AL-4V ALLOY."
- [17] J. Ning, D. E. Sievers, H. Garmestani, and S. Y. Liang, "Analytical Modeling of In-Process Temperature in Powder Bed Additive Manufacturing Considering Laser Power Absorption, Latent Heat, Scanning Strategy, and Powder Packing.," *Materials (Basel)*, vol. 12, no. 5, Mar. 2019.
- [18] J. Ning and S. Y. Liang, "Analytical Modeling of Three-Dimensional Temperature Distribution of Selective Laser Melting of Ti-6Al-4V," Sep. 2018.
- [19] B. Schoinochoritis, D. Chantzis, and K. Salonitis, "Simulation of metallic powder bed additive manufacturing processes with the finite element method: A critical review," *Proceedings of the Institution of Mechanical Engineers, Part B: Journal of Engineering Manufacture*, vol. 231, no. 1, pp. 96–117, Jan. 2017.
- [20] A. Otto, R. G. Vázquez, U. Hartel, and S. Mosbah, "Numerical analysis of process dynamics in laser welding of Al and Cu," *Procedia CIRP*, vol. 74, pp. 691–695, 2018.
- [21] Z. Fan and B. Li, "Meshfree simulations for additive manufacturing process of metals," *Integr. Mater. Manuf. Innov.*, vol. 8, no. 2, pp. 144–153, Jun. 2019.
- [22] A. Otto and M. Schmidt, "Towards a universal numerical simulation model for laser material processing," *Physics Procedia*, vol. 5, pp. 35–46, 2010.
- [23] R. G. Vázquez, H. M. Koch, and A. Otto, "Multi-physical Simulation of Laser Welding," *Physics Procedia*, vol. 56, pp. 1334–1342, 2014.
- [24] "Boussinesq Approximation," www.comsol.de. [Online]. Available: <https://www.comsol.de/multiphysics/boussinesq-approximation>. [Accessed: 02-Jul-2021].
- [25] "ANSYS AM MODULE," ansys.com. [Online]. Available: <https://www.ansys.com/products/additive>. [Accessed: 04-Jul-2021].
- [26] T. Holzmann, "Linear and Circular Spot Motion and Additional."
- [27] "laplacianFoam," openfoam.com. [Online]. Available: <https://www.openfoam.com/documentation/guides/latest/doc/guide-applications-solvers-basic-laplacianFoam.html>. [Accessed: 08-Jul-2021].
- [28] "OpenFOAM Documentation," openfoam.com. [Online]. Available: <https://www.openfoam.com/documentation/user-guide>. [Accessed: 05-Jul-2021].
- [29] "Introduction to COMSOL Multiphysics," doc.comsol.com. [Online]. Available: <https://doc.comsol.com/5.6/docserver/#1/com.comsol.help.comsol/helpdesk/helpdesk.html>. [Accessed: 09-Jul-2021].
- [30] "COMSOL LINEAR SYSTEM SOLVERS," doc.comsol.com. [Online]. Available: https://doc.comsol.com/5.5/doc/com.comsol.help.comsol/comsol_ref_solver.27.118.html?fbclid=IwAR0K_g58zqoviLENxiFlzA2_RN5v5c-pAOGcBBDzYLQsReUF36V1WYcevn0. [Accessed: 11-Jul-2021].

- [31] "OpenFOAM 5 installation guide," *openfoamwiki.net*. [Online]. Available: https://openfoamwiki.net/index.php/Installation/Linux/OpenFOAM-5.x/Ubuntu#Ubuntu_18.04. [Accessed: 14-Jul-2021].
- [32] K. Antony, N. Arivazhagan, and K. Senthilkumaran, "Numerical and experimental investigations on laser melting of stainless steel 316L metal powders," *J. Manuf. Process.*, vol. 16, no. 3, pp. 345–355, Aug. 2014.
- [33] "UBUNTU DOCUMENTATION," *ubuntu.com*. [Online]. Available: <https://help.ubuntu.com/>. [Accessed: 14-Jul-2021].
- [34] J. Lundkvist, "CFD Simulation of Fluid Flow During Laser Metal Wire Deposition using OpenFOAM," 2019.

ΕΚΤΕΤΑΜΕΝΗ ΠΕΡΙΛΗΨΗ

Ανάπτυξη και σύγκριση μοντέλων μεταφοράς θερμότητας για κατεργασία SLM σε OpenFoam και σε εμπορικό πακέτο πεπερασμένων στοιχείων

ΠΕΡΙΛΗΨΗ

Η διπλωματική με το παραπάνω θέμα εστιάζει στην προσομοίωση της κατεργασίας προσθήκης υλικού, Selective Laser Melting (SLM) υλοποιώντας ένα μοντέλο μεταφοράς θερμότητας, σε δύο διαφορετικά λογισμικά, το COMSOL 5.6 και το OpenFOAM v5. Το μοντέλο αυτό περιλαμβάνει τον μηχανισμό μεταφοράς θερμότητας με αγωγή. Η δέσμη laser η οποία χτυπά το υλικό ακολουθεί γκαουσιανή κατανομή. Πρώτα απ' όλα, δίνεται μια σύντομη παρουσίαση της κατεργασίας SLM. Στη συνέχεια σχηματίζονται οι παραδοχές του μοντέλου αυτού. Επιπλέον παρουσιάζεται ο μαθηματικός χειρισμός των εξισώσεων και των οριακών συνθηκών του laser, καθώς και η δημιουργία του κώδικα για το OpenFOAM και το μοντέλο για το COMSOL. Επιπλέον, γίνεται εκτενής περιγραφή της διαδικασίας που ακολουθείται για την μοντελοποίηση, καθώς και παρουσίαση της κατάστρωσης του μοντέλου στα δύο αυτά λογισμικά. Στο OpenFOAM, χρησιμοποιήθηκε ο επιλύτης *laplacianfoam*, ενώ στο COMSOL, το Heat Transfer in Solids Module. Τα αποτελέσματα συγκρίθηκαν σε τρεις διαφορετικές ταχύτητες laser, καθώς επίσης και ο χρόνος εκτέλεσης, η διαχείριση πόρων του λειτουργικού συστήματος και το περιβάλλον εργασίας χρήστη. Κατά τη σύγκριση, και τα δύο λογισμικά λειτούργησαν επαρκώς και συνάγεται το συμπέρασμα ότι για διαφορετική εφαρμογή κάθε λογισμικό μπορεί να είναι πιο ικανό από το άλλο.

Συμπερασματικά, ο αναγνώστης θα είναι σε θέση να απαντήσει σε ερωτήσεις όπως: ποια είναι η μεθοδολογία μοντελοποίησης για τα δύο προγράμματα; πώς μπορεί να μοντελοποιηθεί η μεταφορά θερμότητας με αγωγή στη κατεργασία SLM; πόσο πολύ μπορεί να εμπλουτιστεί η προσομοίωση της κατεργασίας αυτής; ποιο λογισμικό είναι το πιο κατάλληλο για ποια εφαρμογή; πώς τα προγράμματα OpenFOAM και COMSOL διαχειρίζονται τους πόρους του υπολογιστή;

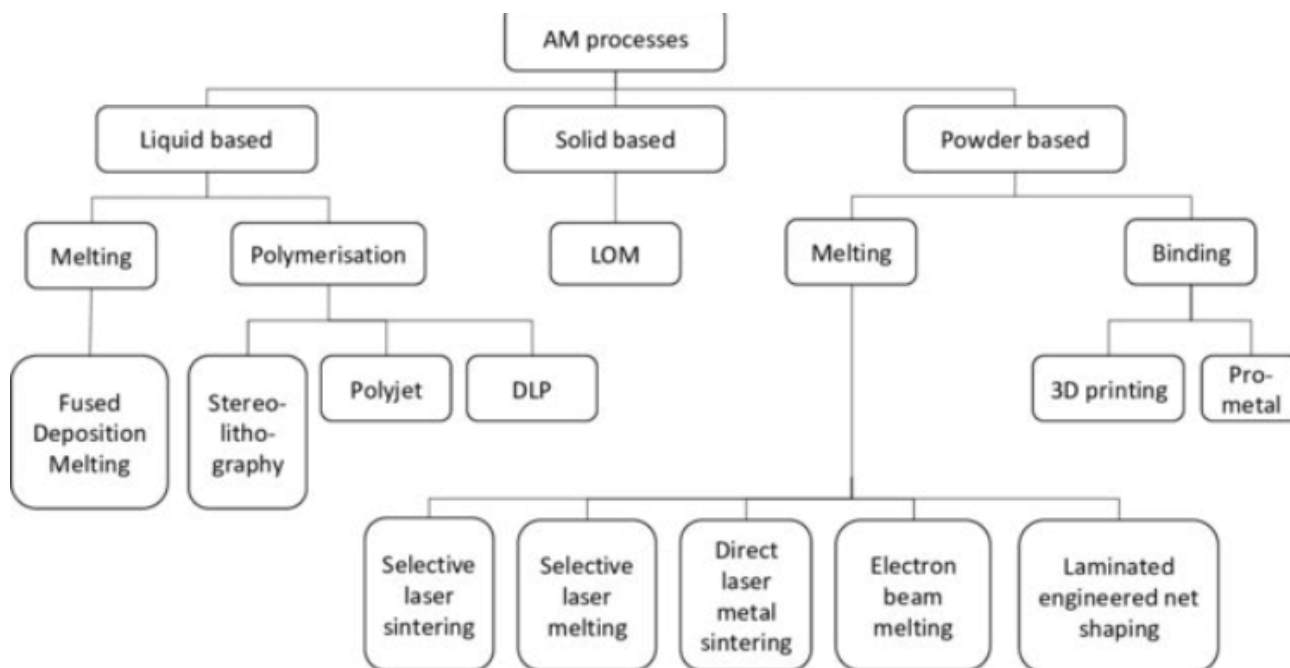
1. ΕΙΣΑΓΩΓΗ

Objectives

Ο αναγνώστης στο τέλος του Κεφαλαίου 1 θα είναι εξοικειωμένος με τις κατεργασίες προσθήκης υλικού και ειδικά την τεχνολογία SLM. Επίσης, καθώς περιλαμβάνεται μια εκτεταμένη παρουσίαση του λογισμικού FEM (εμπορικά διαθέσιμο και ανοιχτού κώδικα), μπορούν να γίνουν αντιληπτά τα πλεονεκτήματα και τα μειονεκτήματα της επιλογής του ενός από τα δύο λογισμικά. Τέλος, πραγματοποιείται μια παρουσίαση των βασικών συστημάτων από τα οποία αποτελείται μια μηχανή SLM.

1.1 ΤΕΧΝΟΛΟΓΙΑ SLM

Οι κατεργασίες με προσθήκη υλικού έχουν ήδη εισέλθει στη βιομηχανία με επιτυχία και γίνεται ενδελεχής έρευνα σε αυτόν τον τομέα. Οι τεχνικές που χρησιμοποιούνται μέχρι σήμερα παρουσιάζονται στην παρακάτω εικόνα:



ΣΧΗΜΑ 1.1 ΤΕΧΝΟΛΟΓΙΕΣ ΠΡΟΣΘΗΚΗΣ ΥΛΙΚΟΥ [1] FIG 1

Η Selective Laser Melting (SLM) ή Laser Powder Bed Fusion (LPBF) είναι μια κατεργασία προσθήκης υλικού (AM) που μπορεί να παράγει σύνθετες τρισδιάστατες γεωμετρίες μέσω της τήξης και της στερεοποίησης της πούδρας που χρησιμοποιείται. Αυτή η διαδικασία επαναλαμβάνεται για κάθε στρώση του sliced model που παράγεται από λογισμικό σχεδίασης με τη βοήθεια υπολογιστή[2]

Η παραπάνω τεχνολογία έχει ορισμένα κύρια χαρακτηριστικά κοινά σε άλλες παρόμοιες τεχνολογίες (SLS, DMLS κ.λπ.). Αυτά περιλαμβάνουν:

- Μια θερμική πηγή, η οποία λιώνει τα σωματίδια πούδρας και τα συγχωνεύει μαζί (laser).
- Ένας μηχανισμός για τον έλεγχο της τήξης των σωματιδίων σε μια συγκεκριμένη περιοχή.
- Δυνατότητα προσθήκης επόμενης στρώσης.
- Δυνατότητα εξομάλυνσης κάθε στρώσης, πριν από την προσθήκη της επόμενης στρώσης.

1.3 ΠΛΕΟΝΕΚΤΗΜΑΤΑ ΚΑΙ ΜΕΙΟΝΕΚΤΗΜΑΤΑ

Ορισμένα πλεονεκτήματα αυτής της διαδικασίας, σε σύγκριση με άλλες τεχνικές προσθήκης υλικού και κλασικές κατεργασίες, είναι:

- Υψηλή πυκνότητα και αντοχή των εξαρτημάτων.
- Ανακύκλωση της μη τηγμένης πούδρας με αποτέλεσμα την ελάχιστη σπατάλη υλικών.
- Δημιουργία εξαρτημάτων με περίπλοκες τρισδιάστατες γεωμετρίες.
- Δεν παράγεται green part. Έτσι, δεν υπάρχει ανάγκη για επόμενες φάσεις της κατεργασίας, όπως συσσωμάτωση.

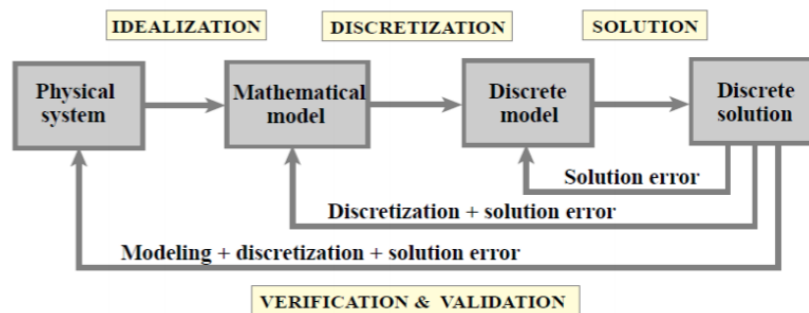
Τα θετικά σημεία της κατεργασίας είναι αρκετά για να δικαιολογήσουν την εμφάνισή της σε πολλούς κλάδους, αν και τα μειονεκτήματά της δεν είναι αμελητέα. Παρακάτω παρουσιάζονται μερικά από αυτά:

- Δαπανηρή κατεργασία, ειδικά για εξαρτήματα που δεν έχουν σχεδιαστεί για κατασκευή με αυτή τον τρόπο.
- Περιορισμένες γεωμετρικές ανοχές και διαστάσεις.
- Επιφανειακή κατεργασία απαιτείται συνήθως μετά τη διαδικασία.

1.5 ΛΟΓΙΣΜΙΚΟ ΠΕΠΕΡΑΣΜΕΝΩΝ ΣΤΟΙΧΕΙΩΝ

1.5.1 ΕΙΣΑΓΩΓΗ

Οι αριθμητικές τεχνικές έχουν αναδυθεί και εξελιχθεί για να ικανοποιήσουν τις τρέχουσες ανάγκες πολλών τομέων της μηχανικής. Μία από αυτές, είναι η Μέθοδος Πεπερασμένων Στοιχείων (FEM), η οποία δίνει μια προσέγγιση στις κύριες εξισώσεις. Αντί της επίλυσης των αναλυτικών εξισώσεων, η περιοχή λύσης μπορεί να προσεγγιστεί με την επίλυση των εξισώσεων για ένα σύνολο διακριτών σημείων. Μπορούν να πραγματοποιηθούν προσομοιώσεις σε σύνθετα σχήματα, καθώς υπάρχουν διαφορετικοί τύποι στοιχείων που καλύπτουν διαφορετικά προβλήματα[3].



ΣΧΗΜΑ 1.10 ΔΙΑΓΡΑΜΜΑ ΡΟΗΣ ΜΕΘΟΔΟΥ ΠΕΠΕΡΑΣΜΕΝΩΝ ΣΤΟΙΧΕΙΩΝ [3]

1.5.2 ΛΟΓΙΣΜΙΚΟ ΑΝΟΙΚΤΟΥ ΚΩΔΙΚΑ

Το λογισμικό ανοικτού κώδικα είναι λογισμικό με άδεια χρήσης στην οποία ο κάτοχος των πνευματικών δικαιωμάτων παραχωρεί τα δικαιώματα χρήσης, μελέτης και αλλαγής του πηγαίου κώδικα. Αυτό είναι πολύ αναγκαίο σε περιπτώσεις όπου ο προγραμματισμός ενός προσαρμοσμένου επιλύτη (solver) είναι αναπόφευκτος. Τέτοια λογισμικά είναι το OpenFOAM και το Kratos Multiphysics.

1.5.3 ΕΝΑΛΛΑΚΤΙΚΟ ΕΜΠΟΡΙΚΑ ΔΙΑΘΕΣΙΜΟ ΛΟΓΙΣΜΙΚΟ

Το εμπορικά διαθέσιμο λογισμικό είναι ένα λογισμικό υπολογιστή που βρίσκεται υπό άδεια στην οποία ο κάτοχος των πνευματικών δικαιωμάτων δεν επιτρέπει καμία τροποποίηση του λογισμικού ή αναδιανομή του. Τέτοιο είναι COMSOL, ANSYS κ.λπ.

2. ΒΑΣΙΚΗ ΘΕΩΡΙΑ – STATE OF THE ART

ΣΤΟΧΟΙ

Αυτό το κεφάλαιο θα εξοικειώσει τον αναγνώστη με τις κύριες εξισώσεις πίσω από το λογισμικό FEM. Επιπλέον θα παρουσιαστεί μια εξήγηση σε ορισμένα από τα state-of-the-art μοντέλα SLM.

2.1 ΚΥΡΙΕΣ ΕΞΙΣΩΣΕΙΣ

Το μοντέλο που δημιουργήθηκε σε αυτή τη διπλωματική είναι ένα απλό μοντέλο μεταφοράς θερμότητας με αγωγή, για να διερευνήσει τις διαφορές των δύο λογισμικών. Έτσι, οι κυρίαρχες εξισώσεις είναι,

$$\rho C_p \frac{\partial T}{\partial t} - \nabla \cdot (k \nabla T) = 0 \quad \text{Eq. (2.2)}$$

και,

$$k \nabla T = q_{conv} + q_{rad} + q_{abl} \quad \text{Eq. (2.3)}$$

Στο δεξί μέρος της εξίσωσης αθροίζεται η θερμότητα κατά τη συναγωγή, την ακτινοβολία και την εξάτμιση του υλικού. Σε αυτή την περίπτωση, μόνο η θερμότητα συναγωγής μοντελοποιείται, έτσι q_{rad} και q_{abl} είναι ίσο με μηδέν.

2.2 STATE OF THE ART

2.2.1 ΑΝΑΛΥΣΗ ΤΗΣ ΔΥΝΑΜΙΚΗΣ ΤΗΣ ΚΑΤΕΡΓΑΣΙΑΣ ΣΥΓΚΟΛΛΗΣΗΣ ΜΕ LASER

Η ανάγκη για ανάλυση και ανάπτυξη προσομοιώσεων melt pool είναι δυνατή να προέλθει και από άλλες κατεργασίες, όπως η διαδικασία συγκόλλησης με laser. Χρησιμοποιώντας το OpenFOAM ως κύριο λογισμικό FEM είναι δυνατόν να δημιουργηθεί μια προσομοίωση multi physics με προσαρμοστική βελτίωση πλέγματος. Επιπλέον, είναι δυνατόν να συνδυαστεί ο μηχανισμός δημιουργίας πορώδους και τα φαινόμενα στερεοποίησης [4].

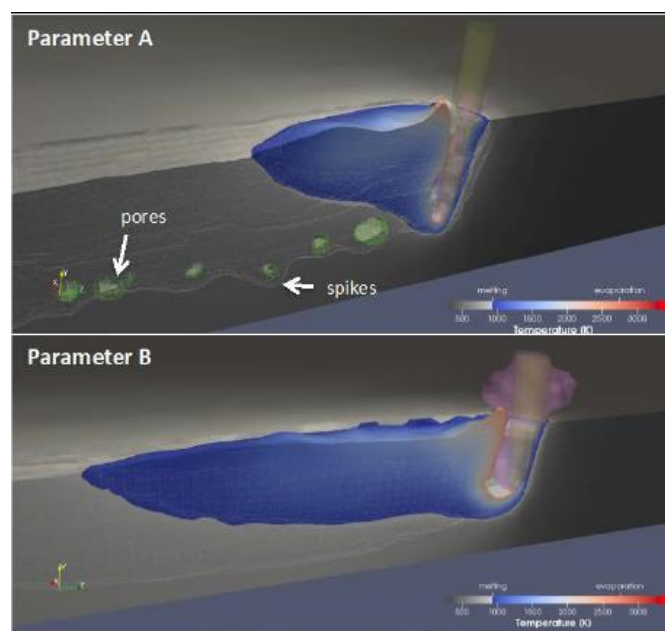
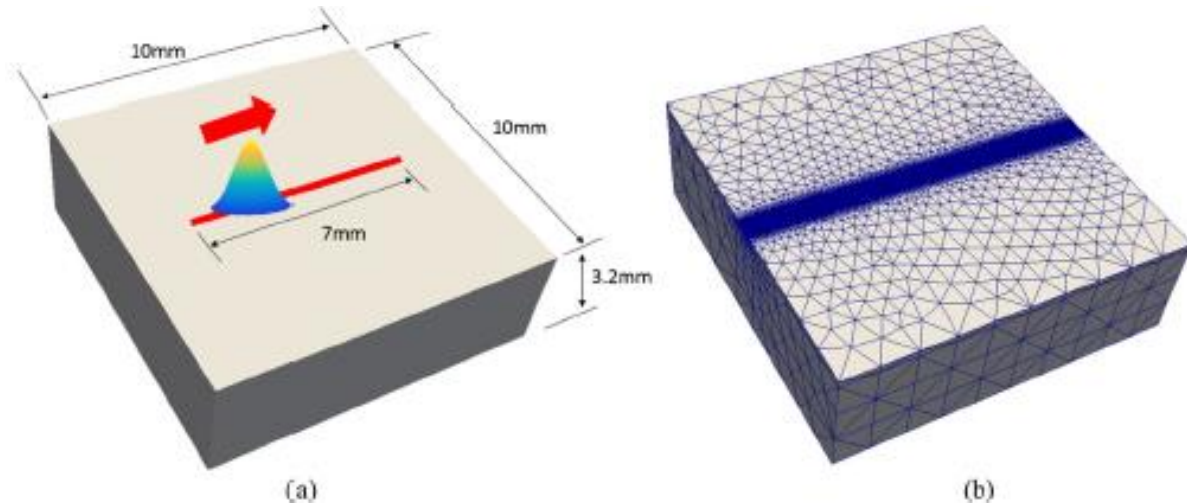


FIG. 2.5 ΜΟΡΦΗ MELT POOL [4]

2.2.2 ΠΡΟΣΟΜΟΙΩΣΕΙΣ ΓΙΑ ΤΗΝ ΠΑΡΑΣΚΕΥΗ ΜΕΤΑΛΛΙΚΩΝ ΑΝΤΙΚΕΙΜΕΝΩΝ ΜΕ ΠΡΟΣΘΗΚΗ ΥΛΙΚΟΥ ΧΩΡΙΣ ΠΛΕΓΜΑ

Ορισμένοι τύποι προβλημάτων προσομοίωσης δεν ήταν σε θέση να κλιμακωθούν αρκετά καλά με το υλικό για να τα λύσουν με συμβατικές μεθόδους. Πρέπει να ληφθούν καινοτόμες προσεγγίσεις για την επίλυση προβλημάτων σε αυτόν τον τομέα για να αλλάξει ριζικά η ροή εργασίας των προσομοιώσεων. Χρησιμοποιώντας λύσεις χωρίς πλέγμα είναι δυνατόν να αντιμετωπιστούν ορισμένα από τα προβλήματα, αν και δεν χρησιμοποιείται ευρέως ως καινούργια μέθοδος διότι έχει ορισμένα μειονεκτήματα [5].

Παρακάτω είναι ορατή η μέθοδος πλέγματος για προσομοίωση διεργασίας SLM και μια προσέγγιση χωρίς πλέγμα.



ΣΧΗΜΑ 2.8 ΔΗΜΙΟΥΡΓΙΑ ΠΛΕΓΜΑΤΟΣ ΓΙΑ ΠΡΟΣΟΜΟΙΩΣΗ ΤΗΣ SLM [5]

Το πλέγμα είναι εξαιρετικά λεπτό στη διαδρομή laser και αυτό καταναλώνει πολλούς πόρους υπολογιστή για να βρει λύση, καθιστώντας έτσι το χρόνο εκτέλεσης μεγαλύτερο.

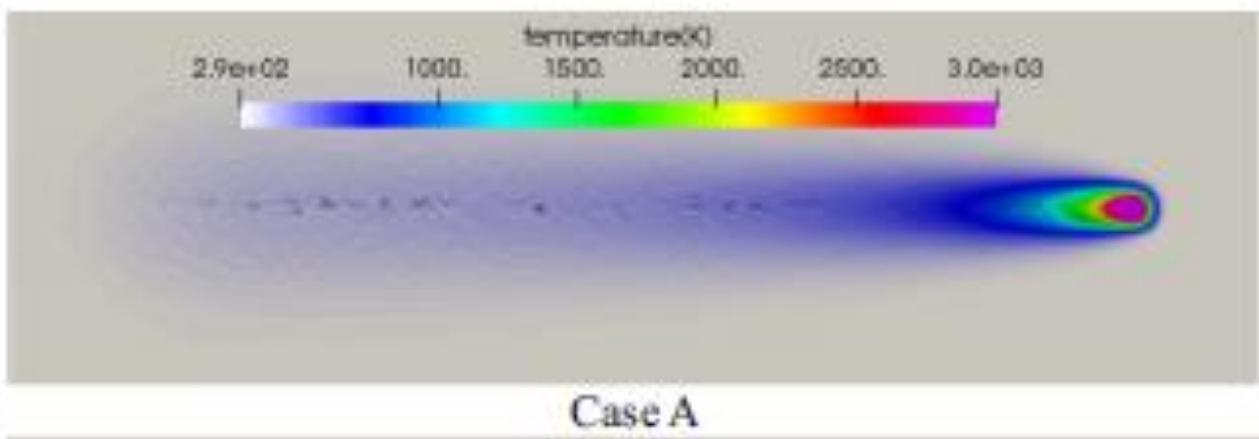
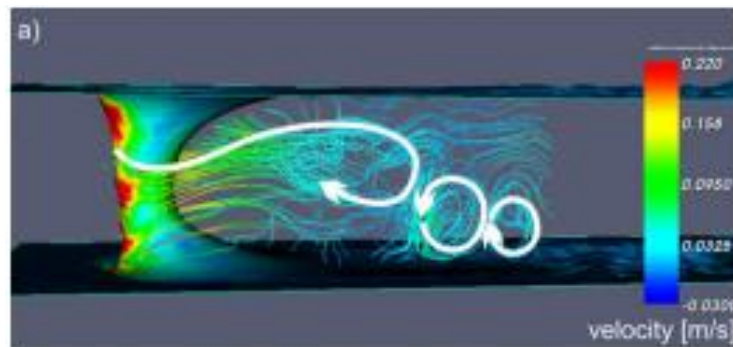


FIG 2.7 ΠΡΟΣΟΜΟΙΩΣΗ SINGLE TRACK ΧΩΡΙΣ ΠΛΕΓΜΑ [5]

2.2.3 ΑΡΘΡΑ ΓΙΑ ΤΗ ΣΥΓΧΩΝΕΥΣΗ ΠΟΛΛΩΝ ΜΟΝΤΕΛΩΝ ΦΥΣΙΚΗΣ ΤΗΣ ΚΑΤΕΡΓΑΣΙΑΣ

Τέλος, είναι ευρέως αναγκαίο ένα καθολικό μοντέλο για τις κατεργασίες προσθήκης υλικού, όπως η κατεργασία SLM. Αυτό είναι γνωστό από ερευνητές σε όλον τον κόσμο και έχει καταβληθεί μεγάλη προσπάθεια για να ολοκληρωθεί ένα τέτοιο μοντέλο.

Η δυναμική ρευστών, η μεταφορά θερμότητας, η οπτική και μια προσέγγιση προσομοίωσης σε πολλαπλές κλίμακες μεγέθους είναι μερικά από τα πράγματα που πρέπει να ενωθούν προκειμένου να παραχθεί ένα καθολικό μοντέλο.



ΣΧΗΜΑ 2.10 ΡΕΥΣΤΟΔΥΝΑΜΙΚΗ ΠΡΟΣΟΜΟΙΩΣΗ ΤΟΥ MELT POOL [6]

Καταλήγοντας, όπως προαναφέρθηκε, η ανάγκη για πληρέστερα μοντέλα της διαδικασίας SLM είναι υποχρεωτική προκειμένου να κατανοήσουμε τους μηχανισμούς της. Έτσι, οι ερευνητές προσπαθούν συνεχώς να αναπτύξουν και να τελειοποιήσουν τις θεωρίες τους και να τις δοκιμάσουν μέσω των περιβαλλόντων προσομοίωσης. Ωστόσο, αυτά τα μοντέλα χρειάζονται πολλούς υπολογιστικούς πόρους που δεν είναι διαθέσιμοι από όλους. Έτσι, σε αυτή τη διπλωματική εργασία δημιουργήθηκε ένα απλό, αλλά αποτελεσματικό, θερμικό μοντέλο για να δοκιμάσει τα δύο λογισμικά και να δείξει στην ερευνητική κοινότητα τις επιλογές που υπάρχουν όσον αφορά στην αποτελεσματική μοντελοποίηση της κατεργασίας SLM.

2.2.5 ANSYS MODULE ΚΑΤΕΡΓΑΣΙΩΝ ΠΡΟΣΘΗΚΗΣ ΥΛΙΚΟΥ

Μια άλλη, νέα, μέθοδος προσομοίωσης της διαδικασίας SLM είναι το module AM του λογισμικού Ansys. Το λογισμικό αυτό μπορεί να ελέγξει αν ένα σχέδιο πληροί τις προϋποθέσεις για εκτύπωση ή και να συλλέξει δεδομένα για τη διαχείριση της κατεργασίας. Μπορεί επίσης να προσομοιώσει την κατεργασία σε ολόκληρο το εύρος της εκτύπωσης για τον υπολογισμό των παραμενουσών τάσεων και της συρρίκνωσης για να αντισταθμιστεί το σφάλμα στο αρχείο STL. Τέλος, το λογισμικό αυτό μπορεί να αναλύσει τη γεωμετρία του αρχείου και μπορεί να προβλέψει την αποτυχία κατά την εκτύπωση [7].



ΣΧΗΜΑ. 2.9 ΕΥΡΟΣ ΧΡΗΣΗΣ ΤΟΥ ANSYS AM MODULE

3. ΠΑΡΑΔΟΧΕΣ ΜΟΝΤΕΛΟΥ ΚΑΙ ΙΔΙΟΤΗΤΕΣ ΥΛΙΚΟΥ

3.1 ΠΑΡΑΔΟΧΕΣ ΜΟΝΤΕΛΟΥ ΚΑΤΑ ΤΗΝ ΠΡΟΣΟΜΟΙΩΣΗ ΤΗΣ ΚΑΤΕΡΓΑΣΙΑΣ SLM

Πολλοί παράγοντες εμπλέκονται σε αυτή τη διαδικασία AM, οπότε έπρεπε να θεσπιστούν περιορισμοί και συμβιβασμοί ως παραδοχές σε αυτό το έργο για τη δημιουργία ενός λειτουργικού μοντέλου. Ως εκ τούτου, οι παραδοχές εμφανίζονται παρακάτω.

- Δεν υλοποιήθηκε μοντέλο στερεοποίησης.
- Η ρευστοδυναμική του melt pool δεν υλοποιήθηκε σε αυτό το έργο.
- Δεν υλοποιήθηκε μοντέλο πορώδους.
- Το μοντέλο απώλειας υλικού δεν συμπεριλήφθηκε σε αυτό το έργο.
- Μια γκαουσιανή διανομή εφαρμόστηκε για την ακτίνα λέιζερ.
- Δεν υπάρχει σχηματισμός keyhole έτσι, ο μηχανισμός ανάκλασης είναι ήσσονος σημασίας. Για αυτό δεν υλοποιήθηκε μοντέλο δευτερεύουσας ανάκλασης της δέσμης του laser.
- Οι δυνάμεις που δημιουργούνται από την αλληλεπίδραση πλάσματος με την melt pool δεν εφαρμόζονται σε αυτό το μοντέλο, ούτε η θωράκιση πλάσματος (plasma shielding).
- Στην προσομοίωση δεν εξετάστηκε η απώλεια θερμότητας κατά την αλλαγή φάσης (λανθάνουσα θερμότητα).
- Το προφίλ της δέσμης laser είχε κυκλικό σχήμα.
- Ο συντελεστής μεταφοράς θερμότητας, κατά την συναγωγή, μεταξύ του υλικού και του περιβάλλοντος θεωρήθηκε σταθερός και ανεξάρτητος από τη θερμοκρασία.

3.2 ΙΔΙΟΤΗΤΕΣ ΥΛΙΚΟΥ

Το υλικό είναι καθαρό Αλουμίνιο. Η βιβλιοθήκη υλικών του λογισμικού COMSOL έχει τις θερμοφυσικές ιδιότητες των υλικών εξαρτώμενες από την θερμοκρασία. Για λόγους απλούστευσης στην παρούσα εργασία χρησιμοποιούνται σταθερές τιμές.

Aluminum properties	Value	Unit
Density ρ	2702	kg/m ³
Heat Transfer Coefficient for heating h	150	W/m ² /K
Thermal Conductivity k	10	W/mK
Material thermal diffusivity DT	8e-05	m ² /s

ΠΙΝΑΚΑΣ 3.1 ΙΔΙΟΤΗΤΕΣ ΑΛΟΥΜΙΝΙΟΥ

4. ΑΝΑΠΤΥΞΗ ΜΟΝΤΕΛΟΥ ΜΕ ΧΡΗΣΗ OPENFOAM

ΣΤΟΧΟΙ

Σε αυτό το κεφάλαιο θα παρουσιαστεί μια σύντομη εισαγωγή στη μοντελοποίηση με το OpenFOAM. Μετά την ανάγνωση του κεφαλαίου, ο αναγνώστης, θα γνωρίζει τη μεθοδολογία μοντελοποίησης στο λογισμικό OpenFOAM.

4.1 ΜΟΝΤΕΛΟ

Για απλή μεταφορά θερμότητας χρησιμοποιήθηκε ο επιλύτης LaplacianFoam. Επιπλέον, το πρόβλημα της μοντελοποίησης laser στο OpenFOAM λύθηκε με την εισαγωγή του laser ως οριακή συνθήκη (BC) με δέσμη γκαουσιανής κατανομής. Εγκαταστάθηκε ως μια ελεύθερη βιβλιοθήκη στην προϋπάρχουσα βιβλιοθήκη OpenFOAM και στη συνέχεια εφαρμόστηκε σε έναν τυπικό επιλύτη, όπως τον *laplacianFoam* [8].

4.1.1 LAPLACIAN ΕΠΙΛΥΤΗΣ (SOLVER)

LaplacianFoam επιλύτης: Αυτός είναι ένας βασικός επιλύτης για τη μεταφορά θερμότητας. Μπορεί να προσομοιώσει τόσο σταθερά όσο και δυναμικά προβλήματα. Ο επιλύτης για να βρεί την θερμοκρασία T λύνει την Εξίσωση 4.1:

$$\frac{\partial}{\partial t}(T) - \nabla \cdot (D_T \nabla T) = S_T \quad \text{Eq. (4.1)}$$

η οποία είναι όμοια με την καταστατική εξίσωση 2.1 που περιγράφεται στο κεφάλαιο 2. Ο όρος D_T είναι ο συντελεστής θερμικής διάχυσης, όπως ο όρος k που χρησιμοποιείται στην εξίσωση 2.3 [9].

Αξίζει να σημειωθεί ότι, χρησιμοποιώντας συστήματα πρώτου βαθμού η λύση θα είναι λιγότερο ακριβής, αλλά θα χρειαστεί λιγότερο χρόνο επεξεργασίας από τις δευτέρου βαθμού λύσεις.

4.1.2 ΟΡΙΑΚΕΣ ΣΥΝΘΗΚΕΣ LASER

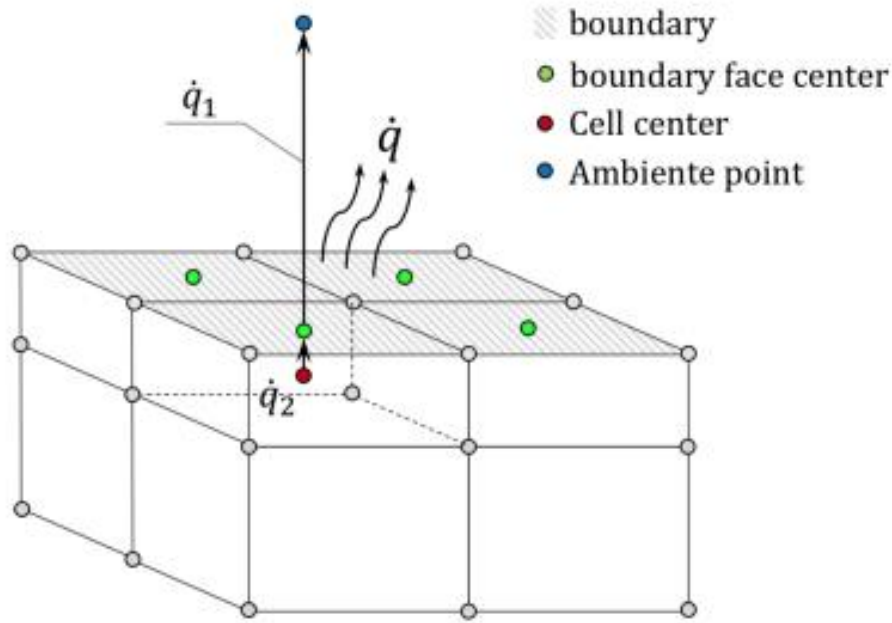
Η ακτίνα λέιζερ διαμορφώνεται ως κατανεμημένη πηγή θερμότητας με κατανομή Gauss και περιγράφεται από την εξίσωση,

$$f_{Gauss}(x,y) = \frac{1}{2\pi\sigma_x\sigma_y\sqrt{1-\rho_{shape}^2}} \exp\left[-\frac{1}{2(1-\rho_{shape}^2)}\left(\frac{x^2}{\sigma_x^2} + \frac{y^2}{\sigma_y^2} - \frac{2\rho_{shape}xy}{\sigma_x\sigma_y}\right)\right] \quad \text{Eq. (4.2)}$$

4.1.3 ΟΡΙΑΚΕΣ ΣΥΝΘΗΚΕΣ ΣΥΝΑΓΩΓΗΣ

Εφαρμόστηκε μια οριακή συνθήκη για να μιμηθεί την ψύξη στην επιφάνεια.

Για να είναι σε θέση να υπολογιστεί η οριακή συνθήκη, η διαφορά μεταξύ της θερμοκρασίας της επιφάνειας και του περιβάλλοντος έπρεπε να αξιολογηθεί και να χρησιμοποιηθεί. Η θερμοκρασία, T , μετράται σε $[K]$, η απόσταση δ μεταξύ του κέντρου των κελιών και του κεντρικού σημείου της επιφάνειας των κελιών, μετράται σε $[m]$. Η θερμική αγωγιμότητα, k , μετράται σε $\left[\frac{W}{mK}\right]$, ο συντελεστής μεταφοράς θερμότητας με συναγωγή $\left[\frac{W}{m^2K}\right]$ και η θερμότητα \dot{q} , σε $\left[\frac{W}{m^2}\right]$.



ΣΧΗΜΑ. 2.3 ΥΛΟΠΟΙΗΣΗ ΟΡΙΑΚΗΣ ΣΥΝΘΗΚΗΣ ΣΥΝΑΓΩΓΗΣ ΣΤΟ ΠΛΕΓΜΑ

Από την εξίσωση 4.5 προκύπτει ότι η θερμότητα στο υλικό, μετρούμενη στη δεξιά πλευρά της εξίσωσης πρέπει να είναι ίση με αυτή που μετράται στην άλλη πλευρά της διεπαφής υλικού-περιβάλλοντος.

$$h \cdot (T_{Face} - T_{Amb}) = k \cdot \frac{T_{Cell} - T_{Face}}{\delta} \quad \text{Eq. (4.5)}$$

λόγω της διατήρησης της ενέργειας,

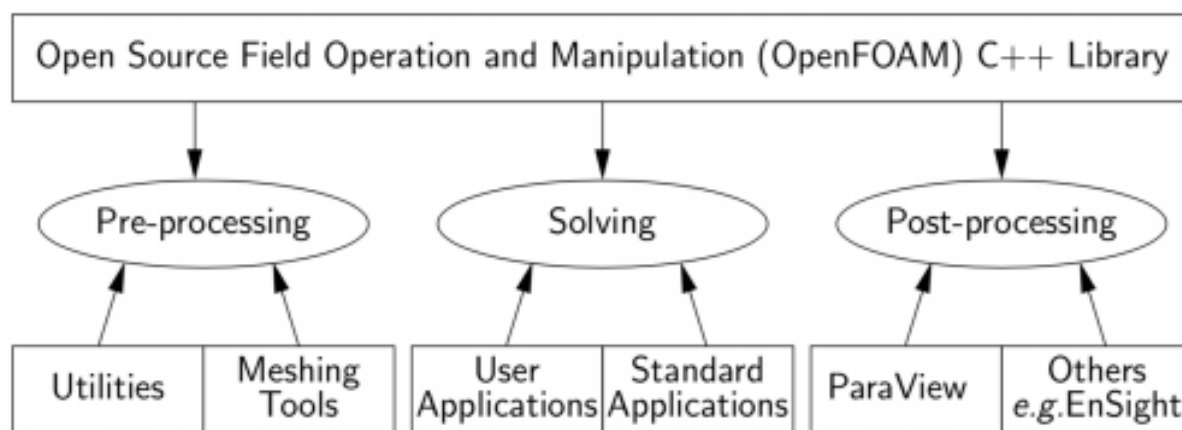
$$\dot{q}_1 = \dot{q}_2 \quad \text{Eq. (4.6)}$$

όπου, η κουκκίδα στον όρο q σημαίνει διάνυσμα κάθετο στην επιφάνεια. Έτσι, η θερμότητα στο εξωτερικό του ορίου είναι,

$$-\dot{q}_1 = h \cdot (T_{Face} - T_{Amb}) \quad \text{Eq. (4.7)}$$

4.2 ΠΕΡΙΒΑΛΛΟΝ OPENFOAM

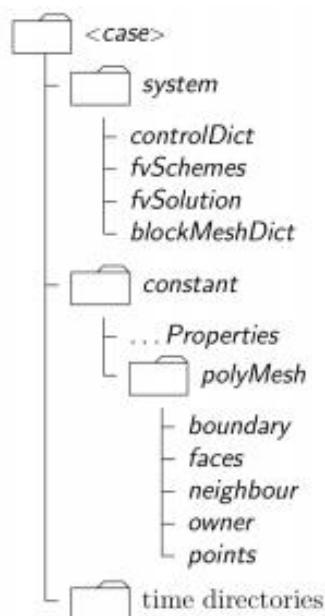
Open-source Field Operation and Manipulation είναι μια βιβλιοθήκη γραμμένη σε C++ για λύση πολύπλοκων προβλημάτων μηχανικής με την μέθοδο πεπερασμένων στοιχείων. Παρακάτω η δομή μιας προσομοίωσης με αυτό το λογισμικό είναι ορατή.



ΣΧΗΜΑ. 4.1 ΔΟΜΗ OPENFOAM [10]

Όπως φαίνεται στο Σχήμα 4.1, η προεπεξεργασία μπορεί να πραγματοποιηθεί σε προγράμματα CAD ή γράφοντας κώδικα για να δημιουργηθεί ένα πλέγμα απευθείας στο OpenFOAM. Η μετα-επεξεργασία γίνεται κυρίως στο ParaView, για μια γραφική ερμηνεία των αρχείων εξόδου από το OpenFOAM [10]

Μια επισκόπηση της δομής του καταλόγου παρουσιάζεται στο σχήμα 4.2. Ο φάκελος <case> είναι ο κύριος φάκελος και θα πρέπει να μετονομαστεί όπως επιθυμεί ο χρήστης. Υπάρχουν τρεις κύριοι υποφάκελοι, system, constant και time directories.



ΣΧΗΜΑ. 4.2 ΔΟΜΗ ΦΑΚΕΛΟΥ <CASE> [10]

4.3 ΠΛΕΓΜΑ ΚΑΙ ΓΕΩΜΕΤΡΙΑ

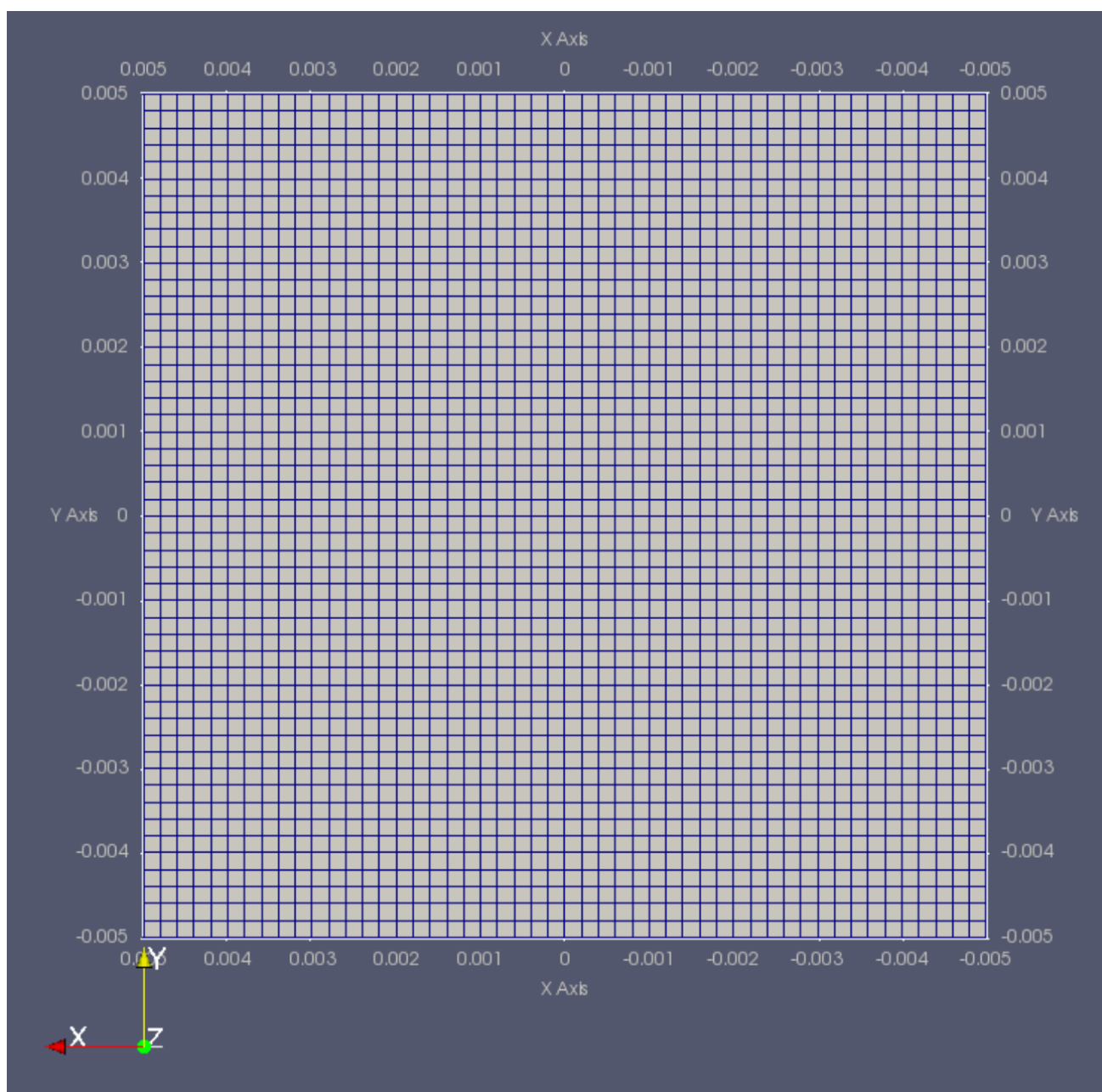
Ένα τρισδιάστατο πλέγμα δημιουργήθηκε για την παρούσα εργασία. Το πλέγμα δημιουργήθηκε στο OpenFOAM. Οι διαστάσεις είναι,

Dimensions of Box [mm]	X	Y	Z
	10	10	10

TABLE 4.1 ΔΙΑΣΤΑΣΕΙΣ ΓΕΩΜΕΤΡΙΑΣ

Το πλέγμα είναι κατασκευασμένο από 25000 εξάεδρα στοιχεία συνολικά.

Μια κάτοψη της γεωμετρίας πλέγματος παρουσιάζεται εδώ,



ΣΧΗΜΑ. 4.5 ΚΑΤΟΨΗ ΠΛΕΓΜΑΤΟΣ

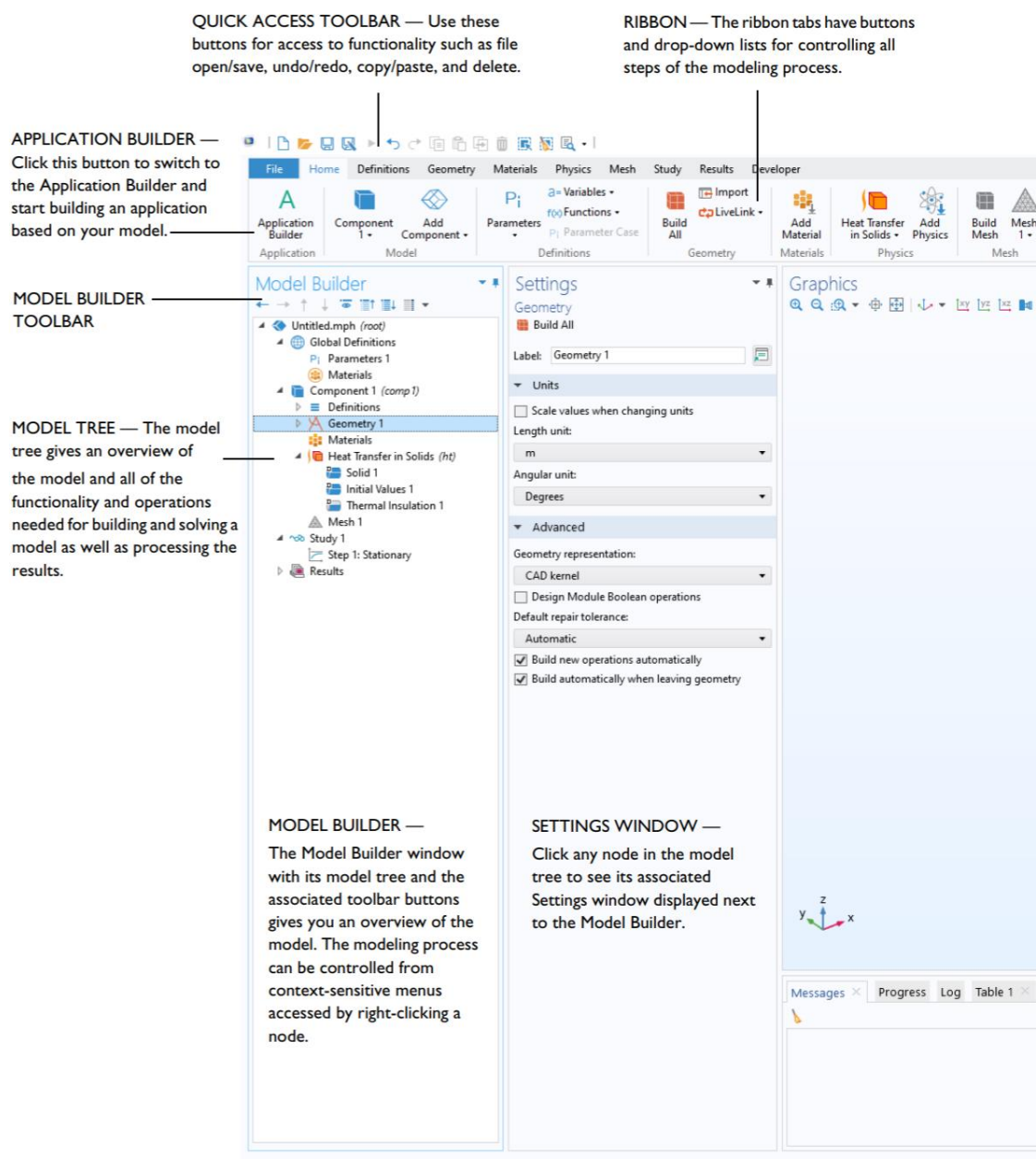
5. ΑΝΑΠΤΥΞΗ ΜΟΝΤΕΛΟΥ ΜΕ ΧΡΗΣΗ ΤΟΥ COMSOL

ΣΤΟΧΟΙ

Στο κεφάλαιο αυτό θα γίνει μια εισαγωγή στη μοντελοποίηση με το λογισμικό COMSOL. Στο τέλος του κεφαλαίου ο αναγνώστης θα εξοικειωθεί με τη ροή εργασίας μοντελοποίησης στο COMSOL.

5.1 COMSOL

Το COMSOL είναι ένα εμπορικά διαθέσιμο λογισμικό FEM το οποίο περιλαμβάνει γραφικό περιβάλλον εργασίας (GUI). Είναι ένα λογισμικό all-in-one, καθώς παρέχει την δυνατότητα δημιουργίας σχεδίων 2-3D και επεξεργασίας των αποτελεσμάτων μετά την προσομοίωση.

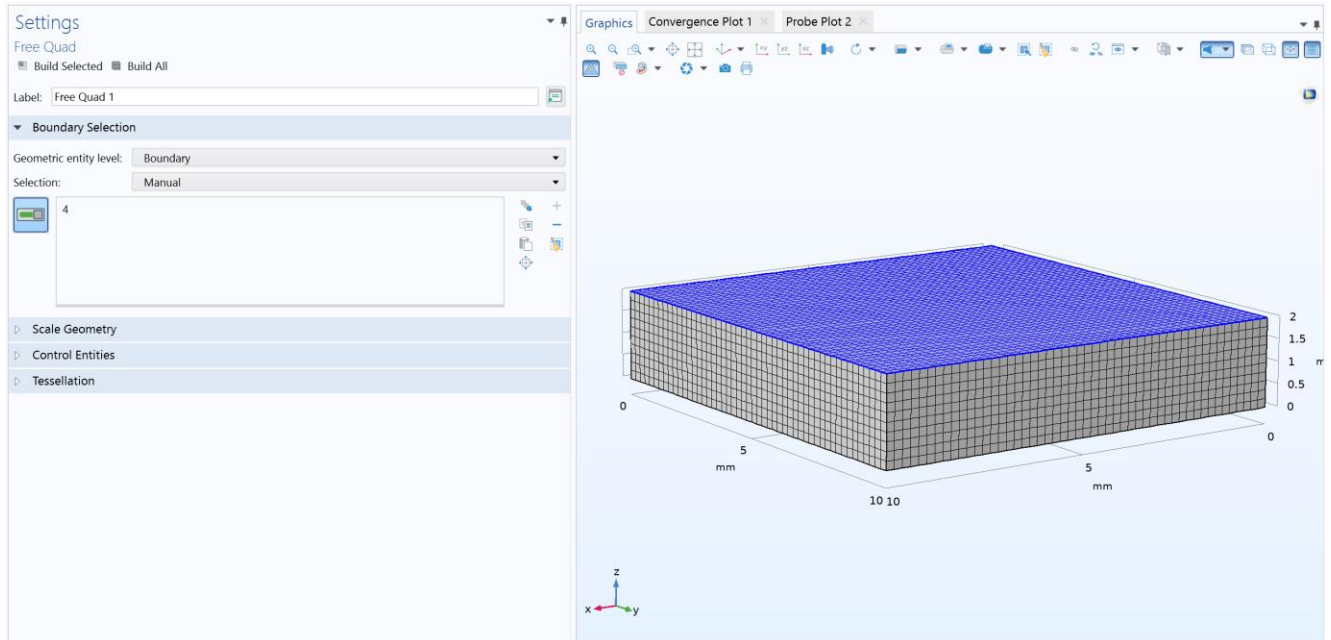


ΣΧΗΜΑ. 5.1 COMSOL MULTIPHYSICS ΓΡΑΦΙΚΟ ΠΕΡΙΒΑΛΛΟΝ [11]

Στο σχήμα 5.1, είναι εμφανείς όλες βασικές πληροφορίες για το περιβάλλον εργασίας του λογισμικού COMSOL.

5.2.1 ΓΕΩΜΕΤΡΙΑ ΚΑΙ ΠΛΕΓΜΑ

Χρησιμοποιώντας την καρτέλα πλέγματος, είναι ορατή η επιλογή ενός κουμπιού Free Quad. Το Free Quad είναι ένας τρόπος δημιουργίας μη δομημένων τετράγωνων επιφανειακών (2D) στοιχείων. Στην καρτέλα Ρυθμίσεις της εντολής Free Quad, το *Geometric entity level* έχει οριστεί σε Boundary και ο χρήστης θα πρέπει να επιλέξει μια επιφάνεια της γεωμετρίας στην οποία θα εφαρμοστεί αυτό το πλέγμα. Στην περίπτωση αυτή επιλέγεται η επιφάνεια της κάτοψης.



ΣΧΗΜΑ. 5.5 ΡΥΘΜΙΣΕΙΣ FREE QUAD

Μετά το τέλος των παραπάνω βημάτων, ο χρήστης θα πρέπει να επιλέξει την Sweep εντολή για να επεκτείνει αυτά τα στοιχεία στην άλλη πλευρά της γεωμετρίας και να τα κάνει τρισδιάστατα εξάεδρα στοιχεία. Το αποτέλεσμα του πλέγματος φαίνεται στο σχήμα 5.5. Το πλέγμα που παράγεται αποτελείται από 25000 εξάεδρα στοιχεία συνολικά.

5.2.3 PHYSICS

Για να επιλέξει τη φυσική της προσομοίωσης, ο χρήστης θα πρέπει να πλοηγηθεί στην καρτέλα Physics και να επιλέξει την επιθυμητή ενότητα για την περίπτωση που αναπτύσσει. Υπάρχουν διαθέσιμες ενότητες single-physics και ενότητες multi physics στο COMSOL. Στη συγκεκριμένη περίπτωση χρησιμοποιήθηκε η παρακάτω ενότητα,

- Heat Transfer in Solids (ht)
 - Solid 1
 - Initial Values 1
 - Thermal Insulation 1
 - Heat Flux 1
 - Surface-to-Ambient Radiation 1
 - Deposited Beam Power 1

ΣΧΗΜΑ. 5.7 HEAT TRANSFER IN SOLIDS

Καταστατική εξίσωση επιλύτη του COMSOL:

$$\rho C_p \frac{\partial T}{\partial t} + \rho C_p \mathbf{u} \cdot \nabla T + \nabla \cdot \mathbf{q} = Q + Q_{\text{ted}}$$

$$\mathbf{q} = -k \nabla T$$

Eq. 5.1

Η Εξίσωση 5.1 είναι η Εξίσωση 2.1, αλλά στην μορφή του επιλύτη του COMSOL.

Δέσμη laser:

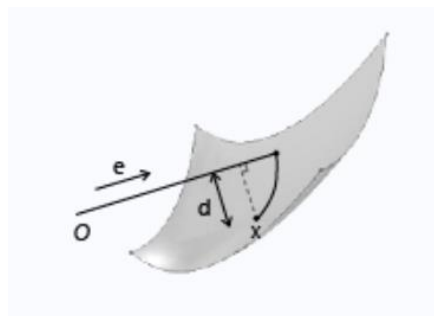
Στην COMSOL η ακτίνα laser προσομοιώνεται εύκολα με τη χρήση της επιλογής *Deposited Beam Power* που περιλαμβάνεται στο *Heat Transfer in Solid Physics*. Οι παράμετροι της δέσμης καθορίζονται στην καρτέλα Ρυθμίσεις, όπως φαίνεται παρακάτω:

ΣΧΗΜΑ. 5.8 ΡΥΘΜΙΣΕΙΣ DEPOSITED BEAM POWER

Η κατανομή της δέσμης laser είναι γκαουσιανής μορφής και περιγράφεται από την Εξίσωση 5.2,

$$f(\mathbf{O}, \mathbf{e}) = \frac{1}{2\pi\sigma^2} \exp\left(-\frac{d^2}{2\sigma^2}\right), \quad d = \frac{\|\mathbf{e} \times (\mathbf{x} - \mathbf{O})\|}{\|\mathbf{e}\|}$$

Eq. 5.2



ΣΧΗΜΑ. 5.8 ΚΑΤΑΝΟΜΗ GAUSS ΔΕΣΜΗΣ LASER

Το παραπάνω είναι το αντίστοιχο της *LaserConvectionBC* βιβλιοθήκης που φαίνεται στην εξίσωση 2.4.

6. ΑΠΟΤΕΛΕΣΜΑΤΑ ΚΑΙ ΣΥΓΚΡΙΣΗ ΤΩΝ ΛΟΓΙΣΜΙΚΩΝ ΣΤΟΧΟΙ

Στο κεφάλαιο αυτό θα παρουσιαστούν και θα συγκριθούν τα αποτελέσματα των δύο λογισμικών. Επίσης, θα παρουσιαστεί μια σύντομη σύγκριση της διαχείριση πόρων από τα λογισμικά.

ΧΑΡΑΚΤΗΡΙΣΤΙΚΑ ΥΠΟΛΟΓΙΣΤΗ

Device name DESKTOP-K11I1SC

Processor Intel(R) Xeon(R) E-2176M CPU @ 2.70GHz 2.71 GHz

Installed RAM 32.0 GB (31.8 GB usable)

System type 64-bit operating system, x64-based processor

ΕΠΕΞΕΡΓΑΣΤΗΣ

Xeon E-2176M είναι ένας 6-core, 12-threads επεξεργαστής, σχεδιασμένος για χρήση σε φορητό υπολογιστή, χρονισμένος στα 2.70GHz και έχοντας Intel turbo boost στα 4.40Ghz.

ΜΝΗΜΗ

32768 MBytes Dual-Channel DDR4 Random-Access Memory (RAM), χρονισμένη στα 2666 MHz.

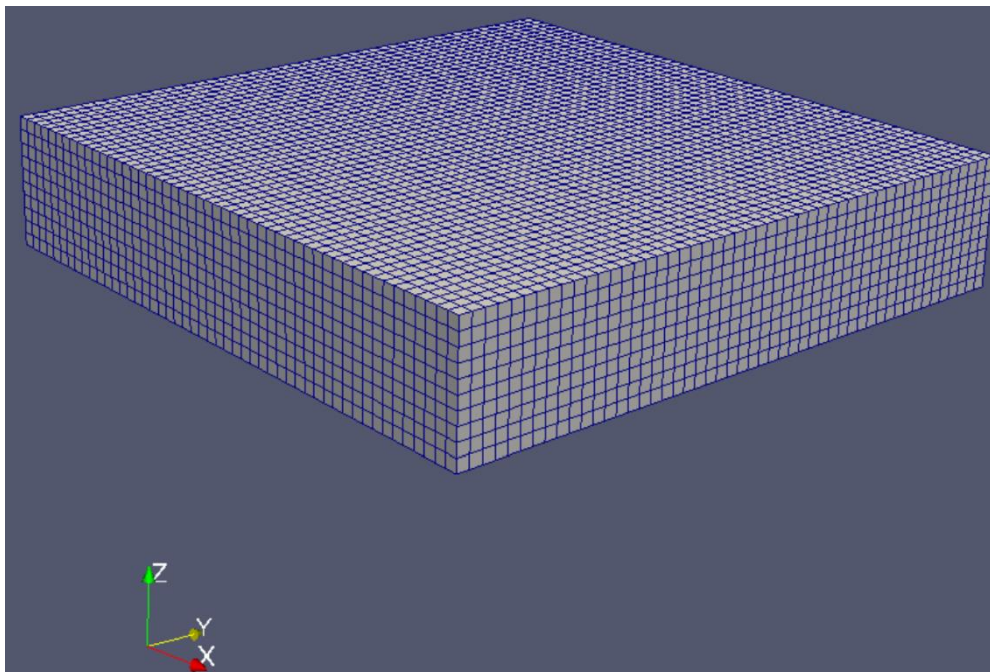
ΤΥΠΟΣ ΣΥΣΤΗΜΑΤΟΣ

Το λειτουργικό σύστημα Windows 10 Pro 64bit χρησιμοποιήθηκε για να τρέξει το COMSOL και το Windows Linux Subsystem με Ubuntu 18.04 LTS εγκαταστάθηκε για να τρέξει OpenFOAM σε περιβάλλον Linux. Οι ακέραιοι του 64bit συστήματος μπορούν να υποστηρίξουν έως και **9.22e+18** στοιχεία ενώ του 32-bit μέχρι **2.147e+09** στοιχεία [12].

6.1 ΠΛΕΓΜΑ

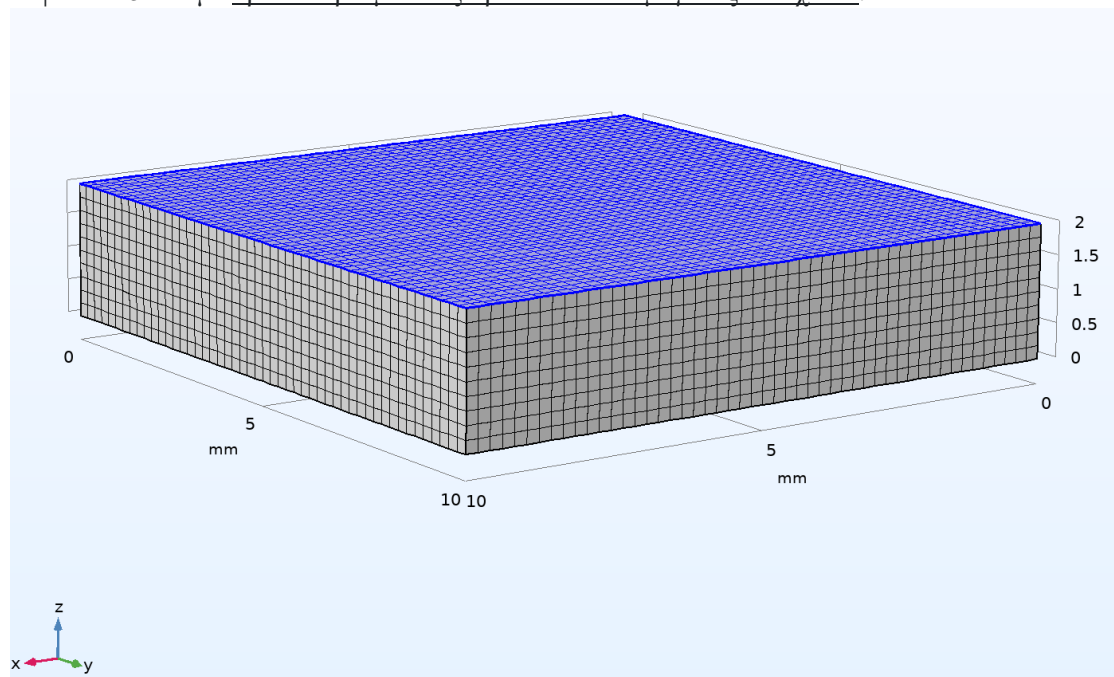
Και τα δύο λογισμικά έχουν την επιλογή να εισάγουν ή να δημιουργούν απευθείας ένα πλέγμα για μια γεωμετρία. Στο openFOAM γίνεται μέσω μερικών ενσωματωμένων μετατροπών πλέγματος.

Επιπλέον, είναι δυνατή η εισαγωγή ενός αρχείου STL και η μετατροπή του σε πλέγμα με την εντολή *snappyHexMesh*. Τα αποτελέσματα του πλέγματος παρατίθενται παρακάτω.



ΣΧΗΜΑ. 6.1 ΠΛΕΓΜΑ ΣΤΟ OPENFOAM

Στο COMSOL, αυτό γίνεται μέσω των καρτελών γεωμετρίας και πλέγματος που αναφέρονται στο κεφάλαιο 5 και με προκαθορισμένο εξαιρετικά λεπτό μέγεθος στοιχείου.



ΣΧΗΜΑ. 6.2 ΠΛΕΓΜΑ ΣΤΟ OPENFOAM

Τα στατιστικά πλέγματος και στα δύο προγράμματα είναι:

Mesh Stats	OpenFOAM	COMSOL
Type	Hexahedral	Hexahedral
Total Elements	25000	25000

ΠΙΝΑΚΑΣ 6.1 ΣΤΑΤΙΣΤΙΚΑ ΠΛΕΓΜΑΤΟΣ

Είναι σημαντικό το πλέγμα να έχει το ίδιο μέγεθος προκειμένου να υπάρξει σωστή σύγκριση των αποτελεσμάτων του κεφαλαίου 6.2.

6.2 ΓΕΩΜΕΤΡΙΑ MELT POOL

Οι θερμοφυσικές ιδιότητες ρυθμίστηκαν ως εξής:

Thermophysical Values	OpenFOAM	COMSOL
Thermal Conductivity	Constant	Constant
Density	Constant	Constant
Specific Heat	Constant	Constant

ΠΙΝΑΚΑΣ 6.2 ΘΕΡΜΟΦΥΣΙΚΕΣ ΙΔΙΟΤΗΤΕΣ

Οι ρυθμίσεις του επιλύτη είναι:

Solver Settings	OpenFOAM	COMSOL
Precision	6 digits	5 digits
Tolerance	0.01	0.01

ΠΙΝΑΚΑΣ 6.3 ΡΥΘΜΙΣΕΙΣ ΕΠΙΛΥΤΗ

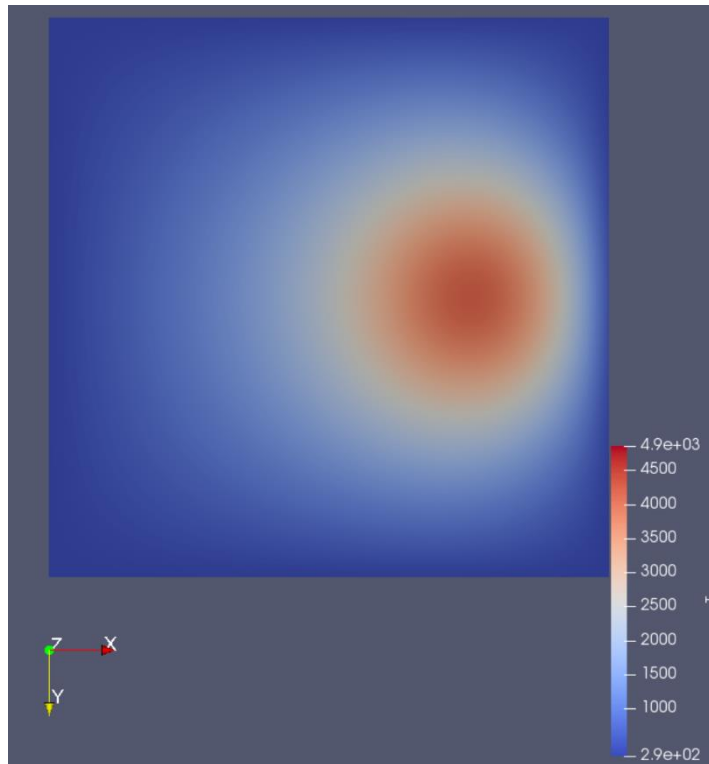
Αξίζει να σημειωθεί ότι οι τιμές θερμοφυσικών ιδιοτήτων διατηρούνται σταθερές. Αυτό θα κάνει τα αποτελέσματα να απέχουν πολύ από τα ρεαλιστικά, αλλά σε αυτή την περίπτωση δεν αποτελεί πρόβλημα, καθώς η προσομοίωση γίνεται με τη σύγκριση των λογισμικών ως πρωταρχικό σκοπό. Οι τιμές των ιδιοτήτων των υλικών στο COMSOL διαφοροποιούνται με την αλλαγή της θερμοκρασίας. Δυστυχώς, το OpenFOAM δεν διαθέτει καθόλου βιβλιοθήκη υλικών. Αυτό σημαίνει ότι ο χρήστης πρέπει να εισάγει τις θερμοφυσικές ιδιότητες του υλικού σε σχέση με την αλλαγή θερμοκρασίας προκειμένου να έχει ρεαλιστικά αποτελέσματα.

Επιπλέον είναι σημαντικό να τονιστεί πως για να γίνει σωστή σύγκριση κάποιες βασικές τιμές έπρεπε να είναι κοινές:

Case settings	OpenFOAM	COMSOL
Initial Temperature [K]	293.15	293.15
Laser Power [W]	350	350
Laser Speed [mm/s]	50	50
Laser Beam σ [m]	0.0015	0.0015

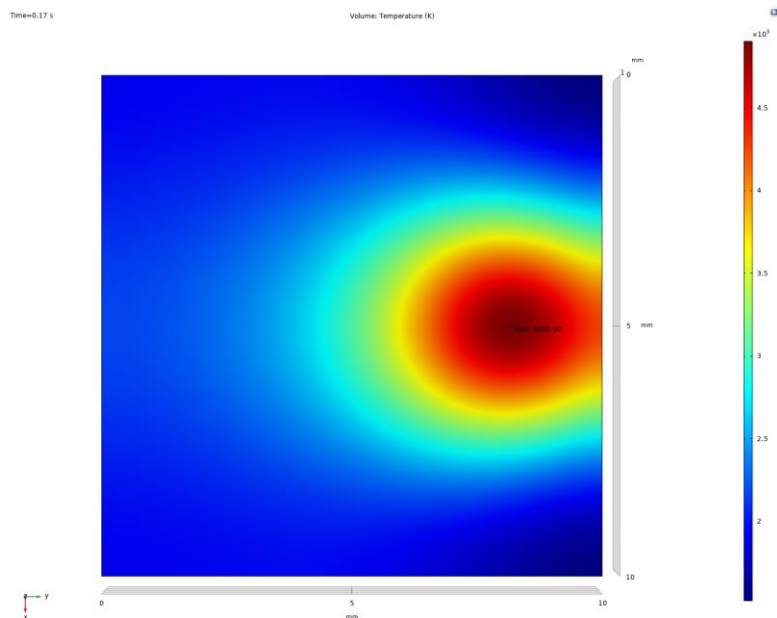
ΠΙΝΑΚΑΣ 6.4 ΒΑΣΙΚΕΣ ΤΙΜΕΣ ΠΡΟΣΟΜΟΙΩΣΗΣ

Τα αποτελέσματα του OpenFOAM παρουσιάζονται παρακάτω,



ΣΧΗΜΑ. 6.3 LASER MELTING CASE ΣΤΟ OPENFOAM. ΧΡΟΝΟΣ ΕΝΑΡΞΗΣ 0s, END TIME 0.2s, ΒΗΜΑ 0.01s.

Στο Σχήμα 6.3 είναι ορατό ότι η δέσμη κινείται προς τη θετική κατεύθυνση του άξονα X. Η μέγιστη θερμοκρασία είναι 4850K. Τα αποτελέσματα του COMSOL παρουσιάζονται παρακάτω.



ΣΧΗΜΑ. 6.9 ΑΠΟΤΕΛΕΣΜΑΤΑ ΠΡΟΣΟΜΟΙΩΣΗΣ LASER MELTING ΣΤΟ COMSOL

Στο σχήμα 6.9 είναι ορατό ότι η δέσμη κινείται προς τη θετική κατεύθυνση του άξονα X. Η μέγιστη θερμοκρασία είναι 4900K.

Ο παρακάτω όγκος δημιουργήθηκε εφαρμόζοντας την συνθήκη $T > 2000$,

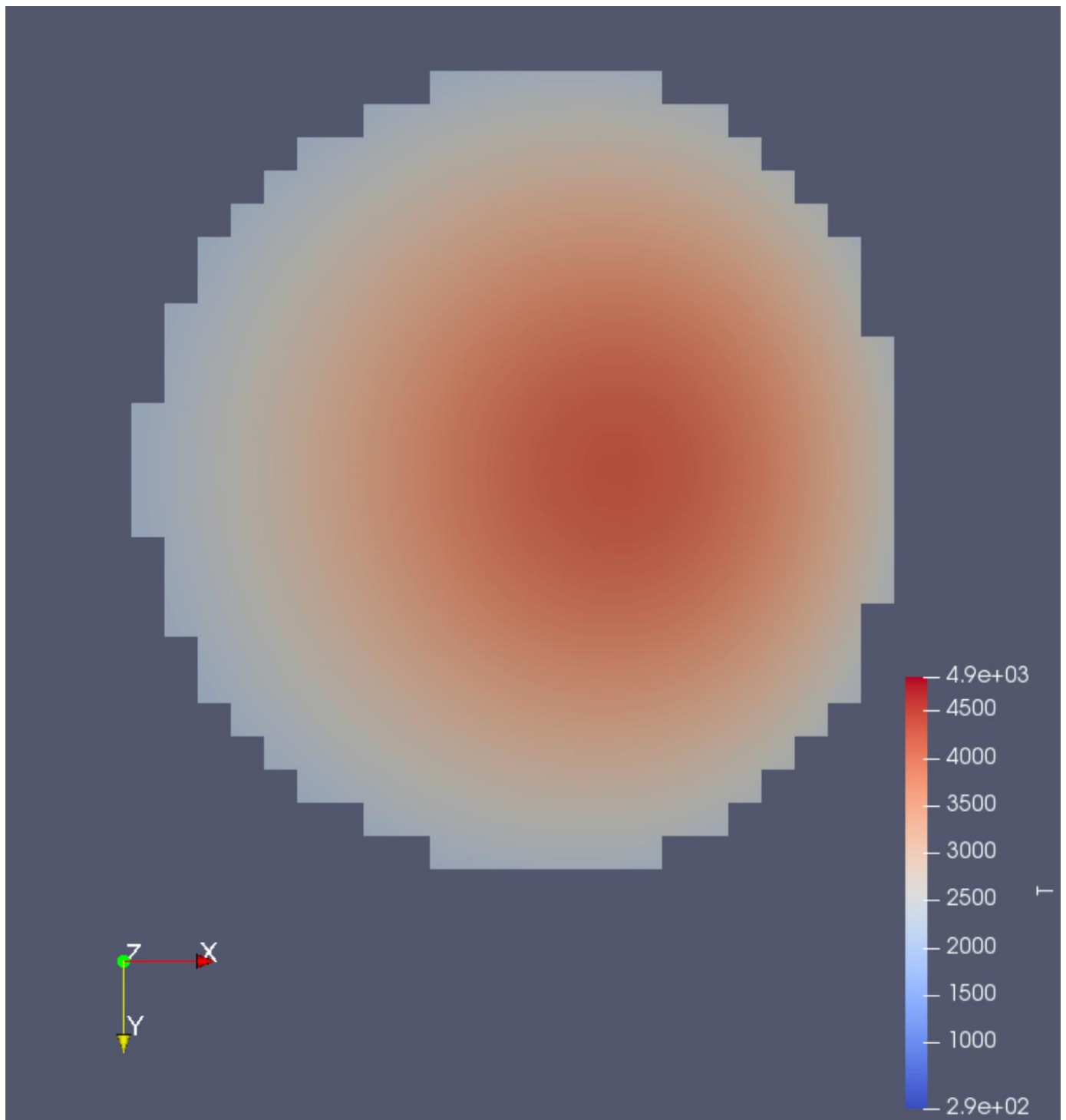
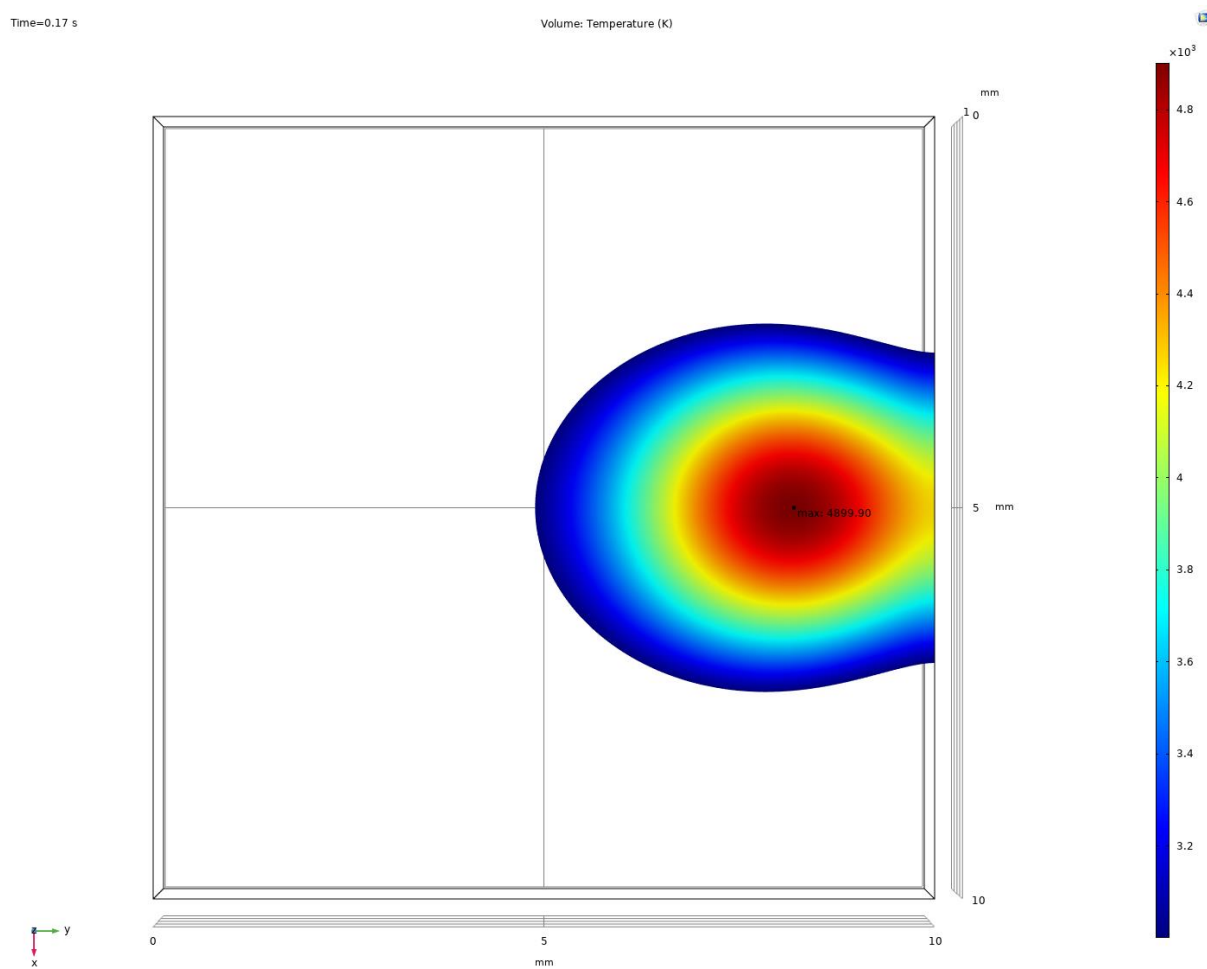


FIG. 6.7 ΠΑΡΑΓΩΜΕΝΟΣ ΟΓΚΟΣ ΓΙΑ ΤΗΝ ΣΥΝΘΗΚΗ $T > 2000K$, ΚΑΤΟΨΗ

Όσον αφορά το COMSOL,

FIG. 6.11 ΠΑΡΑΓΩΜΕΝΟΣ ΟΓΚΟΣ ΓΙΑ ΤΗΝ ΣΥΝΘΗΚΗ $T > 2000\text{K}$ ΣΤΟ COMSOL, ΚΑΤΟΨΗ

Το κριτήριο που επιλέγεται για την αξιολόγηση των αποτελεσμάτων των δύο λογισμικών είναι ο υπολογισμός των παραγόμενων όγκων από τη συνθήκη, $T > 2000\text{K}$, οι οποίοι είναι ορατοί στα σχήματα 6.7 και 6.12. Αυτή είναι μια κοινή και εύκολα εφαρμόσιμη μέθοδος. Οι υπολογισμένοι όγκοι παρουσιάζονται παρακάτω:

Volumes	OpenFOAM	COMSOL
	2.3168e-08	2.1062e-08

TABLE 6.5 ΥΠΟΛΟΓΙΣΜΕΝΟΣ ΟΓΚΟΣ, ΓΙΑ ΤΗΝ ΣΥΝΘΗΚΗ $T > 2000\text{K}$, ΓΙΑ ΤΑ ΔΥΟ ΛΟΓΙΣΜΙΚΑ

Επειδή το εφαρμοσμένο μοντέλο δεν είναι περίπλοκο, τα αποτελέσματα θα πρέπει να είναι εξαιρετικά παρόμοια μεταξύ τους. Έτσι, οι διαφορές των δύο λογισμικών ολοκληρώνονται εδώ. Η μέγιστη θερμοκρασία στο OpenFOAM είναι 4850K , ενώ στην COMSOL είναι 4900K . Αυτό έχει ως αποτέλεσμα μια διαφορά 1.2% μεταξύ τους. Ο παραγόμενος όγκος, από το φίλτρο $T > 2000\text{K}$, στο OpenFOAM είναι 2.3168e-08 , ενώ στο COMSOL είναι 2.1062e-08 , με αποτέλεσμα μια διαφορά 9.1% μεταξύ τους.

Comparison of results	OpenFOAM	COMSOL	Difference
Temperature [K]	4850	4900	1.2%
Calculated filtered volume [m^3]	2.3168e-08	2.1062e-08	9.1%

TABLE 6.6 ΔΙΑΦΟΡΕΣ ΘΕΡΜΟΚΡΑΣΙΑΣ ΚΑΙ ΥΠΟΛΟΓΙΖΟΜΕΝΩΝ ΟΓΚΩΝ ΣΤΑ ΔΥΟ ΛΟΓΙΣΜΙΚΑ

Τέλος, η ίδια μέθοδος εκτελέστηκε επαναληπτικά για δύο ακόμη προσομοιώσεις με ταχύτητα laser ίση με $2 \cdot \text{laser speed}$ και $10 \cdot \text{laser speed}$:

Comparison of results	OpenFOAM	COMSOL	Difference
Temperature [K], $2 \cdot \text{laser speed}$	3292	3356	1.9%
Filtered Volume [m^3], $2 \cdot \text{laser speed}$	4.832e-09	3.9337e-09	18.6%
Temperature [K], $10 \cdot \text{laser speed}$	2080	1998	3.9%
Filtered Volume [m^3], $10 \cdot \text{laser speed}$	3.84e-10	4.8422e-10	20.7%

FIG. 6.7 ΑΠΟΤΕΛΕΣΜΑΤΑ ΓΙΑ: Α) $2 \cdot \text{LASERSPEED}$; Β) $10 \cdot \text{LASERSPEED}$

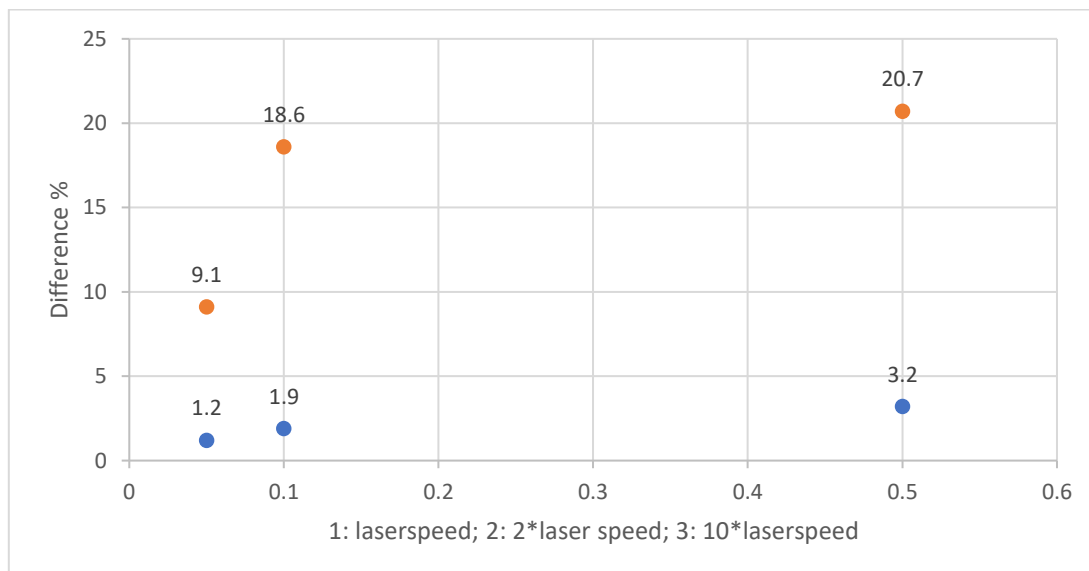
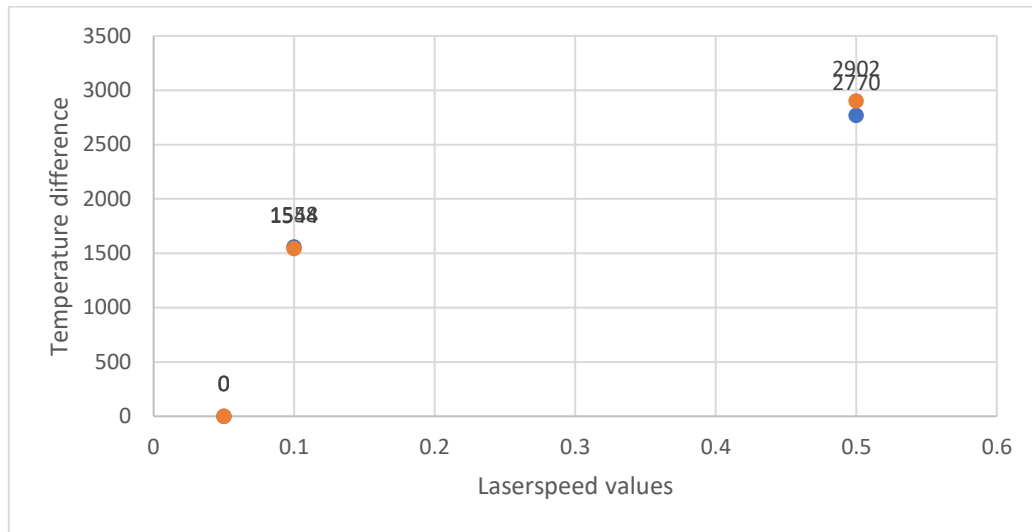


FIG. 6.13 ΔΙΑΦΟΡΑ ΘΕΡΜΟΚΡΑΣΙΑΣ ΚΑΙ ΥΠΟΛΟΓΙΖΟΜΕΝΟΥ ΟΓΚΟΥ ΜΕ ΤΗΝ ΑΥΞΗΣΗ ΤΟΥ LASERSPEED

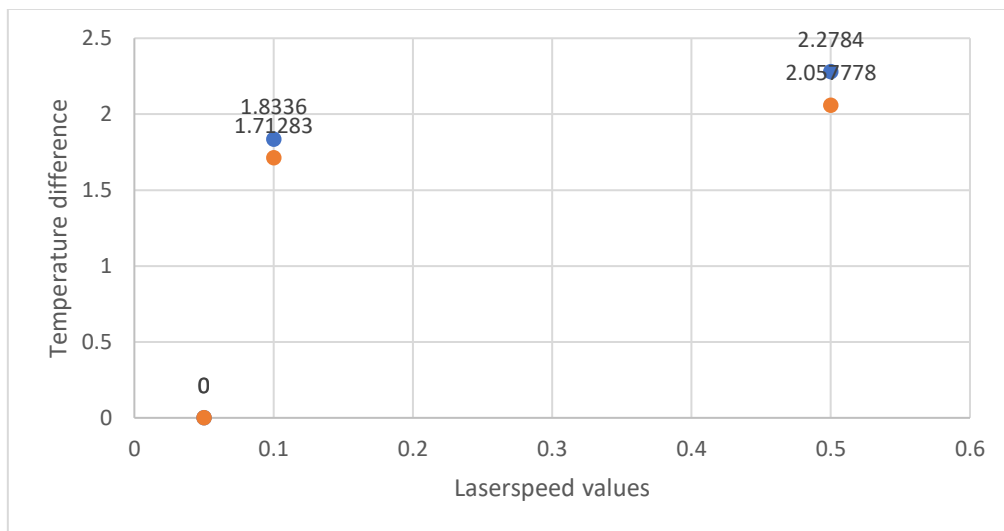
Με μπλέ παρουσιάζεται η διαφορά της θερμοκρασίας ενώ με πορτοκαλί η διαφορά των υπολογιζόμενων όγκων.

Παρακάτω, θα παρουσιαστούν οι διαφορές στις τιμές της θερμοκρασίας και του υπολογιόμενου όγκου για κάθε πρόγραμμα,

X-Values	OpenFOAM Temperature [K]	COMSOL Temperature [K]	OpenFOAM Filtered Volume [e-08m ³]	COMSOL Filtered Volume [m ³]
0.05	4850-4850=0	4900-4900=0	0	0
0.1	4850-3292=1558	4900-3356=1544	2.3168-0.4832=1.8336	2.1062-0.39337=1.71283
0.5	4850-2080=2770	4900-1998=2902	2.3168-0.0384=2.2784	2.1062-0.048422=2.057778



ΣΧΗΜΑ. 6.14 ΓΡΑΦΗΜΑ ΣΤΟ ΟΠΟΙΟ ΕΙΝΑΙ ΕΜΦΑΝΗΣ Η ΔΙΑΦΟΡΑ ΘΕΡΜΟΚΡΑΣΙΑΣ ΓΙΑ ΤΑ ΔΥΟ ΛΟΓΙΣΜΙΚΑ



ΣΧΗΜΑ. 6.15 ΓΡΑΦΗΜΑ ΣΤΟ ΟΠΟΙΟ ΕΙΝΑΙ ΕΜΦΑΝΗΣ Η ΔΙΑΦΟΡΑ ΤΩΝ ΥΠΟΛΟΓΙΖΟΜΕΝΩΝ ΟΓΚΩΝ ΓΙΑ ΤΑ ΔΥΟ ΛΟΓΙΣΜΙΚΑ

Με μπλε παρουσιάζονται οι τιμές για το OpenFOAM και με πορτοκαλί οι τιμές για COMSOL

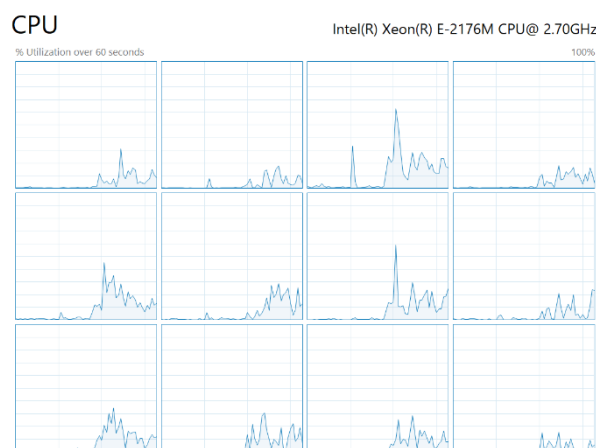
6.3 ΧΡΟΝΟΣ ΕΠΕΞΕΡΓΑΣΙΑΣ, ΔΙΑΧΕΙΡΙΣΗ ΠΟΡΩΝ ΥΠΟΛΟΓΙΣΤΗ ΚΑΙ ΠΑΡΑΛΛΗΛΟΠΟΙΗΣΗ ΚΩΔΙΚΑ

Ο χρόνος επεξεργασίας για τα δύο λογισμικά είναι,

Χρόνος επεξεργασίας	OpenFOAM	COMSOL
Wall clock time [s]	22	423

ΠΙΝΑΚΑΣ 6.6 ΧΡΟΝΟΣ ΕΠΕΞΕΡΓΑΣΙΑΣ ΓΙΑ ΤΑ ΔΥΟ ΛΟΓΙΣΜΙΚΑ

Το OpenFOAM μπορεί να χρησιμοποιήσει τόσο φυσικές όσο και λογικές μονάδες επεξεργασίας, σε αντίθεση με την COMSOL που είναι σε θέση να χρησιμοποιήσει μόνο τους φυσικούς πυρήνες. Επιπλέον, το OpenFOAM υποστηρίζει δυνατότητες GPU Acceleration, ενώ το COMSOL δεν το έχει. Στο σχήμα 6.14 παρουσιάζεται η κατανάλωση πόρων επεξεργαστή κατά την προσομοίωση με OpenFOAM.



ΣΧΗΜΑ. 6.14 ΚΑΤΑΝΑΛΩΣΗ ΠΟΡΩΝ ΕΠΕΞΕΡΓΑΣΤΗ ΑΠΟ ΤΟ OPENFOAM

Αξίζει να σημειωθεί πως στο COMSOL, κάθε φορά που εκτελείται η προσομοίωση, ο χρόνος επεξεργασίας διαφέρει σε μικρό βαθμό. Αυτό οφείλεται στην επιλογή διαφορετικής τιμής αρχικοποίησης από τον επιλύτη.

Για παράδειγμα, η παραπάνω προσομοίωση εκτελέστηκε στο COMSOL αρκετές φορές και τα αποτελέσματα του χρόνου επεξεργασίας είναι:

COMSOL SOLUTION	RUNTIME [s]
1	462
2	434
3	402
4	576
5	423

ΠΙΝΑΚΑΣ 6.7 ΧΡΟΝΟΙ ΑΠΟΚΡΙΣΗΣ ΤΟΥ COMSOL ΕΠΕΙΤΑ ΑΠΟ ΑΡΚΕΤΕΣ ΔΟΚΙΜΕΣ

7. ΣΥΜΠΕΡΑΣΜΑΤΑ

ΣΤΟΧΟΙ

Σε αυτό το κεφάλαιο θα συναχθούν ορισμένα τελικά συμπεράσματα σχετικά με αυτά τα δύο λογισμικά.

Πρώτα απ' όλα, τα αποτελέσματα στο Κεφάλαιο 6.2 δείχνουν μια αυξανόμενη διαφορά μεταξύ των δύο λογισμικών, καθώς η ταχύτητα laser αυξάνεται. Πιθανώς αυτό μπορεί να διορθωθεί βαθμονομώντας τους επιλύτες OpenFOAM.

Τα δύο λογισμικά απευθύνονται σε διαφορετικό κοινό. Το COMSOL είναι ένα εμπορικά διαθέσιμο λογισμικό που χρησιμοποιείται από μεγάλους κατασκευαστές και ερευνητικά εργαστήρια. Το OpenFOAM είναι ένα λογισμικό ανοιχτού κώδικα που χρησιμοποιείται από ερευνητές και κατασκευαστές σε μικρότερη κλίμακα και κυρίως για έρευνα και ανάπτυξη (RnD), καθώς είναι εξαιρετικά προσαρμόσιμο, όπως αναφέρεται στο κεφάλαιο 6.4. Για να χρησιμοποιηθεί το OpenFOAM, συνιστάται ιδιαίτερα η γνώση των συστημάτων Linux και της κωδικοποίησης σε γλώσσα C++, σε αντίθεση με το COMSOL, το οποίο έχει περιβάλλον GUI.

Και τα δύο προγράμματα διαθέτουν χαρακτηριστικά που είναι εξαιρετικά χρήσιμα. Το COMSOL περιλαμβάνει μια βιβλιοθήκη υλικών που διαθέτει ένα μεγάλο σύνολο δεδομένων υλικών και τις θερμοφυσικές τους ιδιότητες, όσον αφορά στην αλλαγή θερμοκρασίας. Από την άλλη, το OpenFOAM, μπορεί να είναι εξαιρετικά προσαρμόσιμο, όπως αναφέρεται στο Κεφάλαιο 6.4 και πολλές βιβλιοθήκες και λύσεις τρίτων είναι διαθέσιμες από τον ερευνητή, καθιστώντας το έτσι ένα εξαιρετικά ισχυρό εργαλείο.

Έτσι, στον παρακάτω πίνακα συνοψίζονται οι ομοιότητες και οι διαφορές του δοκιμασμένου λογισμικού:

	Ομοιότητες	Διαφορές
OpenFOAM-COMSOL	Δυνατότητα εφαρμογής multiphysics μοντέλων	Το περιβάλλον εργασίας χρήστη είναι πολύ διαφορετικό σε αυτά τα δύο λογισμικά και ανάλογα με το χρήστη, μπορεί να είναι εύκολο ή δύσκολο να μάθει
	Ισχυροί και αποτελεσματικοί λύτες	Βιβλιοθήκη Υλικών
	Ευρέως χρησιμοποιημένος, υποστήριξη από την κοινότητα	Διαφορές προσαρμογής, καθώς το COMSOL δεν είναι εύκολα προσαρμόσιμο
		Το πλέγμα ως OpenFOAM δεν υποστηρίζει όλα τα είδη στοιχείων

ΠΙΝΑΚΑΣ 7.1 ΟΜΟΙΟΤΗΤΕΣ ΚΑΙ ΔΙΑΦΟΡΕΣ ΤΩΝ OPENFOAM ΚΑΙ COMSOL

8. ΜΕΛΛΟΝΤΙΚΗ ΕΞΕΛΙΞΗ ΤΟΥ PROJECT

ΣΤΟΧΟΙ

Στο κεφάλαιο αυτό θα παρουσιαστούν μερικές ιδέες για την μελλοντική εξέλιξη του θέματος της εργασίας αυτής. Οι παρακάτω πληροφορίες θα δημιουργήσουν κίνητρα για τη μελλοντική ανάπτυξη του παρόντος project.

8.1 ΣΥΓΧΩΝΕΥΣΗ ΜΟΝΤΕΛΟΥ ΡΕΥΣΤΩΝ ΚΑΙ ΑΛΛΑΓΗΣ ΦΑΣΗΣ

Ένα πιο ολοκληρωμένο μοντέλο θα ήταν αυτό με τη σύζευξη του θερμικού μοντέλου και της ρευστομηχανικής. Αυτό μπορεί να γίνει μέσω του επιλύτη *icoReactingMultiphaseInterFoam*, ο οποίος μπορεί να χειριστεί προσομοιώσεις με πολλαπλές φάσεις υλικών.

8.2 ΜΟΝΤΕΛΟΠΟΙΗΣΗ ΗΛΕΚΤΡΟΜΑΓΝΗΤΙΚΩΝ ΔΥΝΑΜΕΩΝ ΛΟΓΩ ΕΠΙΔΡΑΣΗΣ ΠΛΑΣΜΑΤΟΣ

Κατά τη διάρκεια της SLM κατεργασίας, υφίστανται ηλεκτρομαγνητικές δυνάμεις (δυνάμεις Lorentz) λόγω της παραγωγής πλάσματος, στην περιοχή τήξης. Αυτό το φαινόμενο θα μπορούσε να συνδυαστεί με το παραπάνω μοντέλο μεταφοράς θερμότητας-ρευστών και να παράγει ένα μοντέλο πλησιέστερο στο καθολικό.

8.3 ΣΥΓΚΡΙΣΗ ΤΟΥ ΘΕΡΜΙΚΟΥ ΜΟΝΤΕΛΟΥ ΜΕ ΤΟ ΜΟΝΤΕΛΟ ΡΕΥΣΤΩΝ ΚΑΙ ΗΛΕΚΤΡΟΜΑΓΝΗΤΙΚΩΝ ΔΥΝΑΜΕΩΝ

Τα παραπάνω μοντέλα θα πρέπει να ελεγχθούν για τον αντίκτυπό τους στα συνολικά αποτελέσματα (μέσω στατιστικών τεστ). Τα μοντέλα που δοκιμάζονται πρέπει να είναι το θερμικό μοντέλο, το μοντέλο μεταφοράς θερμότητας-ρευστών και το μοντέλο μεταφοράς θερμότητας-ρευστών-ηλεκτρομαγνητισμού.

8.4 ΣΥΓΚΡΙΣΗ ΔΙΑΦΟΡΕΤΙΚΩΝ ΜΕΓΕΘΩΝ ΠΛΕΓΜΑΤΩΝ

Εδώ πρέπει να γίνει σύγκριση μεταξύ διαφορετικών μεγεθών πλεγμάτων. Αυτό είναι μείζονος σημασίας, καθώς ο χρόνος επεξεργασίας μειώνεται πολύ. Χρησιμοποιώντας τη μέθοδο εκτίμησης Richardson, είναι δυνατόν να προσδιοριστεί το σφάλμα μεταξύ δύο διαφορετικών μεγεθών πλέγματος και να αξιολογηθούν με κριτήριο το χρόνο επεξεργασίας.

8.5 ΣΥΓΧΩΝΕΥΣΗ ΜΟΝΤΕΛΟΥ PLASMA SHIELDING (ΑΠΟΡΡΟΦΗΣΗ ΕΝΕΡΓΕΙΑΣ ΤΗΣ ΔΕΣΜΗΣ LASER)

Κατά τη διάρκεια της διαδικασίας SLM το μέταλλο αλλάζει φάσεις από στερεό σε υγρό, δημιουργώντας έτσι το melt pool. Καθώς η πυκνότητα ενέργειας είναι αυξημένη στην περιοχή αυτή, το μέταλλο μπορεί να αλλάξει φάση από στερεό σε αέριο ή από υγρό σε αέριο. Κατά τη διάρκεια αυτής της κατάστασης, παράγεται πλάσμα και ο ατμός του μετάλλου, όταν ξεπεράσει την ζώνη υψηλής θερμοκρασίας, συμπυκνώνεται και διαμορφώνει σωματίδια τα οποία εμποδίζουν να περάσει όλη η ισχύς του laser στην επιφάνεια του της πούδρας. Αυτό το φαινόμενο ονομάζεται plasma shielding.

8.6 ΔΗΜΙΟΥΡΓΙΑ ΜΙΑΣ ΓΕΝΙΚΗΣ ΒΙΒΛΙΟΘΗΚΗΣ ΛΟΓΙΣΜΙΚΟΥ ΓΙΑ ΤΗΝ ΚΑΤΕΡΓΑΣΙΑ ΠΡΟΣΘΗΚΗΣ ΥΛΙΚΟΥ SLM ΑΝΟΙΧΤΟΥ ΚΩΔΙΚΑ, ΒΑΣΙΣΜΕΝΗ ΣΕ ΛΟΓΙΣΜΙΚΟ ΑΝΟΙΧΤΟΥ ΚΩΔΙΚΑ OPENFOAM

Προκειμένου να εξελιχθεί η διαδικασία SLM, περισσότεροι ερευνητές θα πρέπει να είναι σε θέση να έχουν πρόσβαση σε ελεύθερο λογισμικό. Η παρούσα εργασία μπορεί να αποτελέσει έναυσμα για την ανάπτυξη ενός λογισμικού ανοιχτού κώδικα με βάση το OpenFOAM. Το λογισμικό αυτό θα είναι σε θέση να εκτελέσει πολλαπλούς τύπους προσομοιώσεων όπως, thermal history και υπολογισμό παραμενουσών τάσεων κ.λπ.